COUPLED-INDUCTOR INVERSION, RECTIFICATION AND CYCLOCONVERSION

Thesis by

Sayed-Amr El-Hamamsy

In Partial Fulfillment of the Requirements

for the Degree of

Doctor of Philosophy

California Institute of Technology

Pasadena, California

1986

(Submitted May 13, 1986)

To my parents

who set the standards I have strived to live up to.

ACKNOWLEDGEMENTS

I would like to thank my advisors Professors R. D. Middlebrook and S. M. Ćuk for giving me the opportunity to work in the Caltech Power Electronics Group. They have created ideal conditions for research within the group, and they have allowed their students the freedom to choose the direction of their research on their own.

I am also thankful to Caltech for the Graduate Teaching Assistantships that I have received in the course of my studies here. I am indebted to the Power Electronics Program supported by grants from the GTE Corporation and Emerson Electric Company, as well as the financial support of McDonnell-Douglas Astronautics Corporation, General Dynamics Corporation of Fort Worth, Tx, IBM Corporation of Tucson, Az, and Motorola Government Electronics Division of Phoenix, Az.

Credit is due to the present and former members of the Power Electronics Group for the many discussions and ideas that helped me clarify my own thoughts and avoid some pitfalls in the course of my work. My special thanks go to Ke-Yue Ma for her help with the rectifier circuit and to Rachel Dickenson for her help with the figures.

ABSTRACT

A new PWM approach using three state switching of negatively coupled inductors can be applied to any basic dc-to-dc converter to form single-phase dc-to-ac inverters. Current reference programming gives improvements in linearity, small-signal dynamics, and pulsed-load response. The current programming loops of the flyback and boost inverters are stable at all operating points. New multiple output magnetic structures are introduced that apply space and time multiplexing of magnetics to give non-interacting outputs. The magnetics are analysed for different operating conditions. The inverters with two independent outputs are derived by use of the multiple output magnetics. These are used to form the three-phase versions of the inverters. The corresponding three-phase ac-to-dc rectifiers are also derived with close to ideal current waveforms as well as power factor correction capabilities. Finally, to complete the family of power converters the polyphase ac-to-ac cycloconverters are derived incorporating the qualities of both the inverters and the rectifiers.

TABLE OF CONTENTS

INTRODUCTION

Until recently, signal processing has been the area of rapid expansion in electrical engineering. Signal processing, in general, is any operation on electrical signals, be they analog or digital, where the preservation of the information content of the signal is the primary criterion of quality. In contrast, power processing is any operation on electrical power, be it DC or AC, with the primary criterion of maximizing the efficiency of the procedure. Power processing has remained limited to fixed frequency ac voltage transformations, or to ac-to-dc rectification with uncontrolled rectifiers for a very long time.

However, with the advent of controlled rectifiers, such as thyristors, all the potential for power processing has been released. All the different types of power processing: from dc to dc, dc to ac, ac to dc, and ac to ac, are currently in use. The advent of fast switching power devices, such as bipolar transistors and MOSFETs, allow for higher power switching frequencies. As a result, the magnetic components in these circuits have been drastically reduced in size. The higher switching frequency circuits have more degrees of freedom than the slow switching ones. Several different functions that were considered too hard or expensive to implement are now possible with the fast switching circuits, such as input current wave shaping and power factor correction.

The different power processing circuits have been generated from the fundamental dc-to-dc converters in different ways in recent years. The

power processing circuits are generally known as: inverters for dc-to ac, rectifiers for ac-to-dc, and cycloconverters for ac-to-ac operation. However, there is a constant search for new topologies that are better behaved, use less components and have a fast response to load changes. In this thesis a new family of power processing circuits are introduced that have several distinct advantages over the previous circuits.

A new method of obtaining families of power processing circuits from the different basic dc-to-dc converters is introduced in this thesis. The method is called *coupled inductor inversion*. The basic principle is to replace the single inductor of a standard dc-to-dc converter by a pair of negatively coupled inductors. The new single-phase inverters have *three switched-networks* (3SN) because there are three switches. This results in the creation of an extra degree of freedom in control that is used to implement *current reference programming* (CRP).

The first chapter of the thesis describes the single-phase inverters and compares them to some of the main types of inverters already in existence. It is found that the new type of inverter requires a smaller number of switches than existing inverters. This represents a reduction in size, weight, parts count and complexity of control.

In the second chapter the CRP loop is investigated thoroughly for the inverters derived from the buck, boost, flyback and Ćuk derived inverters. The operation is described with emphasis on the difference between the current programming in these 3SN inverters and in standard 2SN converters. The stability of the current programmed loop is also studied.

There are several advantages that result from the application of current programming in these inverters, the first of which is that the inverters have a linear control-to-output relationship. This results in a waveform with very little distortion, hence very clean sinusoidal outputs are generated from sinusoidal input signals. A second advantage is that the order of the system is reduced by one as the inductor current is constrained and ceases to be an independent state (to first order at least). That results in great simplification of the design of the feedback circuit. The last advantage is that the speed of response to pulsed loads is extremely fast.

In the third chapter the large-signal analysis of the single-phase inverters is performed. A power series expansion of the voltages is used to solve the non-linear time-varying differential equations governing the states. The result is in the form of a time-domain equation for the output voltage. These results, however, clearly show that the properties mentioned above, that were obtained using an idealized model, are very good approximations of the actual inverter.

In Chapter 4, magnetic circuits that are used to obtain multiple outputs are introduced. There are two distinct ways of getting multiple outputs from the same magnetic structure with very little interaction between the different outputs. The first method is called *space multiplexing of magnetics* and the second is *time multiplexing of magnetics*.

The two magnetic structures are analyzed to give expressions for the different inductors as well as the different current and voltage ratios. The analysis for the transition instants is also made and results in an explanation for some unexpected behavior of the currents. This also leads

to prediction of a similar phenomenon when the structure is used as a multiple input structure. These structures are then used with the single-phase inverters to obtain inverters with two independent ac outputs. These two-phase inverters can have any combination of output voltage frequency and phases, and slightly restricted amplitudes (the same that apply to any switching converter).

In the fifth chapter, these inverters are used with a three-phase load to give a three-phase output voltage. The three-phase inverters are then analysed to give the large-signal response as before. The small-signal response is calculated by application of a transformation to a rotating frame of reference. In this frame of reference the three-phase voltages appear as dc quantities and are perturbed. The same small-signal perturbation analysis as applied to dc-to-dc converters is used for the three-phase inverters. That analysis cannot be performed for the single-phase inverters. This is proved in the third chapter. Once more the experimental verification is made with a flyback three-phase inverter.

The coupled inductor three-phase inverters are easily converted into ac-to-dc rectifiers. This is simply achieved by interchanging the loads and the inputs. However, from the control viewpoint the requirements are quite different. The input current ideally should be sinusoidal and if possible in phase with the input voltages. This is not, however, achieved by loss of the current programming capability. It is possible to accomodate the different requirements within this type of rectifier. Hence, the rectifiers have the advantages of current programming while its input current waveforms approach the ideal rectifier characteristics as shown in Chapter 6.

In Chapter 7, the final member of the power processing family is introduced: the ac-to-ac coupled-inductor cycloconverters. The different cycloconverters are described. The analysis for the input section is the same as that of the rectifier, while that of the output is the same as that of the inverter. The cycloconverters with time-multiplexed magnetics are seen to be superior to the ones with space-multiplexed magnetics. They have a substantial reduction in the number of switches as compared to the previous methods. They also exhibit the same properties as the coupled-inductor inverters and rectifiers.

The cycloconverters are in essence the generalized power processing circuit. Application of different switching functions make the circuit behave as a rectifier, an inverter or a dc-to-dc converter with independent multiple outputs. Hence all these functions are a subset of the polyphase ac-to-ac conversion.

CHAPTER 1

Coupled-Inductor Inversion

1.1 Introduction

There has been a lot of interest in recent years to develop dc-to-ac power converters which incorporate high efficiency and good waveforms for ac motor variable speed drives and for uninterruptible power supplies [1,2,3]. Square-wave inverters using silicone controlled rectifiers (SCR) or gate turn-off transistors (GTO) have been in use for many years [4,5], but they have two main drawbacks: the first is that generated outputs are square waveforms which contain a significant amount of the power in higher harmonics of the fundamental, and the second is that the switching frequencies are relatively low thus limiting the range of output frequencies. Lately there have been several types of inverters introduced that use high frequency switching and generate sinusoidal output waveforms.

A family of inverters that uses a new inversion technique is introduced here, and compared to two standard methods of inversion used in fast-switching pulse-width modulated (PWM) inverters with sinusoidal output waveforms. The new inverters are known as *Coupled-Inductor Inverters*. A switched-mode inverter is defined as any switched-mode power processing circuit that accepts a dc input and has an ac output. A PWM inverter is one in which the value and polarity of the output is controlled by the duty ratio of the switches in the circuit. Finally, the switching is considered to be fast if its frequency is much higher than both the

inversion frequency and the natural frequencies of the circuit.

The coupled-inductor inverters are derived from the basic dc-to-dc converters and they have a *three switched-network* (3SN) mode of operation, which adds an extra degree of freedom to the control and permits the application of *current reference programming* (CRP) in a current feedback loop that is independent of the voltage feedback loop. The steady-state values are calculated for the output voltage and inductor current in terms of the duty ratio and the dc input voltage.

1.2 Practical Switch Implementation

Before a description of the coupled-inductor inverter is given certain aspects of practical switches need to be clarified. Because of the high frequencies involved and the size restrictions all the switching in power converters is done electronically. The switches to be implemented may be simple on off switches or may be multi-pole multi-throw switches. The building blocks of electronic switches are diodes and transistors. The transistor is a controlled switch, that is, it is turned on or off by a control signal, whereas the diode is uncontrolled and is turned on and off by circuit conditions. They are both simply on-off switches and are used to implement much more complicated switches. Hence, one must have a basic unit that is used for comparison purposes between different topologies. In this thesis the basic switching unit is defined as a transistor-diode pair.

In dc-to-dc converters with unidirectional power flow there is usually one single-pole double-throw switch that is implemented by a single transistor-diode pair operating in a complementary manner, as shown in Fig. 1(a) for the buck converter. However, if the power flow is bidirectional

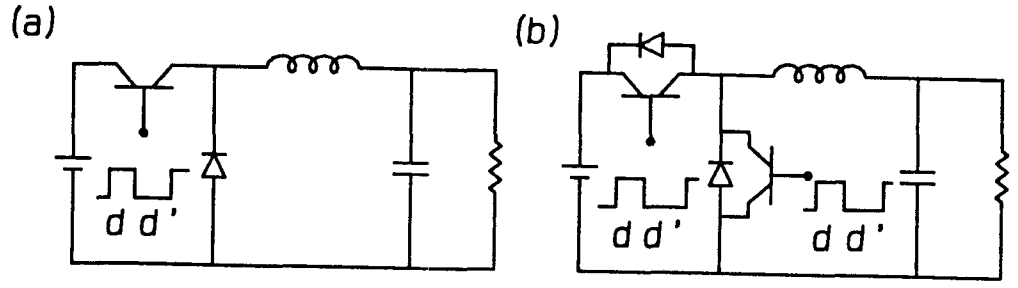

Fig. 1.1 The dc-to-dc buck converter: a) the single quadrant version with a single transistor-diode pair, b) the two quadrant version with two transistor-diode pairs in anti-parallel.

or if some of the states of the converter are ac, this type of switch implementation is not sufficient and a single-pole double-throw switch must have two transistor-diode pairs, as shown in Fig. 1(b) for the buck with bidirectional power handling capability.

Similarly, in an inverter, which by definition has ac states, the basic building blocks for switches are transistor-diode pairs. The pair shown in Fig. 2(a) are connected in parallel to conduct current in both directions and block voltages of one polarity only, whereas the pair in Fig. 2(b) are connected in series and conduct current in one direction but block voltages in both directions. These two switches are known as two quadrant switches, and combining two of the same kind gives a four quadrant switch (Fig. 2(c)). Also for the sake of completeness another possible four quadrant switch is given in Fig. 2(d), where the use of one

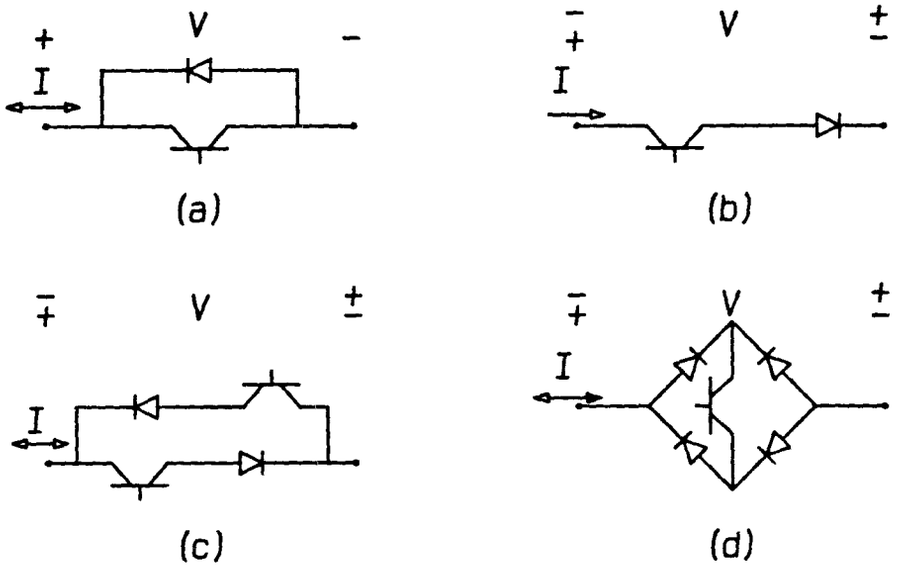

Fig. 1.2 The different switch implementations with transistors and diodes. a) The transistor and diode are in an anti-parallel connection thus blocking one polarity of voltage and carrying bidirectional currents. b) The transistor and diode in series to block bipolar voltages and carry unidirectional currents. c), d) Two different implementations of bidirectional current bipolar voltage switches.

less transistor has been traded-off for two diodes and higher losses due to the two diode drops when the switch is on.

Hence, the number of switches used in a given inverter is taken to be the number of transistor-diode pairs that are needed to implement the multi-pole multi-throw switch of the circuit diagram. For example, the single-pole triple-throw switch of Fig. 3(a) is implemented by either one of the two combinations shown in Fig. 3(b,c). The choice of switches is determined by the topology of the circuit. In general it is advisable to avoid four-quadrant switches for efficiency considerations and parts count reduction.

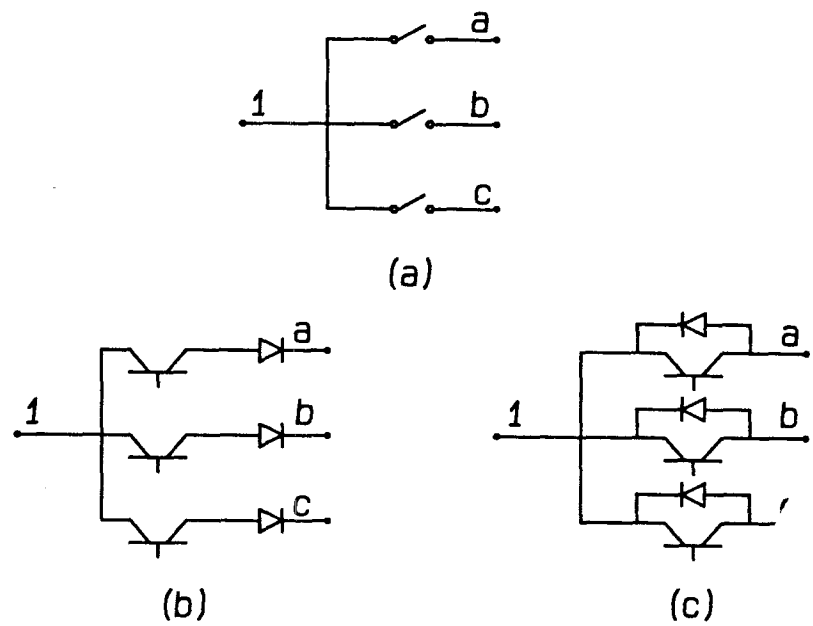

Fig. 1.3 a) An ideal single-pole triple throw switch. b) The implementation of that switch for unidirectional current and bipolar voltage. c) The same switch for single voltage polarity and bidirectional current.

1.3 Fast-switching PWM Inverters

As mentioned above the fast-switching converters have switching times that are much smaller than the natural time constants of the elements composing that converter as well as the inversion period. The advantages of high frequency switching lie in the reduction in size of the magnetic components in the circuit and the ability to filter the switching frequency component from the output waveform. The analysis is also simplified by this condition as the states of the inverter are assumed to be changing in straight lines during the switching period, which results in the dependence of the average states on the duty ratios of the switches [6]. Thus, although the elements are all reactive, ideally, the states of a dc-to-dc converter are dc to first order with a linear ripple around that value.

Hence, it appears that the main problem of dc-to-ac inversion using PWM converters is to obtain bipolar output voltages or bidirectional currents from a system composed of elements carrying unipolar voltages and unidirectional currents. The problem may be formulated in a different manner: the output voltage has to be bipolar, although it is a function of the duty ratio of the switches and the component values, which are all positive.

There have been two main solutions to this problem in recent years, both of which follow the same principle: to make the output depend on an effective duty ratio that is the difference of two actual duty ratios, so the output is bipolar according to the relative values of the two duty ratios. The first method, the push-pull, uses two dc-to-dc converters, with bidirectional power handling capability, to provide a bipolar voltage across a load that is connected differentially between them. The second method has switch configurations that connect the terminals of the dc section of the inverter to the terminals of the ac section in two ways; thus, for example, the flyback inverter of this type has a switch configuration that reverses the inductor carrying a unidirectional current across the load, thus making the load current bidirectional.

1.3.1 Push-Pull Switching Power Amplifiers

The push-pull amplifiers [2,3] consist of two two-quadrant converters with the load connected differentially between them (Fig. 4). The quadrant here refers to the different polarities and directions of voltages and currents that the *converter* can handle (Fig. 5). Thus a converter that has dc output voltage, yet can source or sink a current, is a two-quadrant

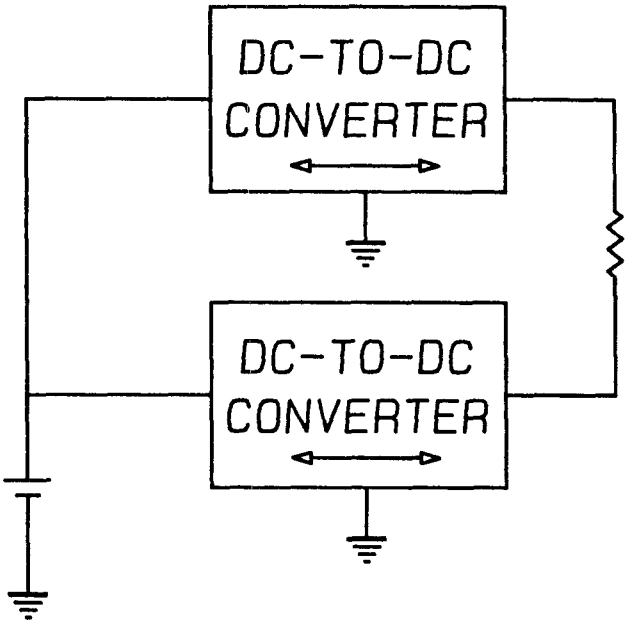

Fig. 1.4 The push-pull switching power amplifier. The load is connected differentially between the two two-quadrant converters.

converter. These are also known as converters with bidirectional power flow. The number of quadrants of a converter is decided by the type of switches used as well as the topology of the converter in question. For example, the inverters under consideration here are four quadrant inverters although the switches are all two quadrant switches.

The two-quadrant converters operate in a complementary manner, so that the voltage generated at the output is a result of the subtraction of the two output voltages. Hence, the ideal gain of the amplifier is:

$$\frac{V}{V_g} = M(D) - M(D')$$

where

$$D' = 1 - D$$

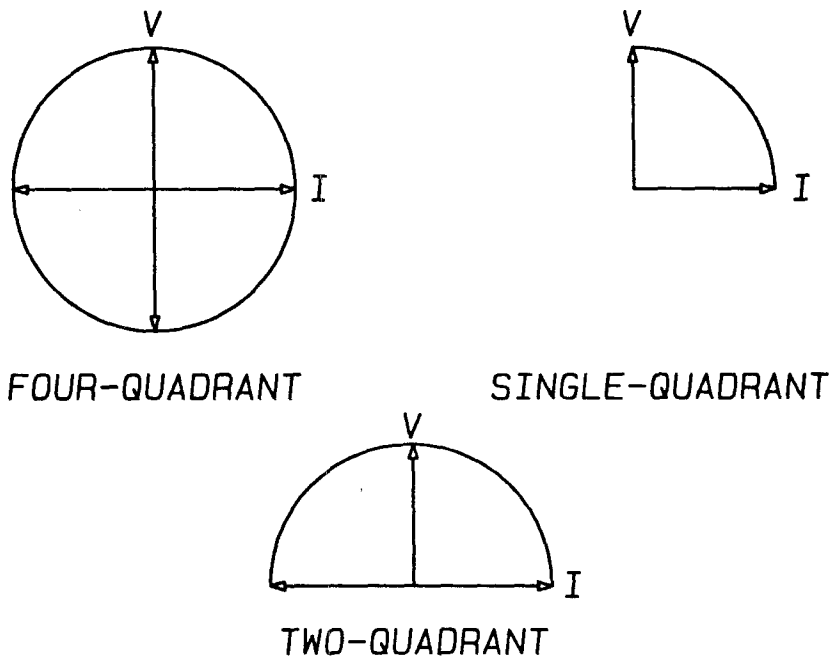

Fig. 1.5 The quadrants define the ability of a power processing circuit to handle different current directions and polarities. This capability depends on the switch implementation as well as on the topology. The figures represent single-quadrant, two-quadrant (bidirectional current), and four-quadrant converters.

and M is the ideal gain of the single converter. The gain is ideal in the sense that parasitics and the effect of loading are neglected. However, all the basic converters, except for the buck, have non-linear ideal gains, and so the resulting inverter gain is also non-linear. It should be pointed out that the inclusion of the parasitic inductor losses linearize the system for certain load conditions and for relatively restricted duty ratio excursions. The use of parasitics to linearize a circuit is not a very good idea, and what is really required is to introduce feedback, or to synthesize a control law that cancels out the non-linearity of the gain.

The switching scheme of the push-pull amplifiers is fairly simple, since only one drive waveform and its complement are needed. The three-phase version of these inverters requires three two-quadrant converters

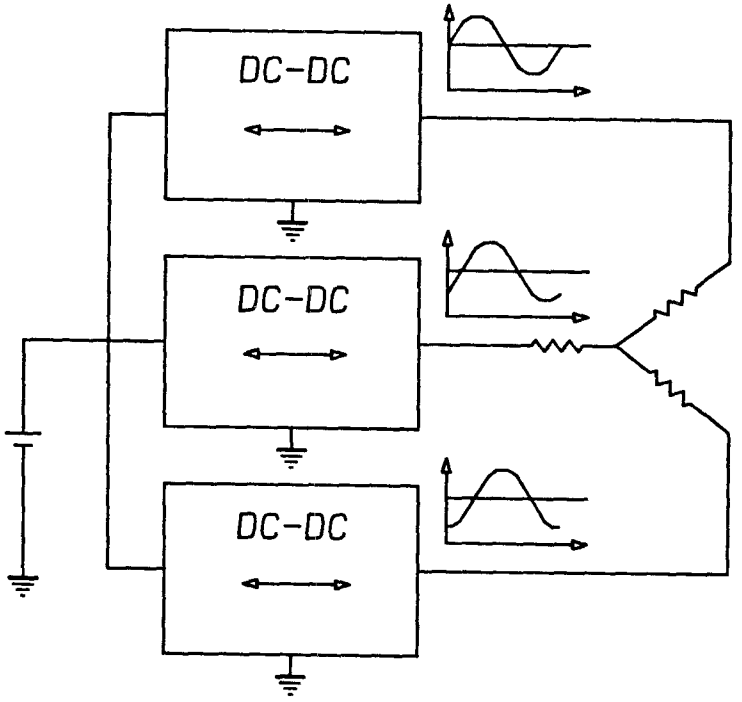

Fig. 1.6 The three-phase push-pull inverter. The output of each converter is dc with a superimposed sinusoid. The sinusoids are out of phase by 120° and are equal in amplitude. Close regulation of the dc value is required to eliminate it from the output.

(Fig. 6), each of which generates one phase plus a dc offset that is neutralized by the subtraction of the other phases. The switches have to sustain voltage stresses that are much higher than the peak output voltage. The dc offset voltage must be very tightly regulated to avoid supplying dc currents to low resistance loads such as motors. On the other hand the system is very robust in situations involving unbalanced loads because of the independence of the three converters.

1.3.2 Fast-switching Sinusoidal PWM Inverters

This type of inverter is described as *sinusoidal* [1] because it generates sinusoidal outputs from sinusoidal inputs when operated without feedback. Thus they are more linear in their gain than the previous inverters. The principle of operation is to use the switch configuration to

connect the dc terminals to the ac terminals in two different ways during one switching cycle, thus using the switching scheme to simulate the existence of the two converters used in the switched-mode power amplifiers. Figure 7 shows a single-phase buck inverter of this type. Each of the inverters derived from one of the basic dc-to-dc converters has different dc and ac parts. For instance the buck inverter's dc part is the source only while the inductor and capacitor are both in the ac section, whereas the boost inverter has the inductor in the dc section.

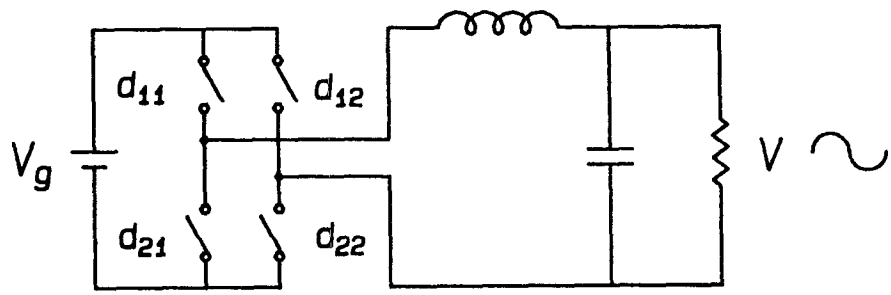

Fig. 1.7 The buck single-phase sinusoidal inverter. The bottom switches d_{21} and d_{22} are complementary with a duty ratio of 0.5. The upper switches d_{11} and d_{12} are modulated sinusoidally.

Several switching schemes can be used to generate sine wave outputs, the simplest of which is to switch the bottom switches at a 0.5 duty ratio in a complementary fashion and to switch the top ones with the following duty ratios:

$$d_{11} = \frac{1}{2} + \frac{d_m}{2}\cos\omega_m t$$

$$d_{12} = \frac{1}{2} - \frac{d_m}{2}\cos\omega_m t$$

d_{11} and d_{12} are the duty ratios of the switches of the same name, and d_m is the modulation amplitude. The resultant gain of the inverter is proportional to the difference of the top switch duty ratios, and hence even inverters based on converters with non-linear gain, such as the boost or flyback, have linear characteristics.

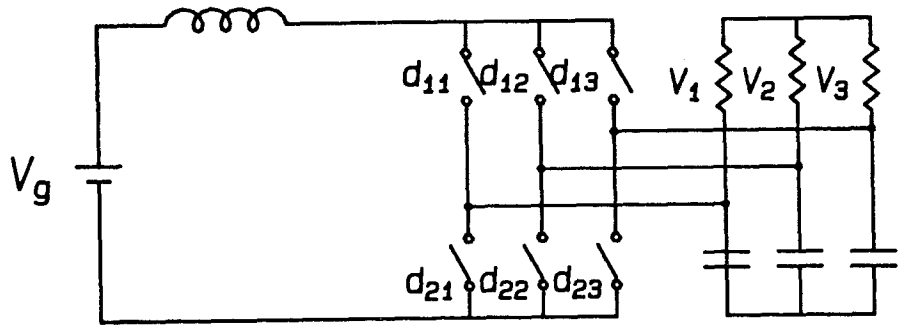

Fig. 1.8 The boost three-phase sinusoidal inverter. The upper switch duty ratios are modulated with balanced three-phase sine waves. The bottom switches each have a duty ratio of one-third.

The three-phase versions are obtained by adding one more pair of switches (Fig. 8). In this case the switching scheme is by modulating the duty ratio of the top switches by a balanced three-phase modulation. The

bottom three switches share the whole period equally between them. Thus the addition of extra phases does not entail the addition of extra converters as in the previous case. There is an overall saving in the size, weight and number of elements as compared to the switching amplifiers. However, there is a price paid in the complexity of the control scheme as each switch needs its own drive waveform.

1.4 Coupled-Inductor Inversion

The new family of inverters, introduced here, uses a pair of negatively coupled inductors to provide current bidirectionality in the output node. The coupled inductors replace the single inductor of the basic dc-to-dc converter to yield the corresponding inverter. Continuity of flux is the basic condition that must be satisfied in a magnetic structure. Thus in a single inductor the current is linked to the flux by Faraday's law, which can be stated as [7]:

$$N\Phi = LI \tag{1.1}$$

and so cannot be reversed instantaneously. However, in a multi-winding structure the relation between the current at the terminals and the flux inside the magnetic core is not one-to-one. Hence, in the case of the negatively coupled inductors shown in Fig. 9, the current at the right-hand-side node reverses direction depending upon which switch is on (d_2 or d_3), yet still satisfies the continuity of flux.

It is clear that inversion is possible with the coupled inductors, and that it also requires a smaller number of switches than the methods presented in Sections 1.3.1 and 1.3.2. The number of switches needed to

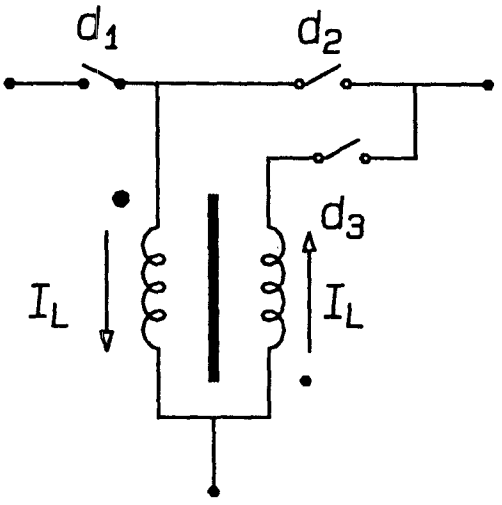

Fig. 1.9 The negatively coupled inductors. There are three switches d_1, d_2 and d_3 one of which is conducting at all times, and only one at any given instant.

reverse a two terminal element across two output terminals is four, as four points need to be interconnected. However, the coupled inductors are always connected to one point and so require only the three switches that are shown in Fig. 9. The actual saving in switches is different according to the dc-to-dc converter from which the inverter is derived; for example, a buck or a boost inverter of the type shown in Section 1.3.2 has four switches in all whereas a flyback has five. The inverters of Section 1.3.1 all have four switches. All the coupled-inductor inverters have three switches. A smaller number of switches implies a large reduction in size, weight, and complexity of control, as there is an equivalent reduction in the number of snubbing elements, heat sinks, base (or gate) drives and control signals. This constitutes one of the main practical advantages of coupled-inductor inversion.

It is of interest to note that the three-phase inverters of Section 1.2.2 have six switches in the buck and boost versions and seven in the flyback or buck-boost versions. That is due to the fact that with a three-phase load there are actually three points that need to be connected to two points only. The three-phase versions of the inverters in Section 1.3.1 are simply three dc-to-dc converters with bidirectional switches with the three phase loads connected differentially between them. It will be shown that the three-phase coupled inductor inverters require only five switches. The savings are thus relatively less important in the three-phase case.

Continuity of flux dictates that the inductor cannot be open circuited as long as the flux is non-zero, which sets a condition on the operation of the switch that is expressed mathematically as:

$$d+d' = 1 \tag{1.2}$$

where d is the duty ratio of the switch and d and d' are non-overlapping. This means that, given an input voltage and a required output voltage, there is a unique duty ratio that results, which also fixes the value of the inductor current for a given load, and so the inductor current cannot be independently set. On the other hand, in the new coupled-inductor inverter there are three switches and the condition on the (non-overlapping) duty ratios becomes:

$$d_1+d_2+d_3 = 1 \tag{1.3}$$

A converter that has three switches with this condition upon them is said to be a three switched-network (3SN) converter [8]. The input to output voltage relation sets a second condition, but there are three

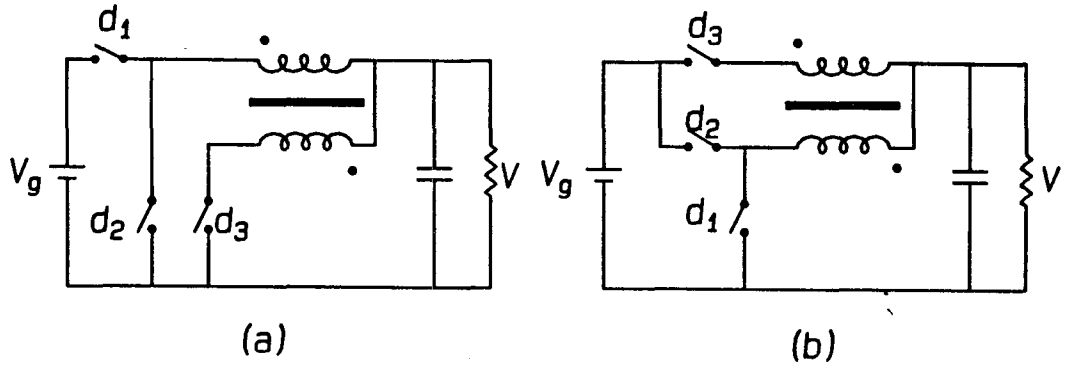

Fig. 1.10 The two possible connections of the coupled inductors in a buck topology. Version (a) is the one chosen as the inverter, while version (b) is the rectifier.

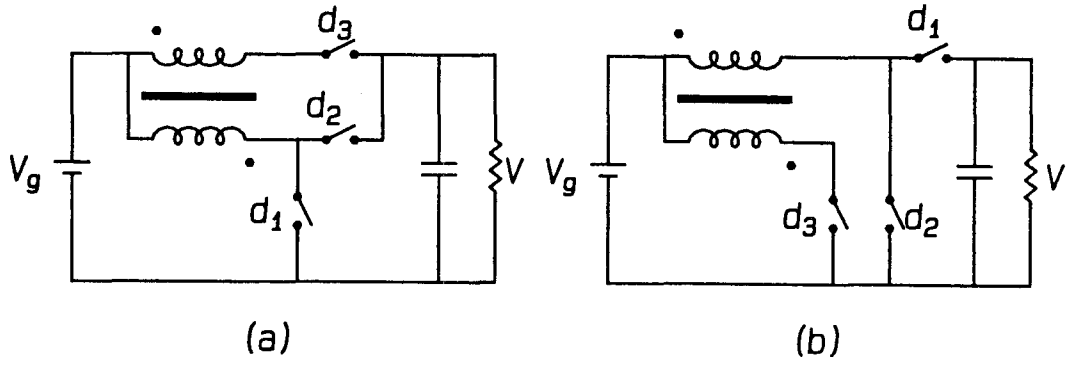

Fig. 1.11 The two possible connections of the coupled inductors in a boost topology. Version (a) is the one chosen as the inverter, while version (b) is the rectifier.

variables and so an infinite number of duty ratio values satisfy both equations. This extra degree of freedom can be used in different ways to improve the performance of the circuit. The way used here is to maintain the inductor current at a fixed value by proper switching of the input switch. This is known as current reference programming (CRP), and will be shown in the next chapter to be a highly satisfactory use of the extra degree of freedom.

1.5 Single-Phase Inverters From Dc-to-dc Converters

In this section the inverters are derived from the four basic dc-to-dc converters [6] (the buck, boost, flyback and Ćuk converters). The steady state capacitor voltages and inductor currents are calculated in terms of the input voltage, duty ratio and load from the volt-second balance as applied to the inductor.

As mentioned before, the coupled inductor replaces the single inductor of the basic dc-to-dc converter to give the corresponding inverter. There are two ways of connecting the inductors in each converter (Figs. 10, 11, 12, 13), both of which yield a circuit with the ability to change the polarity of the output voltage by varying the duty ratio. However,the two versions are not equivalent, and there are practical reasons for preferring one over the other.

As an example, the analysis is done for the two flyback inverters of Fig. 12, then the results are used to justify the choice of one over the other as the preferred inverter. The volt-second balance equation for the coupled inductor in Fig. 12(a) is:

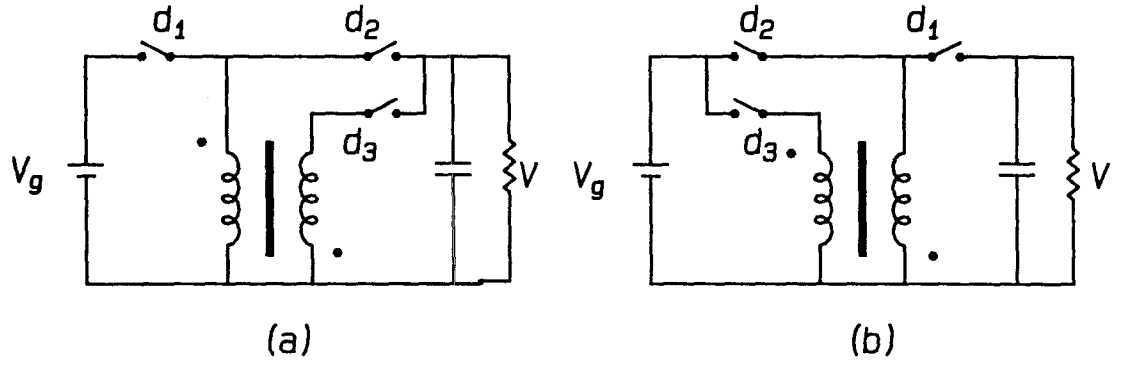

Fig. 1.12 The two possible connections of the coupled inductors in a flyback topology. Version (a) is the one chosen as the inverter, while version (b) is the rectifier.

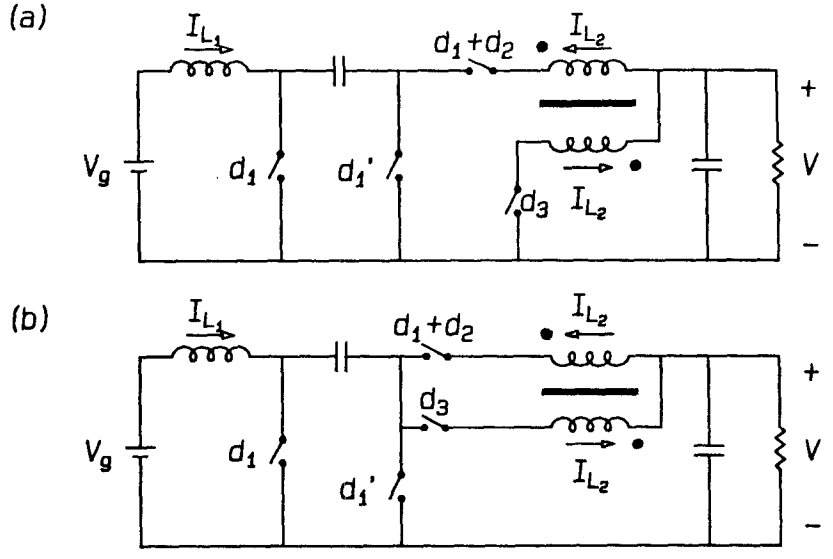

Fig. 1.13 The two possible connections of the coupled inductors in a Cuk topology. Version (a) is the one chosen as the inverter, while version (b) is the rectifier.

$$V_g d_1 T_s = v(d_3 - d_2) T_s \tag{1.4}$$

and the one for the inductor in Fig. 12(b) is:

$$V_g (d_3 - d_2) T_s = v d_1 T_s \tag{1.5}$$

where V_g is the input voltage, v is the output voltage, T_s is the switching period, and d_1,d_2, and d_3 are the duty ratios of the switches of the same name. The difference in sign of d_2 and d_3 is due to the negative coupling. Hence the relation between v and V_g in the first case is:

$$v = V_g \frac{d_1}{d_2 - d_3} \tag{1.6}$$

and in the second:

$$v = V_g \frac{d_2 - d_3}{d_1} \tag{1.7}$$

It is clear that v can be bipolar depending on the relative values of d_2 and d_3 for both inverters. The relation between the output voltage and the average inductor current i_L is obtained from the load current relation:

$$i_{load} = i_L (d_3 - d_2) \tag{1.8}$$

$$v = i_{load} R = i_L (d_3 - d_2) R \tag{1.9}$$

Similarly, for the second inverter the current relations are:

$$i_{load} = i_L d_1 \tag{1.10}$$

$$v = i_{load} R = i_L d_1 R \tag{1.11}$$

Hence in the flyback example the inductor can be connected in two ways: the two switches (d_2 and d_3) can be either on the input or on the output side (Fig. 12). Clearly both are inverters since v can be either positive or negative as can be seen in Eq. (1.6) and (1.7). However, the inductor currents in both inverters do not behave the same way. It is clear from Eq. (1.9) that in the first case the current in the inductor may be dc while the output voltage is ac, as the polarity inversion is then due to the difference duty ratio (d_2-d_3). However, in the second case, as indicated by Eq. (1.11), the dependence is on d_1 which can only be positive, so the inductor current i_L has to change direction at the inversion frequency. Thus the inductor flux changes direction at the inversion frequency in the inverter with the two switches on the input side, and so current reference programming cannot be implemented with a fixed reference current. Since the main advantages of current programming are due to the constraint that is placed on the inductor current, so the use of a varying current reference would be self-defeating. Another disadvantage is that the single switch must be a current bidirectional, as well as a bipolar voltage blocking switch. Since four-quadrant switches are implemented practically with either two transistor-diode pairs or one transistor with a diode bridge as described in Section 1.2.3, it is preferable to avoid using them.

The two arguments presented above are in favor of the inverter with the two switches on the output side. The reduction in the number of switches is one of the first advantages of this method of inversion and it is wiped out if one uses the inverter with a single switch on the output side. Current reference programming provides the inverters with some of their

principal advantages as far as linearity, ease of control and quick response to pulsed loads are concerned. However, that is not to say that the second version is to be discarded; in fact, it will be seen, in Chapter 6, that it is more suitable as the rectifier corresponding to the inverter.

Similar arguments may be used in the case of the buck, the boost and the Ćuk converter (Figs. 10, 11, 13), version (a) of each being the one chosen. The steady state relations between the input and output voltages are easily obtained by applying volt-second balance to the coupled inductor.

Inverter	Voltage Gain	Current Gain
Buck	$V = V_g \frac{d_1}{d_1+d_2-d_3}$	$V = I_L R(d_1+d_2-d_3)$
Boost	$V = V_g \frac{d_1+d_2-d_3}{d_2-d_3}$	$V = I_L R(d_2-d_3)$
Ćuk	$V = V_g \frac{-d_1}{(d_1+d_2-d_3)(1-d_1)}$	$V = I_L R(d_3-d_1-d_2)$
Flyback	$V = V_g \frac{d_1}{d_3-d_2}$	$V = I_L R(d_3-d_2)$

TABLE I The table shows the voltage and current gains of the inverters derived from the four basic dc-to-dc converters. The current gains are all linear functions of the duty ratios, which helps reduce the harmonic, in the output voltage.

Table I gives the steady state gains for different inverters. In each case, an appropriate relationship between duty ratios can give either a positive or a negative voltage at the output. Thus these circuits are truly

PWM inverters, and proper choice of modulation strategy is capable of producing sinusoidal outputs. It is of interest to note that the relation between the voltage and duty ratios in the current equation are all linear. Consequently, if the current is maintained at a fixed level in the inductor, the output voltage to current relation becomes the pertinent one and the output voltage is independent of the input voltage.

1.6 State-Space Analysis of 3SN inverters

The state-space description [9] has been extensively applied to the analysis and modelling of 2SN converters in all the different modes of operation: continuous and discontinuous conduction modes, and current programmed mode. The description is also applied to 3SN converters, thus allowing the application of a very powerful analytical tool to the inverters under consideration. In this section the state-space description of the system is set up in such a way as to be useful for both the low frequency analysis (by averaging of the states) and high frequency analysis (by discrete modelling), that are used in the rest of the thesis.

The analysis takes into consideration the operation of the inverter in the 3SN continuous conduction mode, which implies that the inductor current does not go to zero at any time. During one switching period there are 3 different topologies that apppear, each of which is described by one of the following state-space equations:

$$\dot{\boldsymbol{x}} = \boldsymbol{A}_1\boldsymbol{x} + \boldsymbol{b}_1 V_g \qquad nT_s < t < (n+d_{1n})T_s \tag{1.12}$$

$$\dot{\boldsymbol{x}} = \boldsymbol{A}_2\boldsymbol{x} + \boldsymbol{b}_2 V_g \qquad (n+d_{1n})T_s < t < (n+d_{1n}+d_{2n})T_s \tag{1.13}$$

$$\dot{\boldsymbol{x}} = \boldsymbol{A}_3\boldsymbol{x} + \boldsymbol{b}_3 V_g \qquad (n+d_{1n}+d_{2n})T_s < t < (n+1)T_s \tag{1.14}$$

where $\boldsymbol{x}(t)$ is the state vector V_g is the input voltage and T_s is the switching period. The three topologies are described by the square matrices $\boldsymbol{A}_1, \boldsymbol{A}_2$, and $\boldsymbol{A}_3$, and $\boldsymbol{b}_1, \boldsymbol{b}_2$, and $\boldsymbol{b}_3$ are the input vectors for each topology. The duty ratios satisfy the same conditions given above, the subscript n simply denotes the duty ratio of the n^{th} cycle.

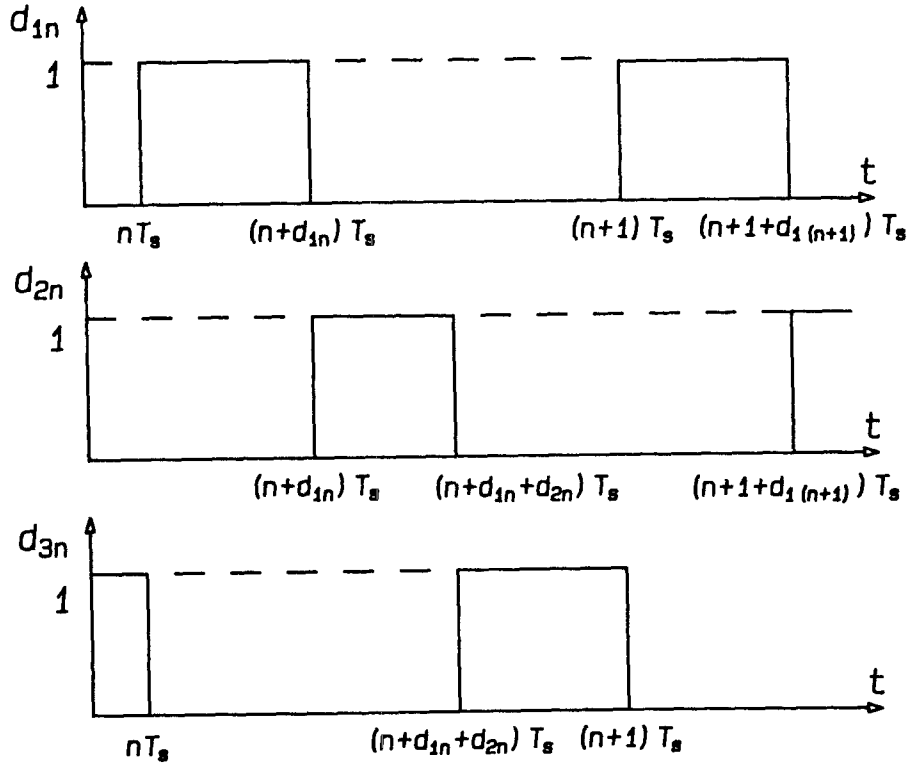

Fig. 1.14 The three switching functions for the coupled-inductor circuits. The switch is conducting when the swiching function is equal to one. The on-times add up to a fixed value T_s.

Three switching functions are defined that allow the three above equations to be combined into one. These are shown in Fig. 14 , and are described mathematically by:

$$d_1(t) = \begin{cases} 1 & \text{if } nT_s < t < (n+d_{1n})T_s \\ 0 & \textit{otherwise} \end{cases} \tag{1.15}$$

$$d_2(t) = \begin{cases} 1 & \text{if } (n+d_{1n})T_s < t < (n+d_{1n}+d_{2n})T_s \\ 0 & \textit{otherwise} \end{cases} \tag{1.16}$$

$$d_3(t) = 1-d_1-d_2 \tag{1.17}$$

Hence, the state space equation of the 3SN converter becomes:

$$\dot{\boldsymbol{x}} = (d_1\boldsymbol{A}_1+d_2\boldsymbol{A}_2+d_3\boldsymbol{A}_3) + (d_1\boldsymbol{b}_1+d_2\boldsymbol{b}_2+d_3\boldsymbol{b}_3)V_g \tag{1.18}$$

The above equation is an exact description of the system and is usually non-linear and time varying. Different techniques are used to linearize the equation or to make it time invariant, each of which is suitable for a specific operating condition or for a certain frequency range. In the course of this thesis several of these techniques are used to provide a complete description of the systems under consideration.

1.7 Conclusion

The use of coupled inductors in switched-mode PWM inverters is introduced in this chapter. The inverters are derived from the basic dc-to-dc converters, and are compared to two other methods of inversion. The inverters operate in a 3SN mode of operation which results in an added degree of freedom to the control. The possibility of maintaining a fixed current in the inductor while still having an ac output leads to the

application of CRP. In the next chapter the CRP loop is discussed in detail, however one advantage of CRP is already apparent: the linearity of the control to output relation. Another advantage of the inversion method is the reduction in the number of switches required for inversion. The state space description of the 3SN inverters is set up in a general form suitable for simplification according to the desired region of analysis.

CHAPTER 2

Current Programming in Three-Switched-Network Inverters

2.1 Introduction

The extra degree of freedom due to the 3SN mode of operation allows the application of CRP to the inverter. The input switch is then turned off whenever the inductor current reaches a fixed reference value. The inductor current is thus constrained and, to first order, is not an independent state. The current loop essentially buffers the output section from variations in the input voltage, and the pertinent relations between the output voltage and the control variables are the current relations as given in Table I. These relations are all linear, and so current programming increases the linearity of the circuit. The inductor current is maintained at its reference value even at small loads, which makes the pulsed-load response very fast.

In this chapter the operation of the current loop is described, and the stability of CRP in 3SN converters is also investigated. It is shown that, as far as the current loop is concerned, a 3SN converter derived from a boost or a flyback converter behaves as a variable switching frequency converter, hence the instability inherent in 2SN converters with current programming does not exist in these 3SN converters. The 3SN coupled-inductor buck and Ćuk converters operate in a slightly different manner and thus have the same behavior as the corresponding 2SN converter. There follows a discussion of the advantages and disadvantages of CRP.

2.2 Operation of the Inverter in CRP

The current programming loop drastically differs from the normal duty ratio programming loop. Whereas in the latter case the output is sensed, an error signal is generated and then compared to a sawtooth clock signal to set the duty ratio, in the former case the switch is simply turned off when the current reaches a reference value [10]. The inductor (or switch) current is sensed by the CRP loop during the period when the energy is being stored in the inductor (the current is ramping up). The sensed signal is compared to the reference value and the switch is turned off when the two are equal (Fig. 1).

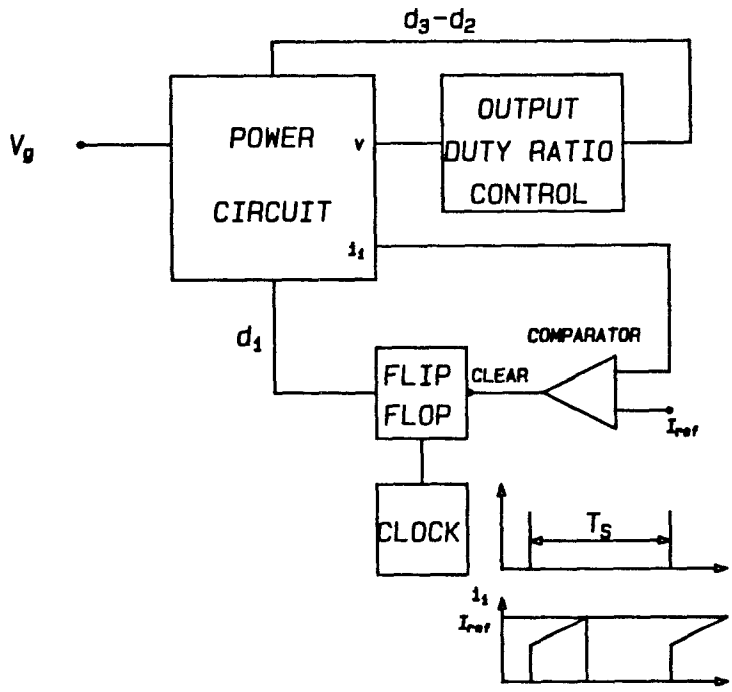

Fig. 2.1 A block diagram of a 3SN converter with current programming. There are two independent loops, a voltage and a current loop.

Standard 2SN converters with current programming have two nested interactive feedback loops [11] (Fig. 2), as they have only one control variable (the duty ratio). However, 3SN converters have two quasi-independent control variables (the duty ratio of the input switch d_1 and the effective duty ratio of the output switches d_3–d_2) and so there are two independent loops. The duty ratios are quasi-independent because they have an upper bound restriction that relates them:

$$d_1 + |d_3 - d_2| \leq 1 \tag{2.1}$$

which means they are independent as long as they are within the region defined by the above equation. In that region, the loops are only independent to first order because non-idealities and finite component values introduce further interaction, as will be seen in the detailed analysis.

The single-phase flyback inverter of Fig. 3 is taken as an example of the operation of the inverter in CRP mode. The other inverters operate in basically the same manner. It has been shown [12] that the current programming loop has a gain that typically is far from infinite. However, for simplicity, in this section the current loop is assumed to have infinite gain. This translates to the assumption of zero current ripple.

The sequence of operation of the inverter is as follows: during period d_1 the inductor is connected to the voltage source, and the current ramps up until it reaches the reference value (Fig. 4(a)). Then the inductor is connected to the load (Fig. 4(b)) and the current flows in the direction shown. Note that because of the voltage polarity shown the current is still ramping up during this period (d_2). Finally, in period d_3, the coupled

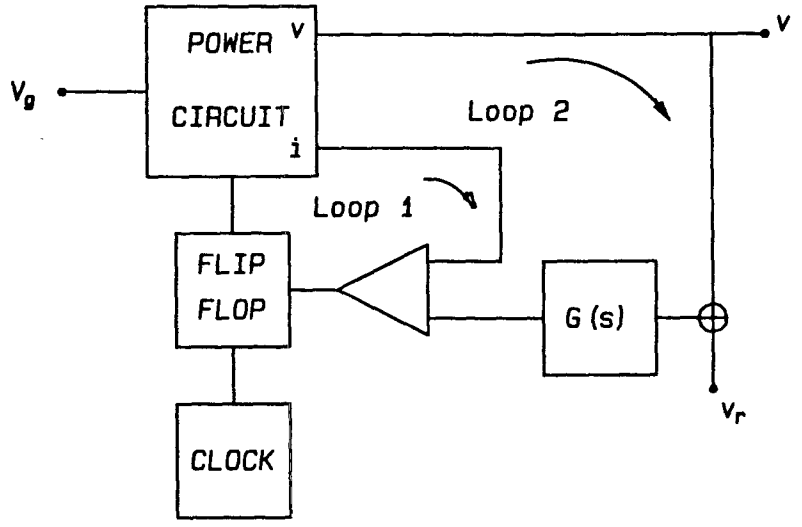

Fig. 2.2 Block diagram representation of a standard 2SN converter with nested, interactive current and voltage feedback loops. The innner loop is the current one. It turns off the switch when the current reaches a reference value. The outer loop sets that reference value to regulate the output voltage.

inductor is connected to the load (Fig. 4(c)) and by continuity of flux the current flows in the shown direction. The current ramps down during this period. The converter is assumed to be at steady state, and so the current value at the beginning of the cycle is equal to the value at the end of the cycle. To maintain this polarity of output voltage d_3 has to be greater than d_2 in such a way that the following equation holds:

$$v = i_L R(d_3 - d_2) \tag{2.2}$$

in which i_L is the average current in the inductor. Uppercase characters indicate dc quantities, while lowercase ones indicate time-varying quantities. In general, the states and the duty ratios are assumed to vary at frequencies much lower than the switching frequency. On the

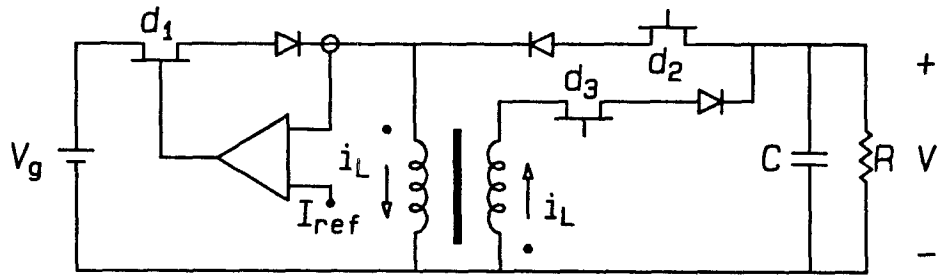

Fig. 2.3 The flyback coupled-inductor inverter with current reference programming. The switch current is sensed and compared to a reference value. The switch is turned off when the current reaches that reference value.

assumption of very small current ripple (large inductor or very high switching frequency), the average current is equal to the reference current, and so:

$$v = I_{ref} R(d_3 - d_2) \tag{2.3}$$

If the input switch is always turned off at the same value of current, the inductor behaves essentially as a current source applied to the output parallel RC impedance, and the output voltage no longer depends on the input voltage but on the average value of the inductor current which flows through the load. This is true as long as certain operating conditions are satisfied. Just as a conventional converter has continuous and discontinuous conduction modes of operation, so do the

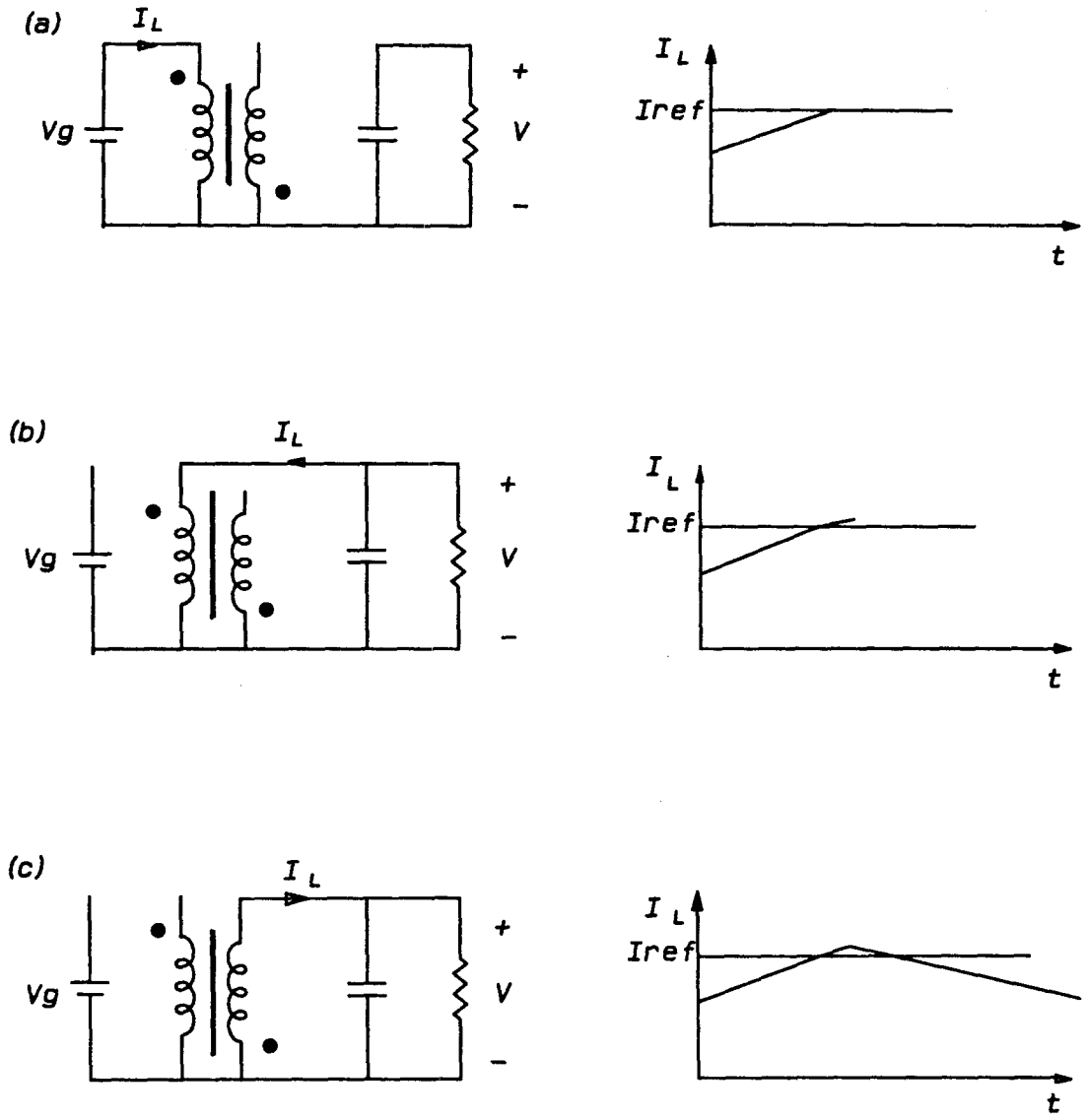

Fig. 2.4 The three-switched networks of the flyback inverter: (a) the inductor is being charged; the current ramps up until it reaches I_{ref}; the input switch is turned off; and (b) the inductor is connected to the load. The current still ramps up because of the shown voltage polarity. In (c) the second output switch is on, the current flows in the reverse direction to (b) and with a negative slope.

inverters. The CRP mode of operation is not achieved if the input voltage is so small that the current never reaches the reference value, or if the load resistance is too low for the required output voltage to be developed from the reference current.

The mechanism of operation of a 3SN converter with CRP is fundamentally different from that of a standard dc-to-dc converter. A lossless flyback converter can have any output voltage for any input voltage, as can be seen from the steady state relation:

$$v = -V_g \frac{d}{1-d} \tag{2.4}$$

As V_g gets smaller, d increases so that v remains constant. The inductor current, meanwhile, increases as it is related to v by:

$$v = i_L(1-d)R \tag{2.5}$$

As long as there is no current limit the output voltage can be maintained. In practical circuits this mechanism is limited by parasitics in the circuit, and there is a minimum input voltage that maintains the output as well as a maximum inductor current.

A 3SN converter with CRP, even under ideal lossless conditions, has a required minimum input voltage to maintain a certain output voltage. The steady state current relation is the one that sets the output:

$$v = I_{ref}(d_3-d_2)R \tag{2.6}$$

Variations in the input voltage do not affect the output as long as the current in the inductor is equal to I_{ref}. However as V_g becomes smaller d_1

becomes equivalently larger, as can be seen from the following equation:

$$v = V_g \frac{d_1}{(d_3-d_2)}$$

This process is limited by the condition on the duty ratios given in Eq. (1.2). At the limit point either d_2 or d_3 is equal to zero since the duty ratios must also satisfy Eq. (1.3), the converter is then a 2SN converter in the current limit region and the output voltage will begin to fall as the input voltage gets smaller. If duty ratio d_1 is allowed to go to any value the reference current will always be reached, but in most circuits a hard limit is set to d_1 and as the input voltage gets smaller the inductor current will not reach I_{ref}. The output voltage would still get smaller.

The condition that needs to be satisfied by the input voltage for correct operation is:

$$V_g \geq V_p \frac{(d_3-d_2)}{1-|d_3-d_2|} \tag{2.7}$$

where V_p is the maximum output voltage as set by the converter specifications, d_3-d_2 is fixed by the control circuit for a given fixed load, and d_1 is replaced by the absolute maximum value it can have according to Eq. (2.1).

It is clear from Eq. (2.6) that the value of the load affects the output for a given duty ratio. In a 2SN converter the output does not depend on the load as long as there is no current limit in the circuit. However, the 3SN converters with CRP are in the current limit mode at all loads and voltages, and there is thus once more an absolute limit on the minimum load resistance for which a specified output voltage can be

maintained. In the ideal case of no losses and no ripple the minimum load resistance is:

$$R_{\min} \geq \frac{V_p}{I_{ref}} \tag{2.8}$$

It is obvious that these conditions are not restrictive enough, and that they can be refined by including all non-idealities and parasitics. However, the basic mechanisms whereby these limitations exist are brought out by the idealisation of the circuit. The insight gained by the more correct analysis is minimal, and does not justify the additional work. Just as most circuit designs take into account component values that vary by as much as 20%, so it is possible to use these relations with a suitable safety factor. However, if the specifications are so restrictive that further refinement is needed, then the above analysis is still useful in showing where the limitations exist and why. For the rest of the analysis it will be assumed that the inverters are in the CRP mode at all times.

2.3 Stability of CRP

The current programmed loop in 2SN converters has been studied extensively [11,12,13], and is known to be unstable whenever the duty ratio exceeds 0.5. A simple geometrical analysis of the current waveform is performed here to account for this instability. The same type of analysis is used to show that the 3SN inverters derived from the boost and the flyback converters are stable for all values of duty ratio. The inverter derived from the buck converter, because of a different control algorithm, behaves as a 2SN converter. Figure 5(a) shows the analysis for a 2SN converter, and it is clear that the condition for stability is that $d \leq 0.5$.

The only way to stabilize the circuit is either to restrict the duty ratio to the stable range or to use a compensating ramp, both of which limit the performance of the converter. The limitation of d to less than 0.5 limits the range of outputs available, and the compensating ramp reduces the loop gain of the current programming feedback loop.

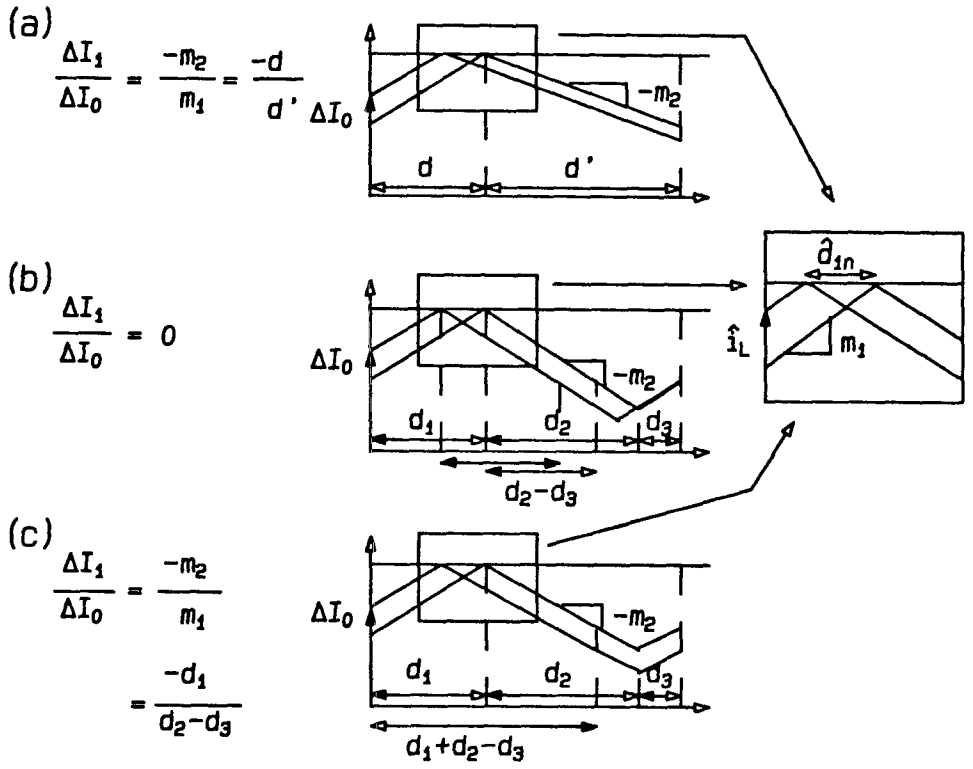

Fig. 2.5 The current waveforms for (a) a standard two switched-network converter, (b) the flyback and boost coupled-inductor inverters, and (c) the buck and Ćuk coupled-inductor inverters. The insert shows the relation between the duty ratio and the current perturbations.

2.3.1 Geometrical analysis of stability

The 3SN inverters normally have a sinusoidal output voltage but, since the inversion frequency is much lower than the switching frequency, and the stability is to be studied at half the switching frequency, the output voltage may be considered constant. This assumption does not affect the stability argument, and merely separates the variation in the length of d_1 due to the output being time varying, from that due to disturbances. Experimental observation shows this to be a reasonable assumption. Thus, the control circuitry can be considered to maintain the quantity (d_3-d_2) constant during the time interval under consideration, a switching period T_s. It can be seen (Fig. 5(b)) that any perturbation ΔI of the current dies out within one cycle. The current loop is thus stable at any duty ratio, and a compensating ramp is not required.

The buck derived inverter behaves differently as its control to output relation is:

$$v = I_{ref}(d_1+d_2-d_3)R \tag{2.9}$$

Thus a disturbance $\hat{d}_1$ in d_1 causes the control circuit to change d_2 by an amount equal to $-\hat{d}_1$ and to let d_3 remain fixed so as to maintain a fixed output voltage. Thus, in effect the inverters operate similarly to a 2SN buck or Ćuk, as can be seen from Fig. 5(c), and the condition for stability is:

$$d_1 \leq |d_2-d_3| \tag{2.10}$$

As it stands this equation is not very useful since it does not yield a certain value beyond which the inverter current loop is unstable. Because

the control to output gain is not symmetrical for the two polarities of the output, there is one more condition on the duty ratios:

$$d_{1\max}+d_{2\max}-d_{3\min} = -(d_{1\max}-d_{3\max}) \tag{2.11}$$

This condition guarantees a symmetrical voltage swing on the output, and also ensures maximum usage of the period by making $d_2 = 0$ in the right-hand side of the equation. It is clear from the operation of the inverter in CRP as described in Section 2.2 that d_1 is the same on both sides of Eq. (2.11). Equation (1.2) then becomes:

$$d_{1\max}+d_{3\max} = 1 \tag{2.12a}$$

for the negative output voltage and:

$$d_{2\max} = 1-d_{1\max}-d_{3\min} \tag{2.12b}$$

for the positive output voltage. The solution of Eq. (2.11), (2.12a) and (2.12b) give the following condition:

$$d_{1\max} = d_{3\min} \tag{2.13}$$

Finally the solution of Eq. (2.13) with the condition for stability (Eq. (2.10)) yields the condition for $d_{1\max}$:

$$d_{1\max} \leq 0.25 \tag{2.14}$$

This is the exact equivalent of the condition for the 2SN buck converter as it implies maximum output voltage of 0.5 V_g. For the Ćuk inverter, this translates to a maximum output voltage of 0.66 V_g, which is less than a 2SN Ćuk [11]. However, it is possible to operate the coupled-inductor Ćuk

inverter in a 4SN mode of operation, without any added switches. In that case, the inverter is capable of achieving any output voltage while remaining stable. However, this is beyond the scope of this work and requires further investigation. Thus, for now, the buck and Ćuk inverters are either restricted to that range of outputs or a compensating ramp is used to maintain the stability of the current loop.

2.3.2 Discrete Modelling Analysis of Stability

A discrete analysis method that is equivalent to the geometrical analysis has also been used to describe the behavior of the high frequency pole in the z-transform domain [13,14]. The same approach is used in the 3SN inverters derived from the boost, flyback and Ćuk converters, to show that the pole is at the origin of the z-plane, which implies that the perturbations die out within one cycle. This type of analysis is not inverter dependent for those three inverters and is done starting from the general state-space description of the system. The analysis for the buck is done in parallel as it differs in some switching function definition only, and it is actually quite similar to the one done for 2SN converters.

The stability analysis for the current programming loop starts from Eq. (1.18). As before the inverter is assumed to have a dc output voltage, which means that d_2-d_3 in the boost, flyback and Ćuk inverters, and $d_1+d_2-d_3$ in the buck are maintained constant. Let the input voltage consist of a dc value with added small signal perturbation:

$$v_g(t) = V_g + \hat{v}_g(t) \tag{2.15}$$

where the standard notation is to use upper case characters for dc

quantities, lowercase ones for time-varying quantities (note that the time variation may be at the inversion frequency or at the switching frequency), and lowercase with carets for small-signal ac perturbations. Similarly, the duty ratios can be written as:

$$d_{1n} = D_1 + \hat{d}_{1n} \tag{2.16}$$

$$d_{2n} = D_2 + \hat{d}_{2n} \tag{2.17}$$

Note that the equations above guarantee that $d_{2n}-d_{3n}$ is constant if:

$$\hat{d}_{2n} = -\tfrac{1}{2}\hat{d}_{1n} \tag{2.18a}$$

and that $d_{1n}+d_{2n}-d_{3n}$ is constant if:

$$\hat{d}_{2n} = -\hat{d}_{1n} \tag{2.18b}$$

The switching functions, introduced in Chapter 1, now consist of a steady state, time varying part and a perturbation. The steady state part is denoted by lowercase letters with bars and so the switching functions become:

$$d_1(t) = \bar{d}_1(t) + \hat{d}_1(t) \tag{2.19a}$$

$$d_2(t) = \bar{d}_2(t) + \hat{d}_2(t) - \hat{d}_1(t) \tag{2.19b}$$

$$d_3(t) = 1 - d_1(t) - d_2(t) \tag{2.19c}$$

$$\bar{d}_1(t) = \begin{cases} 1 & t \in [nT_s,\ (n+D_1)T_s] \\ 0 & otherwise \end{cases} \tag{2.19d}$$

$$\bar{d}_2(t) = \begin{cases} 1 & t\in[(n+D_1)T_s,\ (n+D_1+D_2)T_s] \\ 0 & otherwise \end{cases} \tag{2.19e}$$

$$\bar{d}_3 = 1-\bar{d}_1-\bar{d}_2 \tag{2.19f}$$

$$\hat{d}_1(t) = \begin{cases} sgn(d_{1n}-D_1) & t\in[(n+D_1)T_s,\ (n+d_{1n})T_s] \\ 0 & otherwise \end{cases} \tag{2.19g}$$

$$\hat{d}_2(t) = \begin{cases} sgn(d_{1n}-D_1) & t\in[(n+D_1+D_2)T_s,\ (n+\tfrac{1}{2}d_{1n}+\tfrac{1}{2}D_1+D_2)T_s] \\ 0 & otherwise \end{cases} \tag{2.19h}$$

$$\hat{d}_2(t) = 0 \tag{2.19i}$$

$$sgn(y) = \begin{cases} +1 & \text{if } y>0 \\ 0 & \text{if } y=0 \\ -1 & \text{if } y<0 \end{cases} \tag{2.19j}$$

Equation (2.19h) is defined for the boost, and flyback inverters, while Eq. (2.19i) is defined for the buck and Ćuk inverters. These functions are shown in Fig. 6 . It is clear that these definitions will preserve the condition for operation of the inverters as given by Eq. (2.18a) and D. Owing to these perturbations the state vector now consists of a steady-state, time varying part and a perturbation.

$$\boldsymbol{x}(t) = \bar{\boldsymbol{x}}(t)+\hat{\boldsymbol{x}}(t) \tag{2.20}$$

The perturbed terms are substituted into the state equation (Eq. (1.18)). The steady-state part and the perturbed part can be separated and by setting the perturbations to be equal to zero the steady-state equation results.

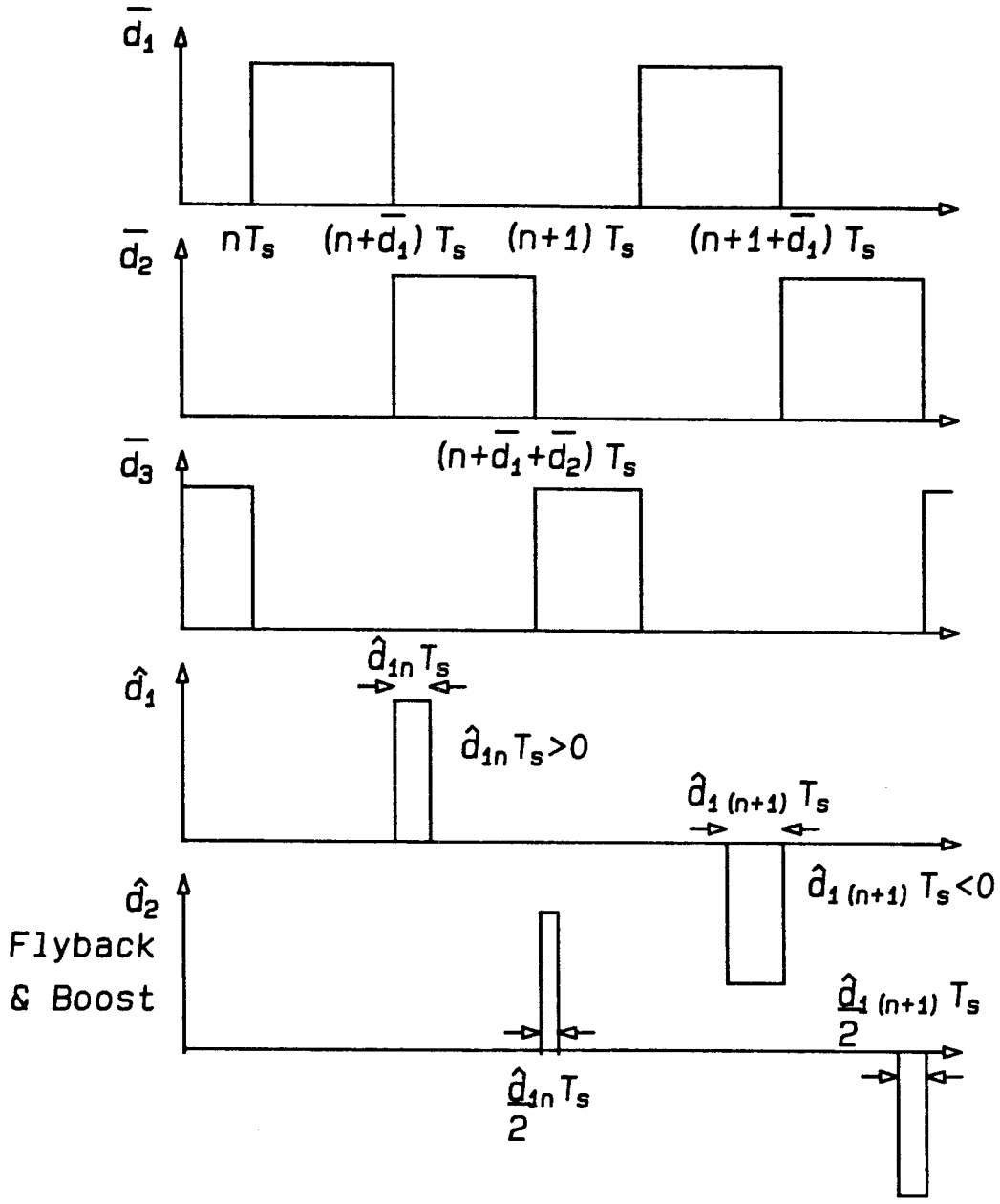

Fig. 2.6 The different switching functions required for the discrete modelling analysis. The top three show the steady state switching functions. The last two show the perturbation switching functions for the flyback and boost inverters. The buck and Cuk inverters require only $\hat{d}_1(t)$.

$$\dot{\bar{x}} = [\bar{d}_1 A_1 + \bar{d}_2 A_2 + \bar{d}_3 A_3]\bar{x} + [\bar{d}_1 b_1 + \bar{d}_2 b_2 + \bar{d}_3 b_3] V_g \tag{2.21}$$

The steady state values of the state variables can be calculated from that equation, and result in the same relations given in Section 1.4. The relevant equation to the stability analysis is the small signal one, and is obtained by subtracting Eq. (2.21) from Eq. (1.18). Furthermore, the perturbations are small, and the equations are linearized by elimination of products of perturbed terms.

$$\begin{aligned}\dot{\hat{x}} &= [\bar{d}_1 A_1 + \bar{d}_2 A_2 + \bar{d}_3 A_3]\hat{x} \\ &+ [\bar{d}_1 b_1 + \bar{d}_2 b_2 + \bar{d}_3 b_3]\hat{v}_g \\ &+ [(A_1 - A_2)\bar{x} + (b_1 - b_2) V_g]\hat{d}_1 \\ &+ [(A_2 - A_3)\bar{x} + (b_2 - b_3)]\hat{d}_2\end{aligned} \tag{2.22}$$

The switching functions $\hat{d}_1(t)$ and $\hat{d}_2(t)$ are narrow pulses occurring at $(n+D_1)T_s$ and $(n+D_1+D_2)T_s$ respectively, and so they are well approximated by two strings of delta functions that are properly weighted.

$$\hat{d}_1(t) \approx \hat{p}_1(t) = \sum_{n=-\infty}^{n=\infty} \hat{d}_{1n} T_s \delta[t-(n+D_1)T_s] \tag{2.23}$$

$$\hat{d}_2(t) \approx \hat{p}_2(t) = \sum_{n=-\infty}^{n=\infty} \hat{d}_{2n} T_s \delta[t-(n+D_1+D_2)T_s] \tag{2.24}$$

Substitution of Eq. (2.23) and (2.24) into Eq. (2.22) gives:

$$\dot{\hat{x}} = [\bar{d}_1 A_1 + \bar{d}_2 A_2 + \bar{d}_3 A_3]\hat{x}$$

$$+ [\bar{d}_1 \boldsymbol{b}_1 + \bar{d}_2 \boldsymbol{b}_2 + \bar{d}_3 \boldsymbol{b}_3]\hat{v}_g \tag{2.25}$$

$$+ [(\boldsymbol{A}_1 - \boldsymbol{A}_2)\bar{\boldsymbol{x}}[(n+D_1)T_s] + (\boldsymbol{b}_1 - \boldsymbol{b}_2)V_g]\hat{p}_1$$

$$+ [(\boldsymbol{A}_2 - \boldsymbol{A}_3)\bar{\boldsymbol{x}}[(n+D_1+D_2)T_s] + (\boldsymbol{b}_2 - \boldsymbol{b}_3)V_g]\hat{p}_2$$

This equation is then integrated over a whole switching period to yield a difference equation relating the perturbation at the beginning of a cycle to the perturbation at the beginning of the previous cycle. There are three regions of integration, the first of which is $[nT_s, (n+D_1)T_s)$. To maintain the causality of the system the first region does not include the time $(n+D_1)T_s$ as the delta function is a result of the perturbation in the state at that time and so cannot be an input to the system. The equation is quite simple as all switching functions in this region are equal to zero, except for $\bar{d}_1$ which is equal to one.

$$\dot{\hat{\boldsymbol{x}}} = \boldsymbol{A}_1 \hat{\boldsymbol{x}} + \boldsymbol{b}_1 \hat{v}_g \quad nT_s \le t < (n+D_1)T_s \tag{2.26}$$

The system is linear time-invariant in that region. As the stability of the system is under consideration, the input voltage modulation $\hat{v}_g$ can be set to zero without any loss of generality. The same applies to the two other regions. The result of the integration is:

$$\hat{\boldsymbol{x}}[(n+D_1)T_s] = e^{\boldsymbol{A}_1 D_1 T_s} \boldsymbol{x}[nT_s] \tag{2.27}$$

The second region of integration is $[(n+D_1)T_s, (n+D_1+D_2)T_s)$. All switching functions except $\bar{d}_2$ and $\hat{p}_1$ are equal to zero and the equation is:

$$\dot{\hat{\boldsymbol{x}}} = \boldsymbol{A}_2\hat{\boldsymbol{x}} + [(\boldsymbol{A}_1-\boldsymbol{A}_2)\bar{\boldsymbol{x}}+(\boldsymbol{b}_1-\boldsymbol{b}_2)V_g]\hat{d}_{1n}T_s\delta[t-(n+D_1)T_s] \tag{2.28}$$

$$(n+D_1)T_s \le t < (n+D_1+D_2)T_s$$

which gives:

$$\hat{\boldsymbol{x}}[(n+D_1+D_2)T_s] = e^{\boldsymbol{A}_2D_2T_s}\hat{\boldsymbol{x}}[(n+D_1)T_s] + e^{\boldsymbol{A}_2D_2T_s}\boldsymbol{K}_1T_s\hat{d}_{1n} \tag{2.29a}$$

$$\boldsymbol{K}_1 = (\boldsymbol{A}_1-\boldsymbol{A}_2)\bar{\boldsymbol{x}}[(n+D_1)T_s] + (\boldsymbol{b}_1-\boldsymbol{b}_2)V_g \tag{2.29b}$$

Finally in the last region of integration $[(n+D_1+D_2)T_s,\ (n+1)T_s)$ the only non-zero switching functions are $\bar{d}_3$ and $\hat{p}_2$.

$$\dot{\hat{\boldsymbol{x}}} = \boldsymbol{A}_3\hat{\boldsymbol{x}} + [(\boldsymbol{A}_2-\boldsymbol{A}_3)\bar{\boldsymbol{x}}+(\boldsymbol{b}_2-\boldsymbol{b}_3)V_g]\hat{d}_{2n}T_s\delta[t-(n+D_1+D_2)T_s] \tag{2.30}$$

$$(n+D_1+D_2)T_s \le t < (n+1)T_s$$

which gives:

$$\hat{\boldsymbol{x}}[(n+1)T_s] = e^{\boldsymbol{A}_3(1-D_1-D_2)T_s}\hat{\boldsymbol{x}}[(n+1)T_s] + e^{\boldsymbol{A}_3(1-D_1-D_2)T_s}\boldsymbol{K}_2T_s\hat{d}_{2n} \tag{2.31a}$$

$$\boldsymbol{K}_2 = (\boldsymbol{A}_2-\boldsymbol{A}_3)\bar{\boldsymbol{x}}[(n+1)T_s] + (\boldsymbol{b}_2-\boldsymbol{b}_3)V_g \tag{2.31b}$$

Equations (2.28) and (2.29a) are substituted into Eq. (2.31a) to give the difference equation:

$$\hat{\boldsymbol{x}}[(n+1)T_s] = e^{\boldsymbol{A}_3(1-D_1-D_2)T_s}\hat{\boldsymbol{x}}[(n+1)T_s] + e^{\boldsymbol{A}_3(1-D_1-D_2)T_s}e^{\boldsymbol{A}_2D_2T_s}\boldsymbol{K}_1T_s\hat{d}_{1n}$$

$$+ e^{\boldsymbol{A}_3(1-D_1-D_2)T_s}\boldsymbol{K}_2T_s\hat{d}_{2n} \tag{2.32}$$

The difference equation is linear and shift invariant, which is equivalent to a differential equation being linear time invariant. The z-transform is applied to that equation to give the transformed equation in

the z-domain:

$$\hat{X}(z) = (zI-M_1)^{-1}M_2K_1T_s\hat{D}_1(z) + (zI-M_1)^{-1}M_3K_2T_s\hat{D}_2(z)$$

$$+ (zI-M_1)^{-1}z\hat{\boldsymbol{x}}(0) \tag{2.33}$$

$$M_1 = e^{A_3(1-D_1-D_2)T_s}e^{A_2D_2T_s}e^{A_1D_1T_s}$$

$$M_2 = e^{A_3(1-D_1-D_2)T_s}e^{A_2D_2T_s}$$

$$M_3 = e^{A_3(1-D_1-D_2)T_s}$$

The introduction of current programming creates a relation between $\hat{d}_{1n}$ and the programmed current. For all converters let the programmed current be the coupled-inductor current and assume that it is the first element of the state vector.

$$\hat{\boldsymbol{x}}(nT_s) = \begin{bmatrix} \hat{i}_L \\ - \end{bmatrix} \tag{2.34}$$

The bar in the state vector indicates that there can be any number of states, but that they will not come into the calculations. From the waveforms in Fig. 5, it can be seen that the relation between the duty ratio perturbation and the current perturbation is:

$$\hat{d}_{1n} = -H_e^T\hat{\boldsymbol{x}}(nT_s) = \left[\frac{-1}{m_1T_s} \quad 0_{m-1}^T\right]\hat{\boldsymbol{x}}(nT_s) \tag{2.35}$$

where m_1 is the slope of the current during period d_1T_s, and 0_{m-1} is a zero vector of order $m-1$ and m is the order of the inverter under consideration. In the z-domain the relation is:

$$\hat{D}_1(z) = -H_e^T \hat{X}(z) \tag{2.36}$$

Equation is substituted in Eq. (2.33) in conjunction with Eq. (2.14a) for the boost, and flyback inverters and Eq. (2.14b) for the buck and Ćuk inverters to yield the relations between the duty ratio and a perturbation at the origin ($\hat{x}(0)$).

$$\hat{D}_1(z) = \frac{-H_e^T(zI-M_1)^{-1}z\hat{x}(0)}{1+H_e^T(zI-M_1)^{-1}\left[M_2K_1T_s+\dfrac{M_3K_2T_s}{2}\right]} \tag{2.37a}$$

$$\hat{D}_1(z) = \frac{-H_e^T(zII-M_1)^{-1}z\hat{x}(0)}{1+H_e^T(zII-M_1)^{-1}M_2K_1T_s} \tag{2.37b}$$

The quantities M_1 and M_2 contain the information about the low frequency behavior of of the system. As the instability in the current programmed loop manifests itself at frequencies close to half the switching frequency, the effect of the low frequency dynamics can be neglected and so the M matrices are approximated by the identity matrix. From Eq. (2.29b) and (2.31b) it is clear that K_1 and K_2 are the differences between the slopes of the states before and after the switching times $[(n+D_1)T_s]$ and $[(n+D_1+D_2)T_s]$ respectively.

$$K_1 = \begin{bmatrix} m_1+m_2 \\ - \end{bmatrix} \qquad K_2 = \begin{bmatrix} -m_2-m_3 \\ - \end{bmatrix} \tag{2.38}$$

The loop gains are given by:

$$T(z) = H_e^T(zII-M_1)^{-1}\left[M_2K_1T_s+\frac{M_3K_2T_s}{2}\right] \tag{2.39a}$$

$$T(z) = H_e^T(zII - M_1)^{-1}M_2K_1T_s \tag{2.39b}$$

Substitution of Eq. (2.38) and application of the high frequency approximation to Eq. (2.39a) and (2.39b) gives the loop gains.

$$T(z) = \left[1 + \frac{m_2 - m_3}{2m_1}\right] \frac{1}{z-1} \tag{2.40a}$$

$$T(z) = \left[1 + \frac{m_2}{m_1}\right] \frac{1}{z-1} \tag{2.40b}$$

In the z-domain the stability criterion for a closed loop causal system is that the poles must lie within the unit circle [15]. The closed loop pole z_p satisfies the condition $T(z) = -1$ and can be easily evaluated from the last equations.

$$z_p = \frac{m_2 - m_3}{2m_1} \tag{2.41a}$$

$$z_p = \frac{m_2}{m_1} \tag{2.41b}$$

In the case of the boost and flyback converters the pole is at the origin if the two slopes m_2 and m_3 are equal. This condition is satisfied only in the case of lossless inverters. However, even in practical cases, the difference between the slopes is very small as it is of the order of the parasitic voltage drops in the circuit and they are always much smaller than the input voltage. Thus ideally these inverters reject the disturbance in one cycle which is the same result as obtained by the simple geometrical analysis of Section 2.3.1.

It is of interest to note that solving the difference equation (2.32) is actually exactly the same process as the geometrical analysis. Thus the geometrical analysis, although outwardly simple minded, is in effect a true reflection of a more complicated mathematical analysis, and so may be used with confidence to get an accurate and quick idea about the stability of such systems.

The buck and Ćuk inverters, as mentioned before, behave similarly to their corresponding 2SN converters with current programming. There is a potential instability at half the switching frequency as the closed loop pole is equal to the ratio between slopes that are of the same order. Equation (2.41b) may be rewritten as:

$$z_p = \frac{m_2}{m_1} = \frac{D_1}{|D_2 - D_3|} \tag{2.42}$$

Thus D_1 has to be less than $|D_2 - D_3|$ which is the same condition obtained in Section 2.3.1, if one takes into account that the dc values for the duty ratios here simply represent the maximum values of the time varying duty ratios used in Section 2.3.1.

2.4 Advantages and Disadvantages of Current Programming

The application of current programming in an independent loop in the 3SN converters results in several advantages. As far as the use of these circuits as inverters is concerned one of the main advantages is the linearity of the steady state control to output characteristics. The steady state relations for the converter in CRP are given by Eq. (2.3). To obtain a sinusoidal output, let:

$$d_3 - d_2 = d_m \cos \omega_m t \tag{2.43}$$

so that

$$v = I_{ref} R d_m \cos \omega_m t \tag{2.44}$$

in which the effect of the output capacitor has been temporarily neglected. Under ideal conditions of no current ripple the output is purely sinusoidal for a sinusoidal control input, and the linearity of the steady state control gain is the result of the current reference programming. This analysis will be made exact in Chapter 3. This relation between output voltage and duty ratio is inherently linear, in contrast to a flyback converter: $v_o = v_g d / d'$, which is inherently non-linear. Residual non-linearity in the new inverter is a result of the actual non-zero current ripple being a function of the output voltage, and it is a second-order effect that can be reduced by proper design. The linearity of the steady state control gain is the reason for the low harmonic content of the output waveform. The CRP has other advantages: single-pole small-signal dynamics and fast pulsed-load response. The small-signal response can be obtained by analyzing the circuit by state-space averaging, but a simple argument as follows shows that it should be a first-order response. The normal converter has two independent states: the inductor current and the capacitor voltage. In the CRP inverter the inductor current is constrained and ceases to be an independent state, and so the order of the system is reduced to one. This is borne out both by more exact analysis and by measurement.

The explanation for the fast pulsed-load response is equally simple. The current in the inductor is maintained at its maximum value even at small loads. When the load is pulsed the control circuitry increases the duty ratio by an equivalent amount. The extra energy required by the load is already stored in the inductor, and the speed of response is limited only by the RC network and the control circuitry. The waveforms in Fig. 7 show the response of the converter to pulsed loads. The inverter is operated as a dc-to-dc converter to avoid problems of synchronization of the waveforms due to the large difference in time bases between the switching frequency and the inversion frequency. In the case of operation as an inverter the results will be the same as the difference in frequencies decouple the two effects.

A converter in CRP mode has an inherent over-current protection, as the maximum current in the inductor is fixed and if there is overload the converter will simply shut itself down. One final advantage is that since the relation between the output voltage and the control variables are decoupled from the input section, it is possible to use that type of converter for independent multiple output applications. This use of the inverters will be discussed in depth in a later chapter.

One of the principal disadvantages of the application of current programming in these inverters is a reduction in the efficiency. The current in the inductor remains at or close to the reference value at all times, thus at small loads or when the output voltage is low the losses in the switches and the inductor parasitic resistance remain the same as when the inverter is at full load or peak output voltage. There is a certain trade-off involved as a small inductor with a big current ripple will result

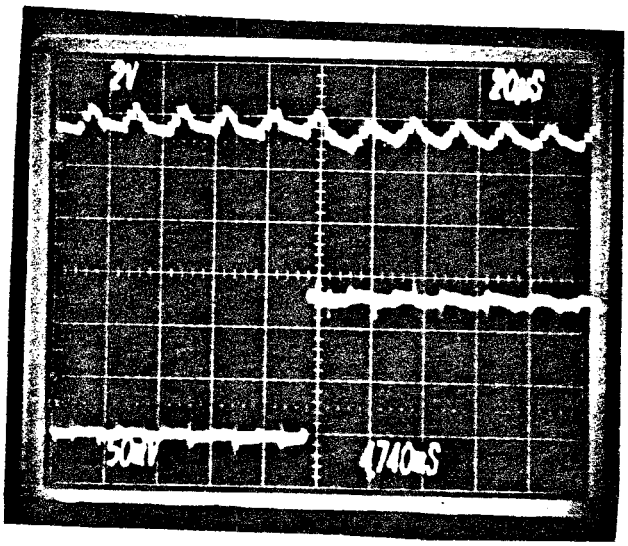

Fig. 2.7 The scope photograph shows the load current and voltage for a pulsed load. The load goes from 30% to full load. The top trace is the voltage which is regulated by a proportional feedback loop. The bottom trace is the current. It is clear that the current reaches full load within one switching cycle represented by three different slopes on the voltage trace.

in more efficient operation but would incur a price in output distortion as can be seen in the next chapter. The efficiency consideration is important in choosing of the value of I_{ref} for a given application.

The second disadvantage of CRP is apparent from Eq. (2.44) as the output voltage is a function of the load. This is in contrast to the 2SN converters where the output voltage is load dependent only as a second order effect due to the parasitics in the circuit. The 3SN inverters are dependent to first order on the load, and so the duty ratio of the output switches regulates the output for load variations. Care must be taken in

the design to ensure proper operation of the inverter under all load conditions. Once more the choice of the value of I_{ref} is crucial in the design stage to guarantee correct operation under different conditions.

2.5 Conclusions

The current reference loop has been analysed in this chapter. The mechanics of its operation as compared to the operation of standard 2SN converters were described. The question of stability was investigated in two different methods. The simple geometrical approach was found to be equivalent to solving the difference equation of the system, thus one can be confident in the application of this method to determine the stability of the CRP loop. The flyback and boost inverters were found to be stable and to require no compensating ramp thus simplifying the design of the control loop. The buck and Ćuk inverters however behave like their 2SN counterparts and require the compensating ramp. The inverters all have linear control to output characteristics, to first-order, as well as a reduction in the number of poles of the system and very fast pulsed-load response. In the next chapter the analysis for the output section is refined to include the dynamics of the output capacitor as well as those of the inductor.

CHAPTER 3

Analysis of Single-Phase Inverters

3.1 Introduction

The analysis of dc-to-dc converters starts from the state-space description of the converter. The converter is assumed to have a dc operating point and that there are some small-signal perturbations applied to the system. The dc operating point is obtained from the state-space equation and the states are perturbed around that operating point thus yielding the small-signal response of the converter. However, this cannot be done in inverter analysis as the steady-state operating point is large-signal ac. Hence, a different approach must be considered.

There are several different ways to analyze dc-to-ac inverters. It is possible, for instance, to rewrite the states of the inverter as a power series expansion with respect to some small parameter and thus to be able to solve a set of linear differential equations. Another method, that is used to analyze three-phase systems, is to transform the system to a rotating frame of reference where the steady-state terms appear as dc terms, and thus one is able to apply perturbational techniques as in dc-to-dc converters. However, the latter is not applicable to single-phase inverters, as will be seen in Section 3.2.1. Hence, for single-phase inverter analysis, the only possibility is to apply some other non-linear analysis technique, the one used here being the power expansion method.

The analysis follows basically the same steps for all the different inverters, and so is done in detail for the flyback inverter only. The differential equations for the other inverters are set up and the solutions are given without going through the detailed algebra. The experimental verification is performed on the flyback and the boost inverters. It is seen that the results of the analysis are very closely matched by the experimental measurements.

3.2 Analysis of Single-Phase Inverters

Dc-to-dc converters have time-varying terms that are usually assumed to be small. Thus it is possible to study the behavior of the system around a steady-state operating point. The inverters, however, by the nature of their operation, are time-varying in a large signal sense, that is, the steady-state is itself time varying. Thus the system needs to be tackled in a different manner. One method that is very attractive to use, because it gives a small-signal response as well as a steady-state response, and that has been successfully applied to polyphase inverters is the abc-ofb transformation [1]. This transformation is applied to the system under consideration to transform it to a rotating frame of reference where the component of the output at the inversion frequency appears as a complex dc quantity. In Chapter 4 there is a more complete discussion of this method, but in this section it is shown to be inapplicable to single-phase systems.

Let the system under consideration be described by its impedance matrix:

$$\boldsymbol{v} = \boldsymbol{Z}\boldsymbol{i} \tag{3.1}$$

where $\boldsymbol{v}$ and $\boldsymbol{i}$ are n^{th} order vectors and Z is the impedance matrix of order $n \times n$. The transformation must satisfy two conditions for the transformed system to have a physical meaning: it should maintain the impedance relation as it is, and it should also preserve the power in the system [16]. The power is defined as:

$$p = \boldsymbol{i}^{*}\boldsymbol{v} \tag{3.2}$$

where $\boldsymbol{i}^{*}$ indicates the conjugate transpose of $\boldsymbol{i}$. Let T be a transformation such that:

$$\boldsymbol{v} = T\boldsymbol{v}' \tag{3.3}$$

and

$$\boldsymbol{i} = T\boldsymbol{i}' \tag{3.4}$$

in which $\boldsymbol{i}'$ and $\boldsymbol{v}'$ are both dc quantities in the new frame of reference. Thus in that frame of reference the impedance matrix is:

$$Z' = T^{-1}ZT \tag{3.5}$$

and the power is given by:

$$p = (T\boldsymbol{i}')^{*}T\boldsymbol{v}' = \boldsymbol{i}'^{*}(T^{*}T)\boldsymbol{v}' = \boldsymbol{i}'^{*}\boldsymbol{v}' \tag{3.6}$$

Thus to satisfy the two conditions cited above the transformation T must be unitary, that is $T^{*}T = I$, the identity matrix. Hence arises the contradiction, for the power p as given in Eq. (3.2) is time varying and the one given in Eq. (3.6) is constant as both $\boldsymbol{i}'$ and $\boldsymbol{v}'$ are dc in the new

frame of reference. So either T is non-unitary and the transformed system has no physical meaning, or i' and v' are time varying which defeats the purpose of the transformation.

Hence it is not possible to use the abc-ofb transformation method in single-phase systems or in non-constant power systems generally. This result rules out the use of such methods as the Canonical Circuit Model for the analysis of the inverters. It is however possible to obtain the canonical circuit model for the 3SN converters when operated as dc-to-dc converters. It would seem useful to do this so as to calculate the loop gain of the current programmed loop. However, the loop gain as calculated from this model is only valid at low frequencies. In the following analysis it is seen that the current loop is not treated as a low frequency loop that regulates the current but as a high frequency loop that sets a fixed value of current at certain times within each cycle and on a cycle per cycle basis.

Thus as far as the analysis of the single-phase inverters is concerned the value of the current loop gain is of minor importance, and the characteristic of interest is that the current actually reaches I_{ref} in the allowed period, which is guaranteed by the conditions for correct operation as defined in Chapter 2. It is still of interest to note that the calculation of the loop gain, from the canonical circuit model, shows that the dc value of the gain is proportional to K where

$$K = \frac{2L}{RT_s}$$

is a "conduction parameter" whose value determines whether the converter operates in continuous or discontinuous conduction mode [17], and to

which the low-frequency current-loop gain in current-programmed 2SN converters is also proportional [11,12].

This analysis is not done here because it hides the cycle by cycle nature of the operation of the current loop, which can be looked at as a constraint on the inductor state rather than a regulation of its value at all times. The difference between the two is rather subtle and resides in the fact that the current loop is not a continuous system but a discrete one. However, once it is assumed that the current reaches I_{ref} at the end of d_1 the differential equations of the system become simple to solve, as there is a fixed initial value for the current in every cycle. This is used in the next section to calculate the output voltage of the flyback inverter.

3.3 Analysis of Flyback Inverter with CRP

In this section the analysis is done with a current loop gain that is finite, which means the droop in the inductor current has to be taken into account. The analysis is done by a power series expansion method that results in a time-domain expression for the output voltage [2]. This expression shows that the inverter behaves essentially as a first-order system and it also gives an estimate for the harmonic content of the output waveforms.

The analysis begins from Eq.(1.18) which is the general state-space description of the 3SN inverters. The state vector for the flyback inverter (Fig. 1(a)) is:

$$\boldsymbol{x} = \begin{bmatrix} i \\ v \end{bmatrix} \tag{3.7}$$

The state matrices $\boldsymbol{A}_1$, $\boldsymbol{A}_2$, $\boldsymbol{A}_3$, are obtained from each of the switched

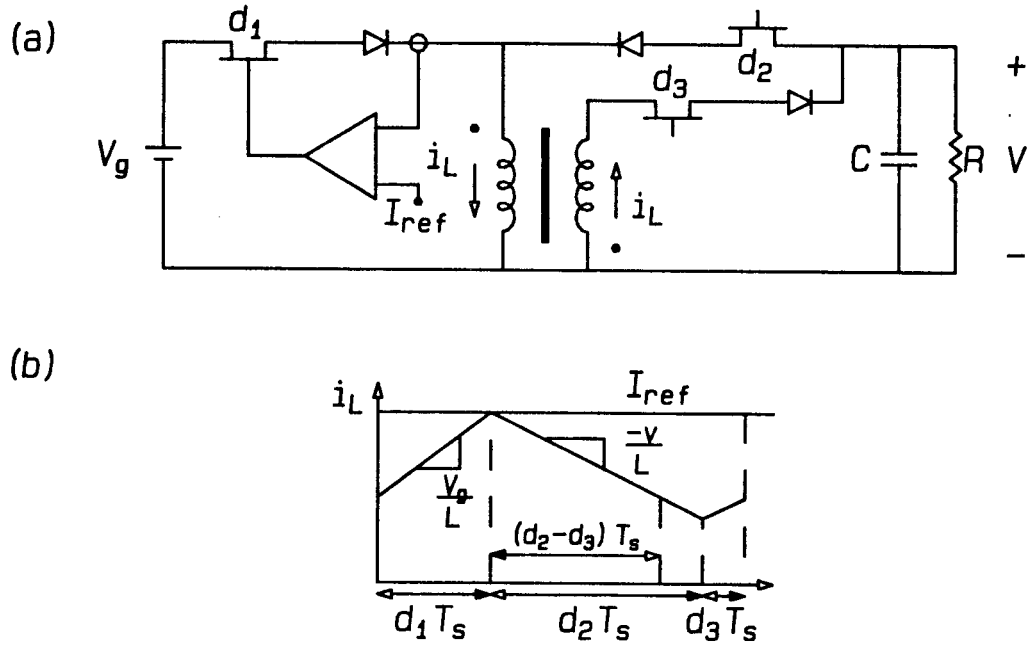

Fig. 3.1 (a) The flyback single-phase coupled inductor inverter with the current programming loop. (b) The inductor current shown as a single rectified current. The different switching intervals are shown, as are the various current slopes.

networks of the inverter which gives, in the case of the flyback inverter,

$$\boldsymbol{A}_1 = \begin{bmatrix} 0 & 0 \\ 0 & -1/R \end{bmatrix} \quad \boldsymbol{A}_2 = \begin{bmatrix} 0 & 1 \\ -1 & -1/R \end{bmatrix} \quad \boldsymbol{A}_3 = \begin{bmatrix} 0 & -1 \\ 1 & -1/R \end{bmatrix} \tag{3.8}$$

and the input vectors are:

$$\boldsymbol{b}_1 = \begin{bmatrix} 1 \\ 0 \end{bmatrix} \quad \boldsymbol{b}_2 = \begin{bmatrix} 0 \\ 0 \end{bmatrix} \quad \boldsymbol{b}_3 = \begin{bmatrix} 0 \\ 0 \end{bmatrix} \tag{3.9}$$

The above equations are substituted in Eq.(1.18), and the time varying switching functions are replaced by the equivalent duty ratio. The last step constitutes the state-space averaging step where the state variables under consideration are no longer the actual state variables but their average value during a cycle. The main assumption made is that of

small ripple in the states, and it is mainly justified for the low frequency characterization of the inverter, that is, when the frequencies under consideration are well below the switching frequency. Thus the *state-space averaged equation* of the flyback inverter is:

$$\begin{bmatrix} L & 0 \\ 0 & C \end{bmatrix} \begin{bmatrix} \dot{i}_L \\ \dot{v} \end{bmatrix} = \begin{bmatrix} 0 & -(d_3-d_2) \\ d_3-d_2 & -1/R \end{bmatrix} \begin{bmatrix} i_L \\ v \end{bmatrix} + \begin{bmatrix} d_1 \\ 0 \end{bmatrix} V_g \tag{3.10}$$

To develop a sinusoidal output voltage let:

$$d_3-d_2 = d_m \cos \omega_m t \tag{3.11}$$

Because of the current programming, the initial value of the current is known and the exact averaged inductor current is given by:

$$i_L = I_{ref} - v \frac{d_m \cos \omega_m t \, T_s}{2L} \tag{3.12}$$

where T_s is the switching period.

The above result is obtained by use of the straight-line approximation of the current waveform, which arises from the difference between the converter time constants and the switching period. Thus the slope of the current is assumed to be simply proportional to the applied voltage divided by the inductor value (Fig. 1(b)). The remaining equation to be solved is that for the output voltage which is obtained by substitution of Eqs.(3.11) and (3.12) into (3.10):

$$\frac{1}{\omega_p} \dot{v} + v(1+\varepsilon) = I_{ref} R d_m \cos \omega_m t - \varepsilon v \cos 2\omega_m t \tag{3.13}$$

where

$$\omega_p = \frac{1}{RC}$$

and

$$\varepsilon = \frac{d_m^2 R T_s}{4L}$$

The solution for the voltage can be written as an expansion in powers of ε:

$$v = v_0 + \varepsilon v_1 + \varepsilon^2 v_2 + \cdots \tag{3.14}$$

and substitution into Eq.(3.13) gives:

$$\frac{1}{\omega_p}(\dot{v}_0 + \varepsilon \dot{v}_1 + \varepsilon^2 \dot{v}_2 + \cdots) + (v_0 + \varepsilon v_1 + \varepsilon^2 v_2 + \cdots)(1+\varepsilon) =$$

$$I_{ref} R d_m \cos \omega_m t - \varepsilon(v_0 + \varepsilon v_1 + \varepsilon^2 v_2 + \cdots)\cos 2\omega_m t \tag{3.15}$$

Thus there results a linear differential equation for each of the powers of ε. Only the equations for the first two powers of ε need be solved as ε is small. The equation for the zeroeth order of ε is:

$$\frac{1}{\omega_p}\dot{v}_0 + v_0(1+\varepsilon) = I_{ref} R d_m \cos \omega_m t \tag{3.16}$$

This equation is easily solved and $v_0(t)$ in the steady-state is given by:

$$v_0 = \frac{I_{ref} R d_m}{\sqrt{(1+\varepsilon)^2 + (\omega_m / \omega_p)^2}} \cos\left(\omega_m t - \tan^{-1}\frac{\omega_m}{(1+\varepsilon)\omega_p}\right) \tag{3.17}$$

The differential equation for the first order of ε is:

$$\frac{1}{\omega_p}\dot{v}_1 + v_1(1+\varepsilon) = -v_0 \cos(2\omega_m t) \tag{3.18}$$

The result for v_0 given by Eq.(3.17) is substituted in the above equation. The term on the right-hand side contains both a fundamental and third-harmonic component of the inversion frequency. Thus there are no even harmonics generated by this inverter, because inclusion of higher orders of epsilon result in the generation of higher orders of odd harmonics only. The equation is solved and gives the expression for v_1.

$$v_1 = \frac{-I_{ref} R d_m}{2\sqrt{(1+\varepsilon)^2+(\omega_m/\omega_p)^2}}\left[\frac{1}{\sqrt{(1+\varepsilon)^2+(\omega_m/\omega_p)^2}}\cos(\omega_m t)\right. \tag{3.19}$$

$$\left. + \frac{1}{\sqrt{(1+\varepsilon)^2+(3\omega_m/\omega_p)^2}}\cos(3\omega_m t - \tan^{-1}\frac{\omega_m}{(1+\varepsilon)\omega_p} - \tan^{-1}\frac{3\omega_m}{(1+\varepsilon)\omega_p})\right]$$

Equation (3.19) is then multiplied by ε and added to Eq. (3.17) to give the output voltage. Some algebraic manipulation is needed to put the expression in a useful form.

$$v = \frac{I_{ref} R d_m}{\sqrt{(1+\varepsilon)^2+(\omega_m/\omega_p)^2}}$$

$$\times\left[\frac{\sqrt{(1+\varepsilon/2)^2+(\omega_m/\omega_p)^2}}{\sqrt{(1+\varepsilon)^2+(\omega_m/\omega_p)^2}}\cos(\omega_m t - \tan^{-1}\frac{\omega_m}{(1+\varepsilon/2)\omega_p})\right. \tag{3.20}$$

$$\left. + \frac{\varepsilon/2(1+\varepsilon)}{\sqrt{(1+\varepsilon)^2+(3\omega_m/\omega_p)^2}}\cos(3\omega_m t - \tan^{-1}\frac{\omega_m}{(1+\varepsilon/2)\omega_p} - \tan^{-1}\frac{3\omega_m}{(1+\varepsilon)\omega_p})\right]$$

The above result shows that the response of the system is basically of the first order. The departure from a pure first order response is proportional to ε, which is usually kept very small by design. This supports the result obtained in Chapter 2 by the argument of state independence. The high linearity of the inverter is also demonstrated by the above equation, as the main part of the voltage amplitude is proportional to d_m, and the non-linearities are all of order ε.

In Eq. (3.20), to first order, the amplitude of the fundamental inversion frequency component is independent of ε, and that of the third harmonic is proportional to ε. Therefore, to keep the distortion low, it is desirable to make ε as small as possible.

The parameter ε is an important indicator of the performance of the circuit. If ε is zero, the nonlinear effects disappear and the result reverts to the ideal case of Eq. (2.45), except with the addition of the RC dynamics previously omitted.

It is of interest to note that the parameter ε can be written

$$\varepsilon = \frac{d_m^2}{2K}$$

Therefore, small ε and consequent low distortion is achieved by making the modulation amplitude d_m small, and by making the CRP loop gain large. This is the same as saying that a large K makes a high CRP loop gain and makes the operation of the converter more ideal because the average inductor current approaches more closely its reference value.

The value of d_m controls the output voltage and so cannot be freely used to satisfy the distortion requirements. However, there is a trade-off between I_{ref} and d_m, as the output voltage is proportional to each

of them, so d_m can be made smaller by increasing I_{ref} for a given output voltage. As ε is proportional to d_m^2, a value of d_m may exist that satisfies both the output voltage and the distortion requirements. As an example, the circuit built for experimental verification (discussed in Section 3.5), with L=1mH, R=25Ω, T_s=16μsec and I_{ref}=0.7$Amps$, has a d_m=0.3 for an output voltage of 5 volts, which gives ε=0.01.

One of the disadvantages of CRP is the dependence of the converter gain, cutoff frequency and harmonic content on the load resistance. However, as an increase in R implies a proportional decrease in d_m, for the same output voltage, that translates to a net reduction of the distortion. Hence the designer should take the full load case into account for calculations of the inverter parameters that satisfy both specifications. The variation of the cutoff frequency cannot be controlled, but as the inverter has a single pole there is no problem of stability, as is demonstrated by the pulsed-load test (Fig. 7 in Ch. 2). However, if the pole moves in such a way that ω_p becomes smaller than ω_m the gain is reduced such that the output is no longer regulated. The design has to take the worst case load into account.

3.4 Analysis of the Buck and Boost Inverters

The analysis of these inverters is very close to that performed for the flyback inverter. There are some minor differences as far as setting up the differential equations is concerned. This results in different expressions for the output voltages for each inverter, hence it is of interest to point out where the discrepancies occur. The main difference appears in the expression used for the slope of the current which is not the same for

each inverter.

3.4.1 Analysis of the Buck Inverter

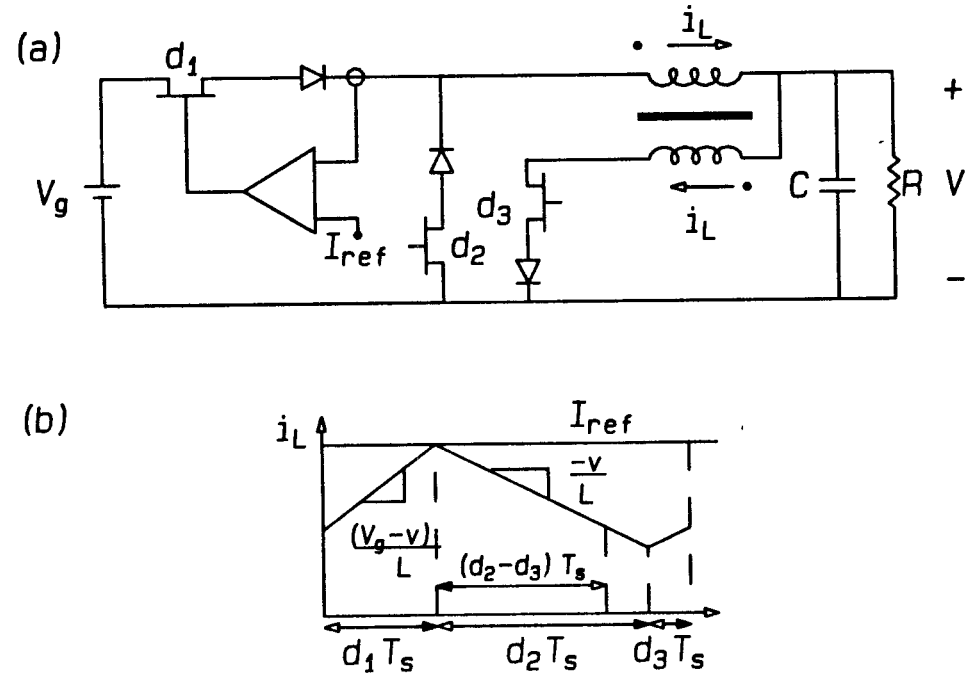

Fig. 3.2 (a) The buck single-phase coupled inductor inverter with the current programming loop. (b) The inductor current shown as a single rectified current. The different switching intervals are shown, as are the various current slopes.

The current ripple in the buck inverter (Fig. 2(a)) is proportional to the output voltage during the period d_2-d_3 (Fig. 2(b)). The expression for the current then becomes:

$$i_L = I_{ref} - v\frac{(d_2-d_3)\,T_s}{2L} \tag{3.21}$$

which contrasts with that given for the flyback inverter by Eq. (3.12). The analysis is not as straightforward as for the flyback since d_2-d_3 is not the effective duty ratio, that being $d_1+d_2-d_3$. Hence a relation must be found between those two values. A steady-state relation is given by the voltage

equation in Table I:

$$v = V_g \frac{d_1}{(d_1+d_2-d_3)} \tag{3.22}$$

This equation assumes zero slope in the *average* inductor current. However, this approximation is justified as it is applied only to a second-order effect and is thus a third-order approximation. Equation (3.22) is used in conjunction with the equation for the effective duty ratio:

$$d_1+d_2-d_3 = d_m \cos\omega_m t \tag{3.23}$$

to give:

$$d_2-d_3 = \left[\frac{v}{V_g}\right] d_m \cos\omega_m t \tag{3.24}$$

The state-space averaged equation for the buck inverter is similar to the one of the flyback inverter although they differ in the definition of the effective duty ratios.

$$\begin{bmatrix} L & 0 \\ 0 & C \end{bmatrix} \begin{bmatrix} \dot{i}_L \\ \dot{v} \end{bmatrix} = \begin{bmatrix} 0 & -(d_m \cos\omega_m t) \\ d_m \cos\omega_m t & -1/R \end{bmatrix} \begin{bmatrix} i_L \\ v \end{bmatrix} + \begin{bmatrix} d_1 \\ 0 \end{bmatrix} V_g \tag{3.25}$$

The application of the equation for the current (Eq. (3.21)) with Eq. (3.24) to the state equation (Eq. (3.25)) gives the differential equation for the output voltage.

$$\frac{1}{\omega_p}\dot{v} + v(1+\varepsilon) = I_{ref} R d_m \cos\omega_m t - \varepsilon v \cos 2\omega_m t$$

$$+ \varepsilon v\left[\frac{v}{V_g}\right](1+\cos 2\omega_m t) \tag{3.26}$$

The power series expansion for v is substituted in Eq. (3.26), and the resulting differential equation for v_0 is the same as Eq. (3.16). The equation for v_1 is:

$$\frac{1}{\omega_p}\dot{v}_1 + v_1(1+\varepsilon) = -v_0 \cos(2\omega_m t) + \frac{v_0^2}{V_g}(1+\cos 2\omega_m t) \tag{3.27}$$

The above equation contains the same term on the right-hand side as Eq. (3.19), in addition to two terms that are proportional to v_0^2. The latter terms generate a dc voltage, a second harmonic and a fourth harmonic in the output. The resulting expression for the output voltage is:

$$v = \frac{I_{ref} R d_m}{\sqrt{(1+\varepsilon)^2+(\omega_m/\omega_p)^2}}\left[v_{o\,flyback} + v_{1\,flyback}\right] \tag{3.28}$$

$$+ \frac{(I_{ref} R d_m)^2 \varepsilon}{2 V_g[(1+\varepsilon)^2+(\omega_m/\omega_p)^2]}\left[1 + \tfrac{1}{2}\cos\left(2\tan^{-1}\frac{\omega_m}{(1+\varepsilon)\omega_p}\right)\right.$$

$$\left. + 2\cos\left(2\omega_m t - \tan^{-1}\frac{\omega_m}{(1+\varepsilon)\omega_p}\right) + \tfrac{1}{2}\cos\left(4\omega_m t - 2\tan^{-1}\frac{\omega_m}{(1+\varepsilon)\omega_p}\right)\right]$$

As for the flyback inverter the harmonics are all of order ε and can thus be made very small by proper design of the inductor or by choosing a sufficiently large switching frequency. Furthermore it is possible to reduce the dc offset in the output to zero by biasing the duty ratio modulation slightly.

The Ćuk inverter output section is similar to the buck converter. The analysis yields results that are the same as far as the harmonic content of the waveforms is concerned. However, the Ćuk inverter in its present form has a 4SN mode of operation without the addition of extra switches. Hence, it requires fairly detailed analysis that is beyond the scope of this thesis and so it is left for future work.

3.4.2 Analysis of the Boost Inverter

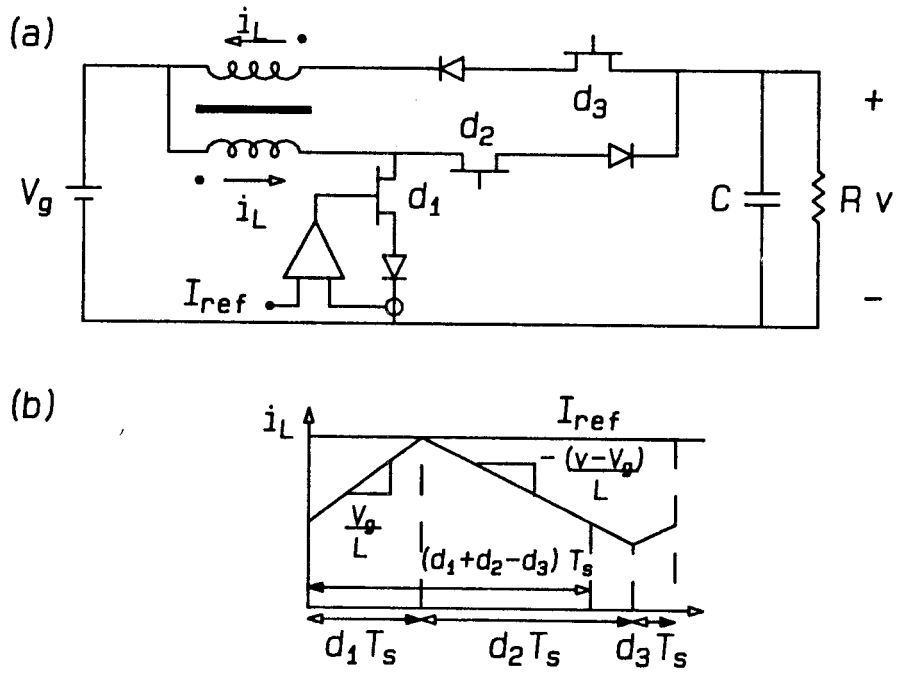

Fig. 3.3 (a) The boost single-phase coupled inductor inverter with the current programming loop. (b) The inductor current shown as a single rectified current. The different switching intervals are shown, as are the various current slopes.

The boost inverter shown in Fig. 3(a) has a current slope during the period d_2-d_3 that is proportional to $(v-V_g)$ (Fig. 3(b)). Thus the average inductor current is given by:

$$i_L = I_{ref} - (v - V_g)\frac{(d_2 - d_3)T_s}{2L} \tag{3.29}$$

Since $d_2 - d_3$ is the effective duty ratio of this inverter the analysis proceeds from this point in the same manner as for the flyback inverter. The state-space averaged equation of the boost inverter is:

$$\begin{bmatrix} L & 0 \\ 0 & C \end{bmatrix} \begin{bmatrix} \dot{i}_L \\ \dot{v} \end{bmatrix} = \begin{bmatrix} 0 & -(d_m \cos\omega_m t) \\ d_m \cos\omega_m t & -1/R \end{bmatrix} \begin{bmatrix} i_L \\ v \end{bmatrix} + \begin{bmatrix} d_1 + d_m \cos\omega_m t \\ 0 \end{bmatrix} V_g \tag{3.30}$$

Substitution of Eq. (3.29) into the state equation (Eq.(3.30)) results in the following differential equation for the output voltage:

$$\frac{1}{\omega_p}\dot{v} + v(1+\varepsilon) = I_{ref} R d_m \cos\omega_m t - \varepsilon(v - V_g)\cos 2\omega_m t + \varepsilon V_g \tag{3.31}$$

Once more the voltage is expanded as a power series in ε. The result for the zeroeth order of ε is the same as Eq. (3.16). The equation for v_1 is:

$$\frac{1}{\omega_p}\dot{v}_1 + v_1(1+\varepsilon) = -(v_0 - V_g)\cos(2\omega_m t) + V_g \tag{3.32}$$

This equation gives a good idea of what the output looks like; for example, there will be even harmonics, mainly the second harmonic in this case as well as some dc offset. Thus the harmonic content of the output is bigger than that of the flyback as it contains even harmonics. The rest of the analysis is the same as before except for some difference in the algebra which is not significant enough to be mentioned here. The output voltage for the boost inverter is given by:

$$v = v_{flyback} + \frac{\varepsilon}{(1+\varepsilon)}V_g + \frac{\varepsilon V_g}{\sqrt{(1+\varepsilon)^2+(2\omega_m/\omega_p)^2}}\cos(2\omega_m t - \tan^{-1}\frac{2\omega_m}{(1+\varepsilon)\omega_p}) \quad (3.33)$$

where $v_{flyback}$ is the voltage of a flyback inverter as given by Eq. (3.20).

There are fewer harmonics in the boost inverter than in the buck inverter. However that is not to say that the total harmonic content of the one is necessarily smaller than the other, it is possible that for certain operating conditions the buck inverter has a smaller harmonic content. However, it is clear that the flyback inverter is the one with the smallest harmonic content of all. The main reason for this is that the output in the flyback is totally decoupled from the input voltage, whereas in the buck and, to a lesser extent, in the boost, the input voltage affects the output as there is a direct connection via the inductor.

3.5 Experimental Verification

A flyback and a boost single-phase inverter were built for experimental verification of the theoretical results obtained in the previous sections. The generation of gate (or base) drive waveforms is not as straightforward as in regular PWM converters because of the gain dependence on (d_3-d_2), while at the same time the length of d_1 is not constant. Before proceeding to the actual measurements some discussion of the control circuit is necessary.

3.5.1 Practical Considerations

The generation of the gate (or base) drive waveforms in 2SN converters is fairly straightforward as there is only one controlled switch in the circuit. The input signal is compared to a fixed frequency ramp. The transistor is then turned off when the two signals are equal. The new period starts when the ramp resets, hence, the total length of the period is constant.

However, the 3SN inverter drive waveforms are not as simple to generate. The main reason is that there are three waveforms to be generated which are only related by the constant frequency constraint expressed by Eq. (1.3). The length of period d_1 is determined by the current programming loop. Thus, the length of the period (d_2+d_3) is variable. One needs to know it to be able to calculate the length of each of d_2 and d_3 that yields the correct value of the effective duty ratio.

The PWM circuit uses a ramp voltage of fixed frequency to relate the lengths of the periods to the different control voltages, and Fig. 4 shows the different periods and the corresponding voltages. For the flyback or boost inverters, the requirement is that d_2-d_3 be proportional to the input control signal v_{in}. From Fig. 4(a) one gets:

$$d_2 T_s = a(v_c - v) \qquad d_3 T_s = a(V_{max} - v_c)$$

where a is the slope of the ramp. Hence, the input voltage to the comparator v_c must be:

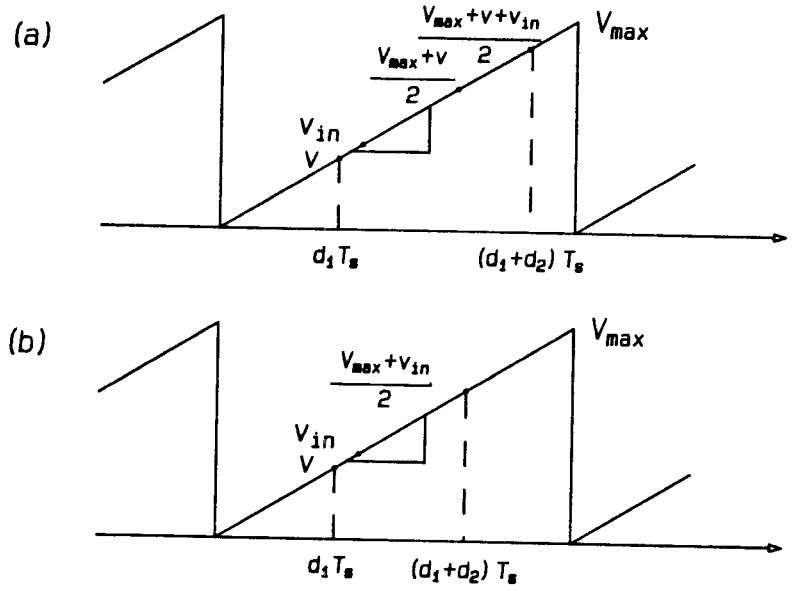

Fig. 3.4 The ramp voltages giving the relations between the switching intervals and the control voltages for (a) the flyback and boost inverters, and (b) for the buck inverter.

$$v_c = \frac{V_{max}+v+v_{in}}{2}$$

where v is the ramp voltage at the end of period d_1. The duty ratios d_2 and d_3 are complements during $(1-d_1)T_s$ and so v_c determines when d_2 ends and d_3 begins.

As mentioned before the length of d_1 is set by the current loop. It is not known *a priori* and changes according to operating conditions. Hence, a means of remembering the value of v is needed. This value is thus held by a sample-and-hold circuit at the turn-off of the input switch. A simple OP-AMP adder is used to calculate the value of v_c (Fig. 5); this is probably not the simplest nor easiest method to generate the waveforms, but simpler ones have yet to be proposed.

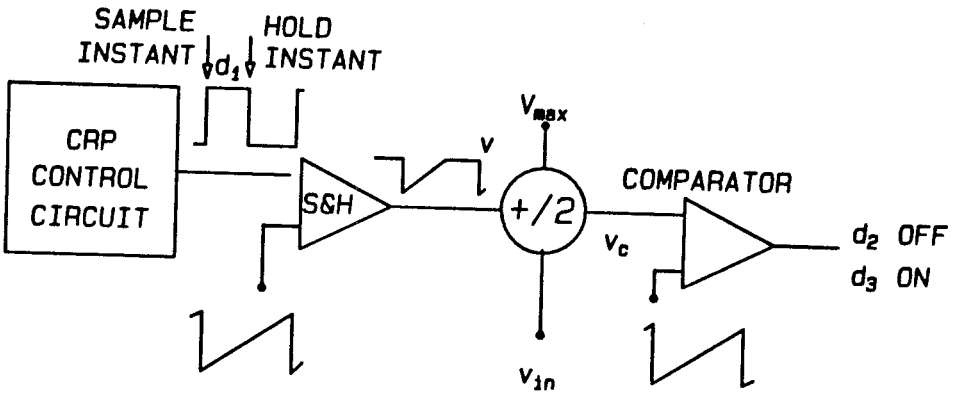

Fig. 3.5 The control circuit used to calculate the duty ratios d_2 and d_3 for the flyback and boost inverters. The sample-and-hold circuit holds the value of v and the OP-AMP adder calculates the control voltage to be input to the comparator for generation of the PWM signal.

The buck or Ćuk inverters require a slightly different value of v_c. This value is also simple to calculate by referring to Fig. 4(b):

$$d_1+d_2-d_3 = a(v+v_c-v-V_{max}+v_c) = av_{in}$$

$$v_c = \frac{(V_{max}+v_{in})}{2} \tag{3.34}$$

Thus for these inverters there is no need for a sample-and-hold circuit, and so there is a certain simplification in the control circuit.

It is clear from the above results that the dc components in the output of the buck, boost and Ćuk inverters can be suppressed by proper choice of a dc offset in the control waveform. It is also possible to use some feedforward scheme to completely eliminate the effects of input

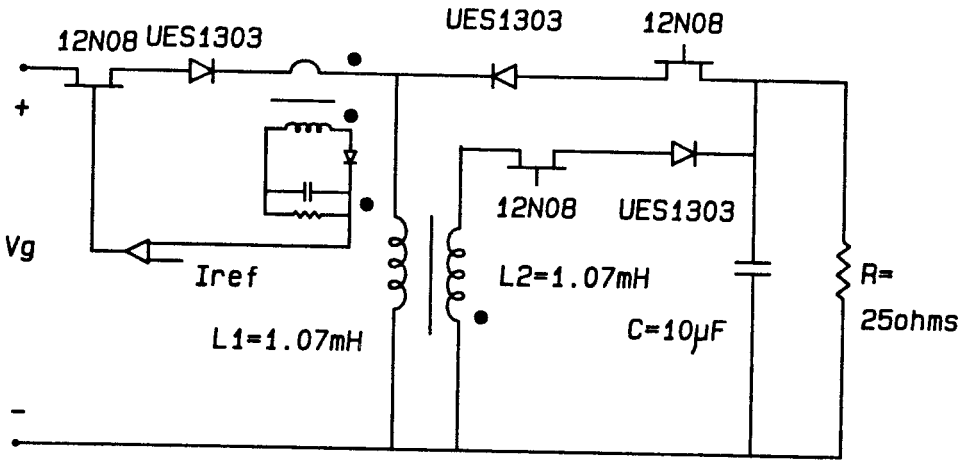

Fig. 3.6 The experimental flyback single-phase coupled-inductor inverter.

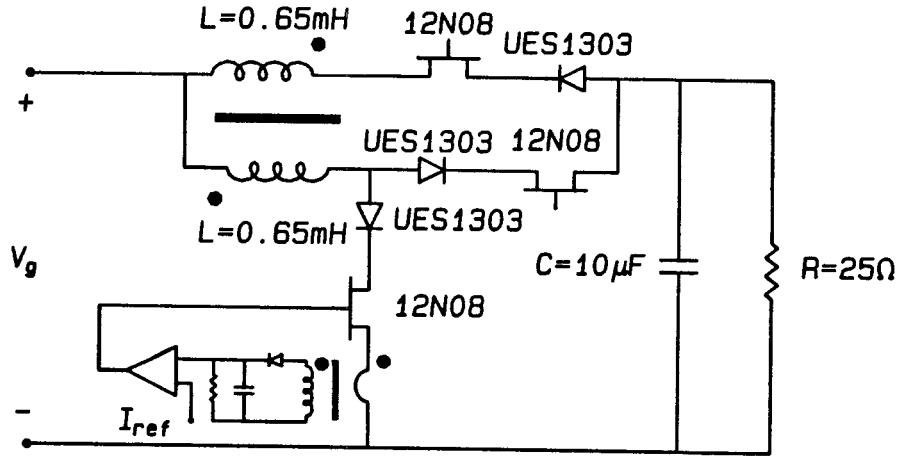

Fig. 3.7 The experimental boost single-phase coupled-inductor inverter.

voltage variations from the output without too much additional complication.

3.5.2 Comparison of Theoretical and Experimental Results

The flyback single-phase inverter shown in Fig. 6, and the boost inverter of Fig. 7 were built. The measurement of the control-to-output transfer function was accomplished with use of the Caltech Power Electronics Group Automatic Measurement System [18] on an HP9826 computer, with the NF analyzer and frequency synthesizer. The theoretical transfer function was calculated, from Eq. (3.20) for the flyback and from Eq. (3.33) for the boost, as the amplitude of the fundamental cosine and its phase at each frequency.

Comparison of the calculation and the measurement shows good agreement for the fundamental components in both the flyback (Fig. 8) and the boost inverters (Fig. 9). The measurement was done by using the synthesizer output as the input signal to the inverter. The inverter output amplitude and phase are then measured relative to the synthesizer output. Figure 10 shows the output of the two inverters.

The measurement of the third harmonic is shown in Fig. 11. The curves are calculated with respect to a one volt rms reference value. Hence, the gain for the fundamental component need not be equal to the ones shown in Fig. 8. There is also no phase measurement as the phases for the harmonics given by the analyzer have no meaning and are completely erratic.

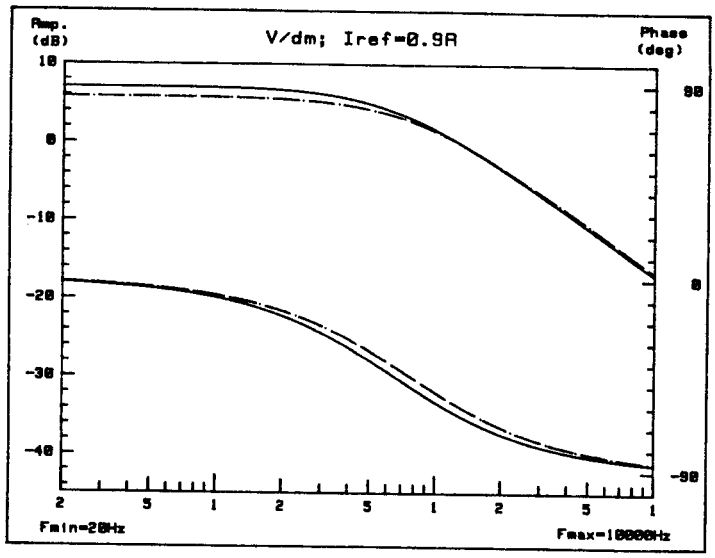

Fig. 3.8 The comparison between the theoretical calculation (solid line) and experimental measurements of the flyback inverter control-to-output characteristics. The measurement is a large-signal one. The response is very close to an ideal single-pole characteristic.

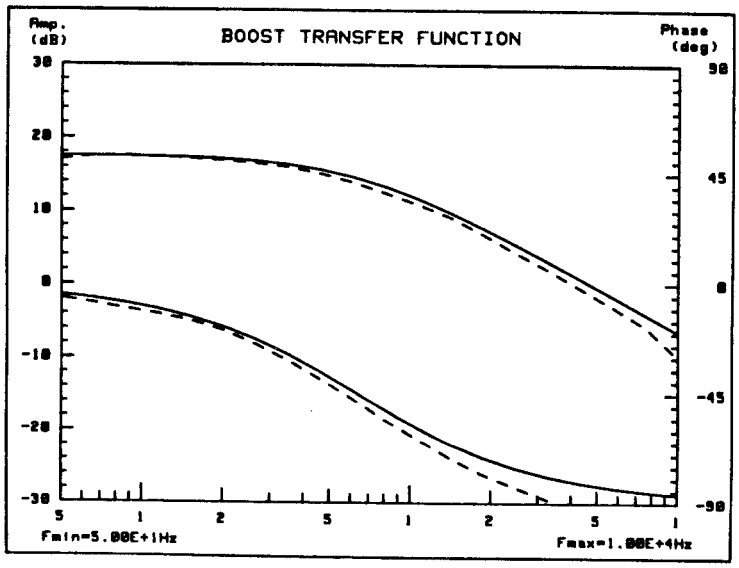

Fig. 3.9 The comparison between the theoretical calculation (solid line) and experimental measurements of the boost inverter control-to-output characteristics. The measurement is a large-signal one. The response is very close to an ideal single-pole characteristic.

Measurement of the harmonics was very hard to do as the values under consideration are at the lower end of the analyzer range. Thus, at the frequency end the measured values are drowned in the noise that is picked by the analyzer. There is a small discrepancy between the measured and calculated values. Most of the difference in the amplitude of the third harmonic is due to the neglect of the losses in the inverter, in particular the resistive losses in the inductor and the MOSFET switches.

An added error is introduced by the control circuit, especially the sample-and-hold circuit. The sample-and-hold does not store the exact value of the ramp at the hold instant but has a certain error. This error appears as part of the input signal and thus contributes to the error in the measurement. However, it is clear to see that the harmonic content of the output voltage is very small as it is 40 dB less than the fundamental. The experimental results do confirm the main theoretical calculations.

3.6 Conclusions

The analysis of the single-phase inverters is completed in this chapter with the analysis of the output waveforms. It is shown that there is no way to apply a transformation to a rotating frame of reference for small-signal calculations. However, the large signal response is calculated by applying a power series expansion method to the non-linear differential equation describing the inverters.

The harmonic content of the output waveforms is calculated for the flyback, boost and buck inverters. The results of this analysis confirm the high linearity of the inverters, as the harmonic content is found to be very small. The inverters are also found to be basically first order systems

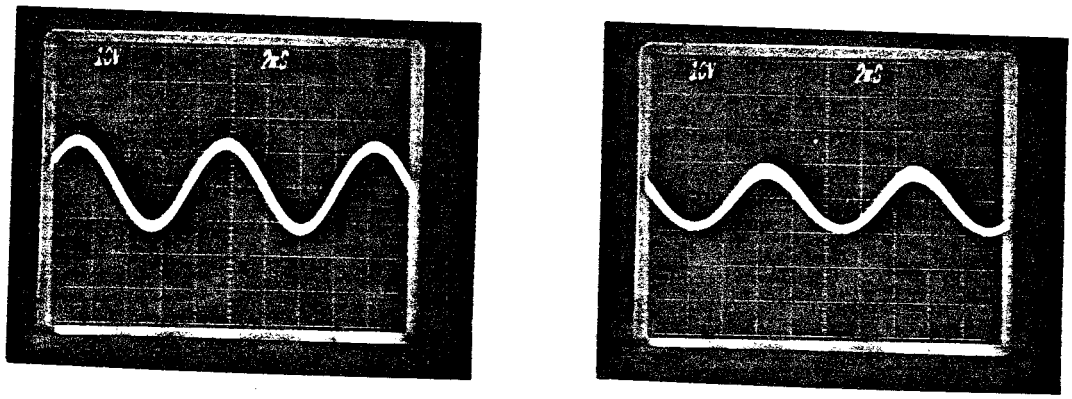

(a)

Fig. 3.10 The output waveforms of (a) the flyback and (b) the boost inverters

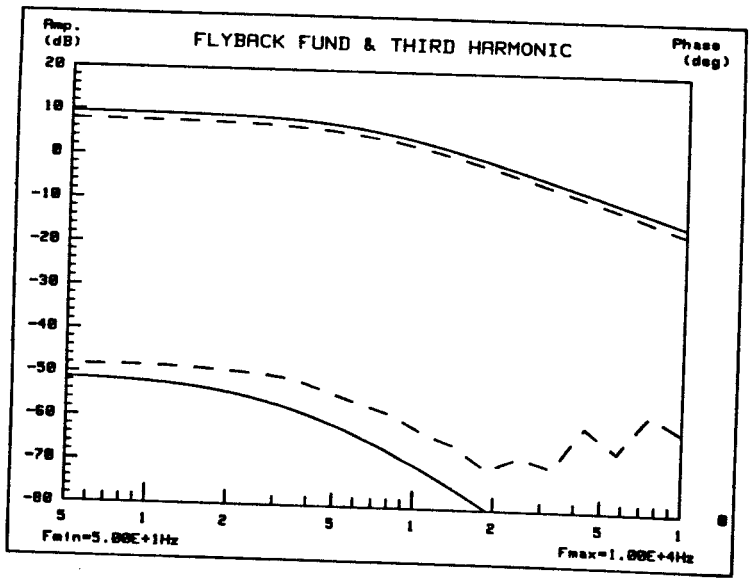

Fig. 3.11 Comparison between the calculated (solid line) and measured (dashed line) fundamental and third harmonic component in the flyback single phase inverter.

as far as the control to output response is concerned. The experimental verification of the results for the flyback and the boost inverters is also performed. The verification of the response for the fundamental components shows that the calculations are very accurate. The confirmation of the results for the harmonics is not as close, mainly owing to practical limitations in the measurement instruments.

CHAPTER 4

Multiple Output Magnetics

4.1 Introduction

Single-phase inverters have their use in applications involving household appliances driven from dc power sources such as solar cells, for instance. They may also be used as power amplifiers in public address systems where distortion requirements are not very stringent. However, the bulk of industrial applications is in three-phase systems. These applications include three-phase motor drives and uninterruptible power supplies. So for the coupled-inductor inverters to have broad applications there is a need for their three-phase versions.

The straightforward method of obtaining the three-phase versions of the coupled-inductor inverters is to use three pairs of switches on the output, one for each phase. However, this approach would nullify one of the principal advantages of this inversion technique, as the number of switches would be greater than that of other inversion methods. A more subtle way of generating a three-phase output is by use of a multiple output magnetic structure. The inverter then has two independent ac outputs. These outputs are used to generate the three-phase voltages, as described in the next chapter.

The basic idea is to split the energy in the system into two (or more) parts, each of which is supplied to a different output. That division of the energy can be done in two ways. The first way is called *space*

multiplexing of inductors, which contrasts with the other possibility which is *time multiplexing of inductors*. The former splits the energy between two inductors separated in space, and in the latter the energy is in one inductor which supplies first one output then the other, either within one switching cycle or alternating cycle by cycle.

The magnetic structure for space multiplexing is introduced in this chapter and is analyzed in different modes of operation. The analysis uses the reluctance model for the magnetics. As the inductors on the structure may be on or off at different times, there are several different operating modes and each needs to be analyzed separately. Time multiplexing of inductors is also discussed in this chapter.

4.2 Description of Multiple Output Structure

Space multiplexing of inductors is achieved by use of a standard E-I core that is slightly modified. The difference between the standard magnetics and multiple output magnetics reside in the position of the gaps and of the windings. Standard inductors or transformers on E-I cores are wound on a bobbin placed on the center leg of the core (Fig. 1). The gap is usually made by putting a piece of non-magnetic material of the required thickness across the three legs of the core.

In the case of multiple output converters the requirements are different. The primary and secondaries must be tightly coupled to ensure maximum energy transfer from input to output. At the same time the secondaries must have as little coupling between them as possible to reduce the interaction between the outputs. One way to achieve this end would be to split the primary into two halves and to wind each half with

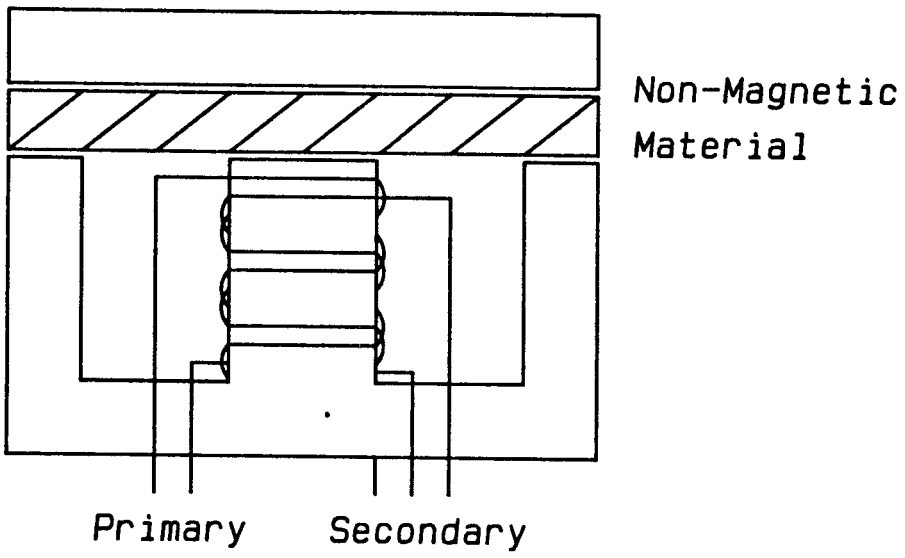

Fig. 4.1 A standard transformer wound on the center leg of an E-I core. The gap is made across the three legs of the core by use of a piece of non-magnetic material (shown hatched).

one of the secondaries on a C core, as shown in Fig. 2(a). Thus by physically separating the two secondaries the two objectives stated above can be satisfied.

The amount of magnetic material is reduced by merging the two cores into one structure (Fig. 2(b)). There is, however, a slight increase in the cross-coupling of the secondaries, but it is minimized as shown in Section 4.4. The two C cores can now be replaced by a single E-I core (Fig. 3). The primary is split in two and each half is tightly coupled to a secondary consisting of the negatively coupled inductors. The gaps in this case are only on the outer legs, thus creating a minimum reluctance path in the center legs. The flux from the secondaries flows preferentially in the center leg which reduces the flux linkage between them. The savings in magnetic material occur if the fluxes in the center legs are in opposite

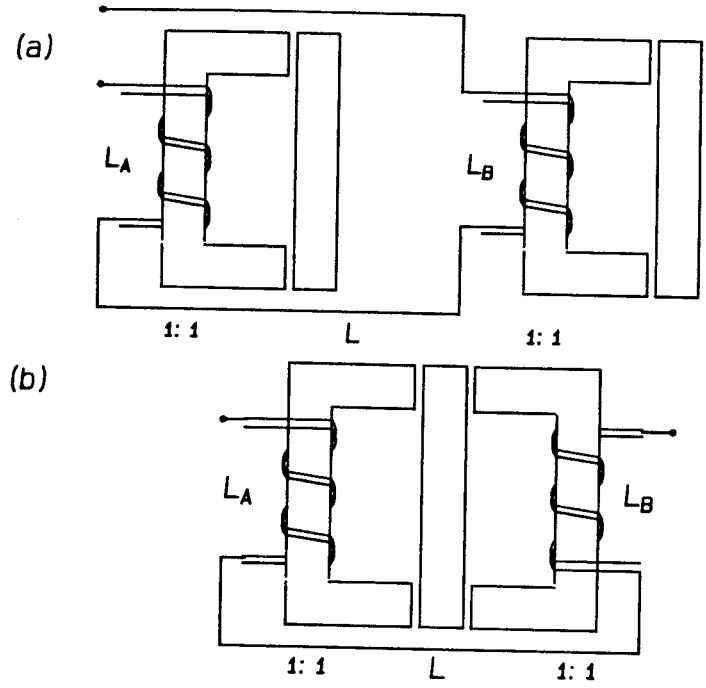

Fig. 4.2 The two separate cores of (a) can be combined as in (b) with savings in the amount of magnetic material.

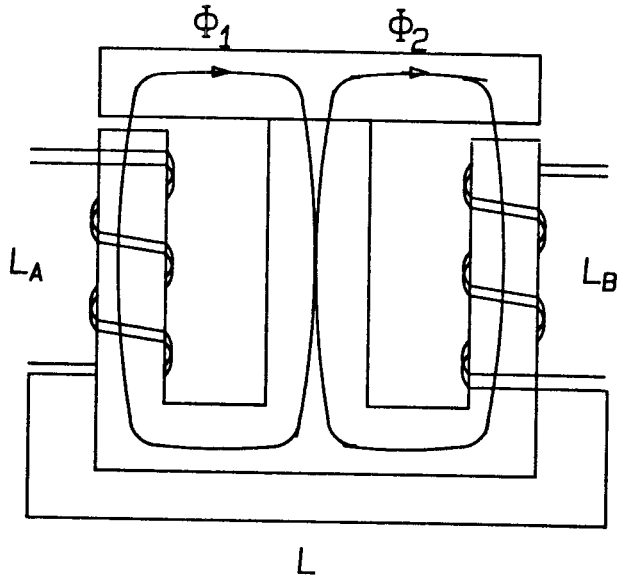

Fig. 4.3 The two windings are on a single E-I core. The fluxes are in opposite directions in the center leg thus there is a reduction in the material of that leg. Note the position of the gaps that reduce the linkage between the two sides.

directions. The resultant flux is very small. Hence, a smaller cross section is needed for that center leg.

This method is not limited to two outputs only, but can be extended to as many outputs as required; Fig. 4 shows a four output magnetic piece. It is of interest to note that the multiple output magnetic structure was first used in an independent multiple output dc-to-dc converter [8], hence it need not be limited to the applications given in this thesis.

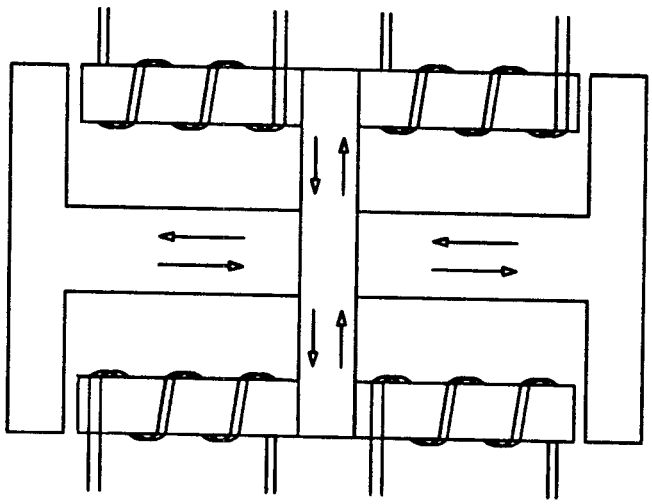

Fig. 4.4 Two E-I cores are used to get four non-interactive windings. Note that the fluxes are all in opposing direction in the common legs. The gaps are positioned such that the interaction is minimized.

4.3 Two-Phase Flyback Inverter

The analysis of the magnetic circuit cannot be done without reference to the external electric circuit. It is the electric circuit that sets the voltages and currents that affect the magnetics. Therefore, the flyback two-phase inverter is briefly described here as the circuit of reference for the magnetic analysis. The inverter is shown in Fig. 5. There is no loss of generality as far as the magnetic analysis is concerned. The use of an actual circuit, however, helps in motivating the analysis. The symbol for the coupling between the inductors, in Fig. 5, is taken henceforward to represent the multiple output magnetics as described in the previous section.

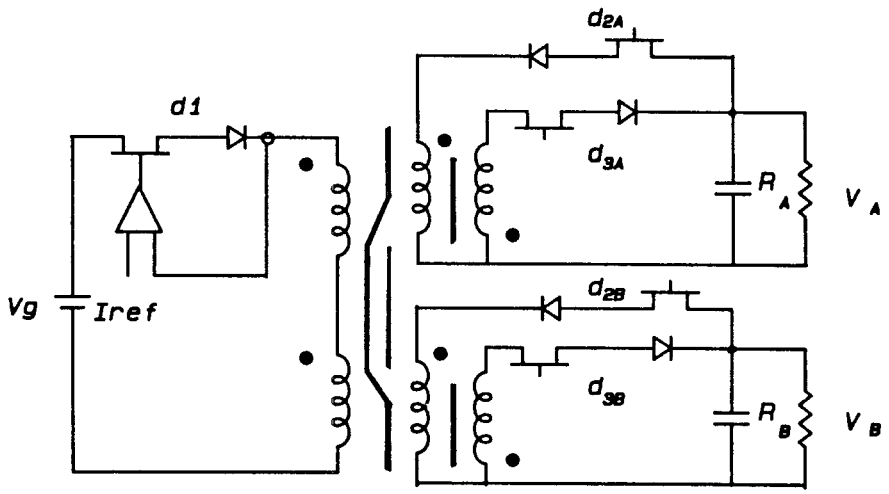

Fig. 4.5 The flyback with two-independent ac outputs. The space-multiplexed magnetic structure is used to separate the two outputs. The use of current programming further separates the outputs as they are now functions of the output duty ratios only.

Each of the two loads has a corresponding pair of output switches. Each output voltage is proportional to the average value of the inductor current that flows through the load. The output voltage is thus controlled by the duty ratios of the corresponding switches. The conditions for operation discussed for the single-phase version apply here as well with some differences that become clearer when the analysis of the magnetics is done. One may assume that the current value in the two output inductors is equal to I_{ref} at the end of d_1 (the conditions for this are derived in the next section). With this assumption each of the two phases behaves as a single-phase inverter, and the voltage outputs are:

$$v_A = I_{ref} R_A (d_{3A} - d_{2A}) \tag{4.1}$$

$$v_B = I_{ref} R_B (d_{3B} - d_{2B}) \tag{4.2}$$

where d_{2A}, d_{3A}, d_{2B}, d_{3B} are the duty ratios of the switches of the same name in Fig. 5.

As the non-overlapping duty ratios need only satisfy the condition:

$$d_1 + d_{2A} + d_{3A} = d_1 + d_{2B} + d_{3B} = 1 \tag{4.3}$$

the effective duty ratios $d_{3A} - d_{2A}$ and $d_{3B} - d_{2B}$ are linearly independent and hence the output voltages are independent of each other. This brief introduction to the two-phase inverter is sufficient for the analysis of the magnetics which is the primary concern of this chapter.

4.4 Reluctance Model Analysis of Multiple Output Magnetics

The inductors on the magnetic structure are switched on and off by the external switches according to the operation of the converter or inverter. Several questions need to be answered: what are the current and voltage transformation ratios, what are the values of the inductances, and what happens to the currents at the switching instants? Several different operating configurations are studied here that occur at different times during the operation of the converter.

The sequence of the operation is not crucial to the analysis. However, one condition has to be maintained: there must always be a path for the inductor current as long as the flux is not zero in a given loop. This condition implies that the two outputs turn on simultaneously when the input switch turns off. If this is not so one of the loops would contain a flux yet have no driving current in the windings. The flux then tries to go to zero instantaneously, which means infinite voltages are generated across the windings.

The reluctance model of a magnetic structure is derived from Ampere's law for the magnetic field intensity stated here for a magnetic core with several windings on it [7]:

$$\oint H \, d\underline{l} = \sum_j n_j i_j \tag{4.4}$$

and Gauss's law for the magnetic flux density:

$$\oint_S B \, d\underline{S} = 0 \tag{4.5}$$

where n_j and i_j are the number of turns and the current in the j^{th}

winding. In a homogeneous medium with a uniform cross section the following relations hold:

$$H = \frac{B}{\mu} = \frac{\Phi}{\mu A} \tag{4.6}$$

where μ is the permeability of the medium and A is the cross-sectional area.

Solution of the line integral of Eq. (4.4) with use of the relations of Eq. (4.6), lead to a set of equation that are equivalent to the loop equations of electric circuit theory. Equation (4.5) in turn yields for the flux Φ a relation equivalent to the node equations for the currents in an electric circuit. Thus the flux is the dual of the current and the magneto-motive force (mmf) given by ni is the dual of the voltage. The dual to the resistance is known as the reluctance and is given by:

$$R = \frac{l}{\mu A} \tag{4.7}$$

where l is the length of the path. Figure 6 shows the general reluctance model for the multiple output magnetics; the fluxes are shown in opposite directions in the center leg. However, the analysis is done for both cases.

The first operating mode to be studied is when the primary is energized and both secondaries are off (Fig. 7). Let the number of turns on both halves of the primary be n_1, the current in the primary be i_1 and assume that the gaps on the outer legs are equal. It is clear that $\Phi_1 = \Phi_2$ and so

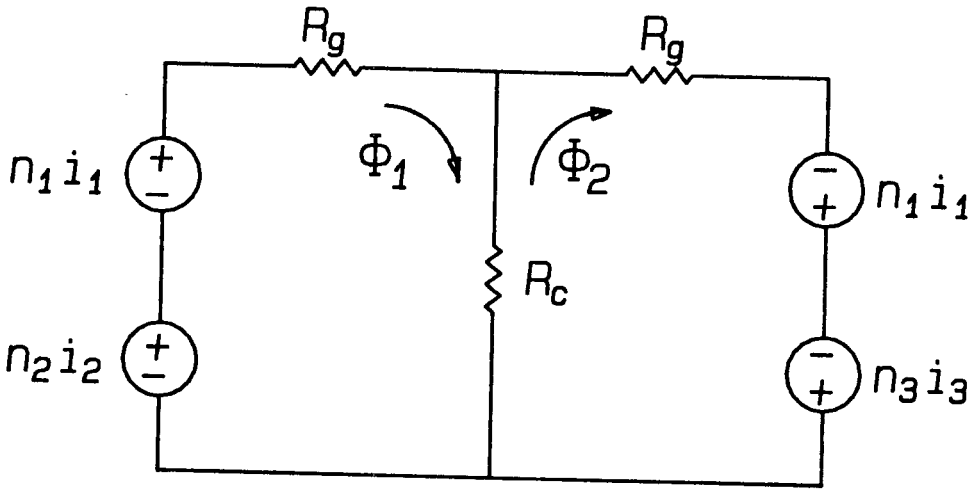

Fig. 4.6 The general reluctance model of the space-multiplexed magnetics showing all the possible mmf sources. The case shown is for opposing fluxes in the center leg.

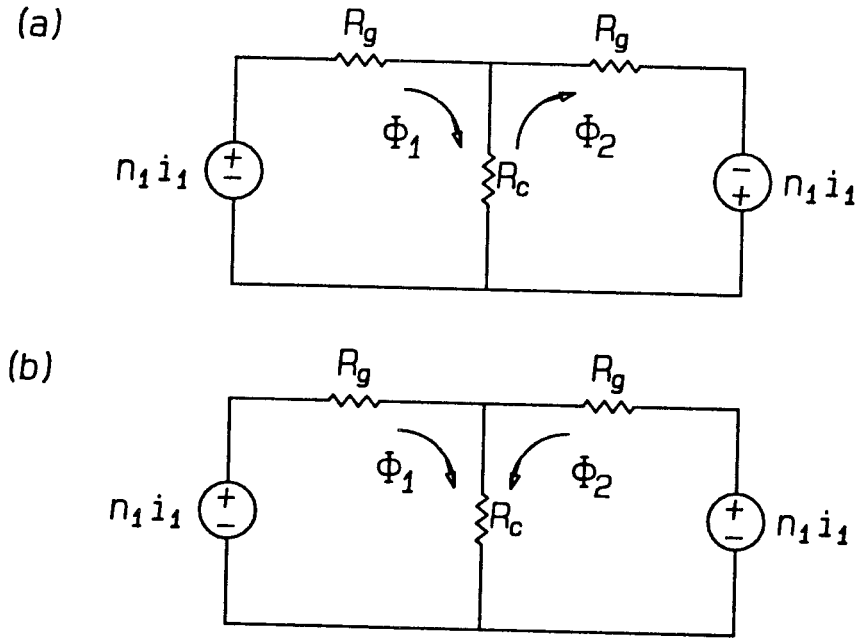

Fig. 4.7 The reluctance model for the space-multiplexed magnetics with (a) opposing and (b) adding fluxes in the center leg.

$$n_1 i_1 = \Phi_1 R_g \tag{4.8a}$$

$$n_1 i_1 = \Phi_1 R_g + 2\Phi_1 R_c \tag{4.8b}$$

$$R_g = \frac{l_g}{\mu_0 A} \qquad R_c = \frac{l_c}{\mu_f A}$$

l_g = length of air gap $\qquad$ l_c = length of center leg

Equation (4.8a) is for the case of the two fluxes opposing each other and Eq. (4.8b) is for the case of the fluxes adding in the center leg.

The ferrite material used for the cores has a permeability (μ_f) that is much higher than that of the air (μ_0), and so the core reluctance in series with the air gap are ignored. The center leg reluctance may also be ignored but is kept as it gives a quantitative measure of the amount of cross-coupling between the secondaries. Faraday's law applied to the primary inductor gives:

$$V_g = -2n_1 \frac{d\Phi_1}{dt} \tag{4.9}$$

Differentiation of Eq. (4.8a) and substitution of (4.9) gives:

$$n_1 \frac{di_1}{dt} = \frac{V_g}{2} n_1 R_g \tag{4.10a}$$

Differentiation of Eq. (4.8b) and substitution of (4.9) gives for the second case:

$$n_1 \frac{di_1}{dt} = \frac{V_g}{2} n_1 (R_g + 2R_c) \tag{4.10b}$$

Hence the primary inductor value for the two cases is given by:

$$L_1 = \frac{2n_1^2}{R_g} \tag{4.11a}$$

$$L_1 = \frac{2n_1^2}{(R_g + 2R_c)} \tag{4.11b}$$

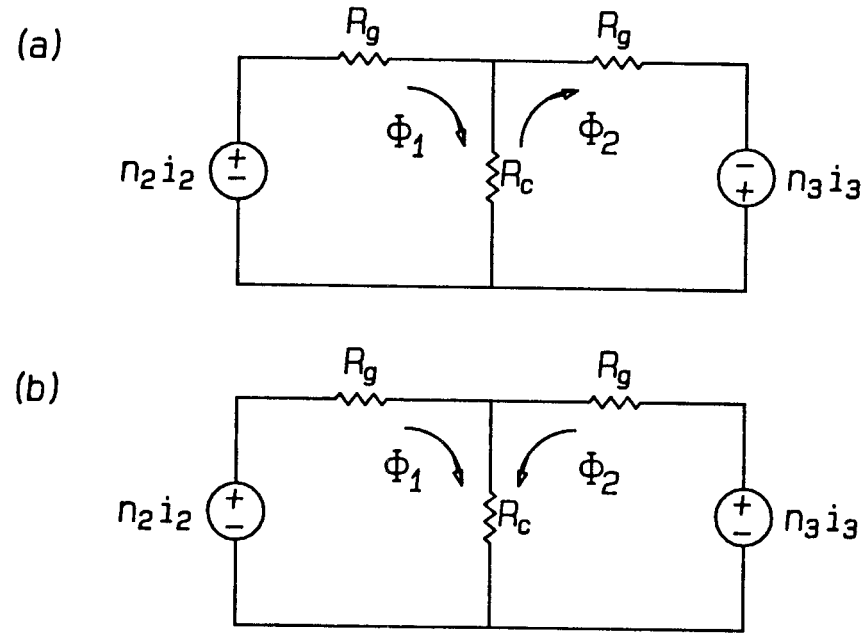

Fig. 4.8 The reluctance model during the output switching periods for (a) opposing and (b) adding fluxes in the center leg. The flux direction does not change during a switching cycle although the current direction does, because of the negative coupling.

The second mode of operation is when the two secondaries are on and the primary winding is off (Fig. 8). At the switching instant, and by continuity of flux, the currents in the secondaries are:

$$i_2(d_1 T_s) = \frac{n_1}{n_2} i_1(d_1 T_s) \qquad i_3(d_1 T_s) = \frac{n_1}{n_3} i_1(d_1 T_s) \tag{4.12}$$

Hence the self-inductance of the secondaries can be calculated in the same manner as for the primary, as well as the mutual inductance. The two loop equations are written out for the case of the opposing fluxes in the

center leg, the other case just differs by the sign of the mutual inductance.

$$n_2 i_2 = \Phi_1(R_g + R_c) - \Phi_2 R_c \tag{4.13a}$$

$$n_3 i_3 = \Phi_2(R_g + R_c) - \Phi_1 R_c \tag{4.13b}$$

Simultaneous solution of these equations gives expressions for Φ_1 and Φ_2 in terms of the two mmf's $n_2 i_2$ and $n_3 i_3$.

$$\Phi_1 = \frac{n_2 i_2 (R_g + R_c) + n_3 i_3 R_c}{(R_g + R_c)} \tag{4.14a}$$

$$\Phi_2 = \frac{n_3 i_3 (R_g + R_c) + n_2 i_2 R_c}{(R_g + R_c)} \tag{4.14b}$$

Hence, the self-inductances of the secondaries are:

$$L_2 = \frac{n_2^2}{(R_g + R_c // R_g)} \qquad L_3 = \frac{n_3^2}{(R_g + R_c // R_g)} \tag{4.15}$$

and the mutual inductance is given by:

$$L_{23} = L_{32} = \pm \frac{n_2 n_3}{\frac{R_g}{R_c}(R_g + 2R_c)} \tag{4.16}$$

The mutual inductance is positive when the fluxes are opposing each other in the center leg and negative in the other case.

4.5 Analysis at the switching instants

The reluctance of the center leg is neglected in the self-inductances with respect to the air gap reluctance. The number of turns on all windings are equal, that is $n_1=n_2=n_3$. Hence the secondary inductors are equal to each other and to half the value of the primary inductor. The initial currents in the secondaries are then equal to the final current in the primary, from Eq. (4.12). This could also be derived by an energy argument taking into consideration that the primary consists of two equal inductors in series. In this case, the open circuit voltage on each secondary is half the total voltage on the primary. The implication is that to get the same current slope the output voltage need only be half the input voltage. This affects the range of operation of the inverters in CRP, as defined in Ch. 2, as well as the region of stability of the current programming loop.

The remaining condition to be examined is at the other switching instant, that is, when the secondaries are turned off and the primary is turned on. The output voltages that are applied to the secondaries are not equal in general, and the effective duty ratios on each output also differ, thus one may expect the final fluxes to be different. When the primary winding is turned on each half winding has a different flux linked to it, yet the current in the two windings have to be equal, as they are in series. Hence, the flux tries to change instantly and generates very high voltage spikes that could destroy the switches. However, a path is provided for a secondary current that allows the magnetic circuit to adjust itself in a gradual manner.

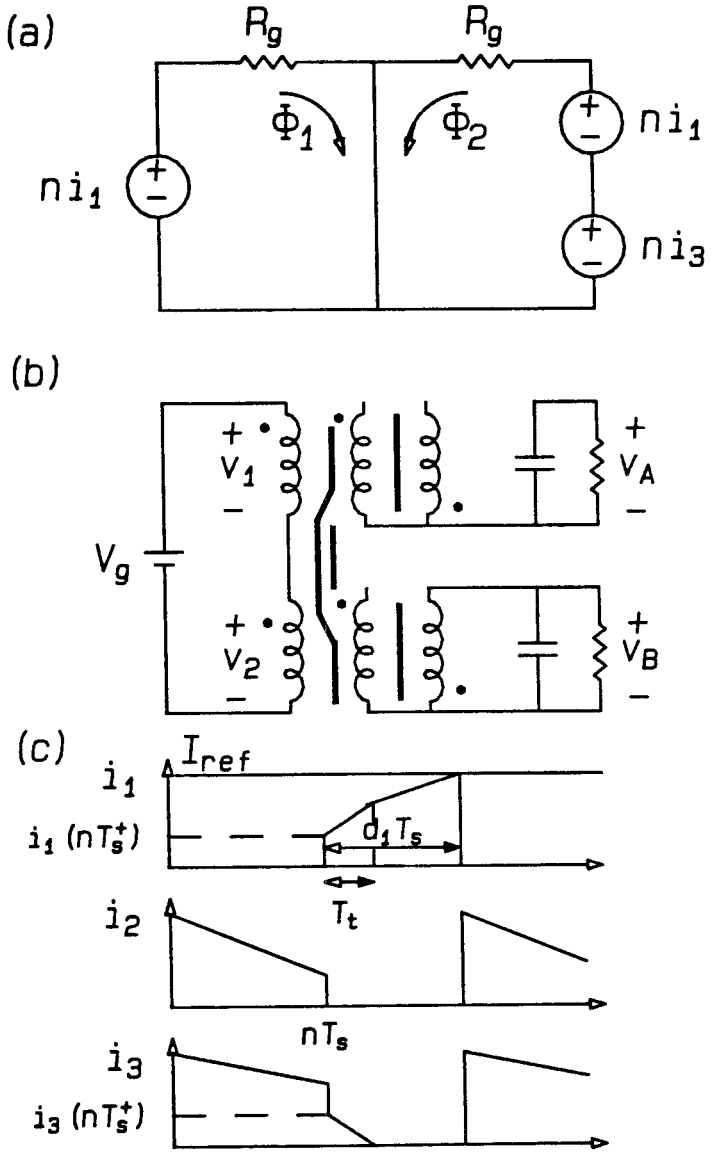

Fig. 4.9 (a) The reluctance model for the magnetics at the switching instant at the end of the output interval. (b) The corresponding electric circuit. (c) The currents in the different windings just before and after the switching instant.

Assume that one of the two fluxes, Φ_2 for instance, is larger than the other Φ_1, and that the transistor d_{2B} (Fig. 5) is on. The other case is symmetrical, and so there is no loss of generality in this assumption. The diode D_{2B} is back-biased and is off as long as the input switch is on and the output voltage has the polarity shown or is smaller than $2\frac{n_1}{n_3}V_g$. Thus the control circuit must sense the polarity of the output voltage and change the drive waveforms such that the correct output transistor is on during the period d_1. The incorrect transistor being on results in distorted waveforms at the output, but is not a destructive mode of operation.

However, in the case under consideration (a significant difference in the final fluxes in the secondaries), the diode corresponding to the winding with the higher flux conducts until the transient condition settles down. The reluctance circuit for this condition is given in Fig. 9(a), the electric circuit in Fig 9(b) and the currents are in Fig. 9(c).

In this part of the analysis the reluctance of the center leg is neglected as it does not affect the results in a significant manner. Also let the turns on the different windings be all equal to n. The output voltages are assumed to be sinusoidal, equal in amplitude and frequency and with a phase angle of 120° between them. The equations for the circuit of Fig. 9(a) are:

$$ni_1 = \Phi_1 R_g \tag{4.17a}$$

$$ni_3 = \Phi_2 R_g - ni_1 \tag{4.17b}$$

It is clear from the above equations that the initial value $i_1(nT_s^+)$ (the $^+$

sign indicates the value just after the switching instant, as there is a discontinuity at that point) of the primary current is equal to the final value of the smaller of the secondary currents (in this case $i_2(nT_s^-)$) and that $i_3(nT_s^+)$ is equal to the difference between the two secondary currents $(i_3(nT_s^-)-i_2(nT_s^-))$. From Fig. 9(b) it can be seen that $v_1 = V_g+v_B$, thus the slope of the flux Φ_1 is:

$$n\frac{d\Phi_1}{dt} = v_1 = V_g+v_B \tag{4.18}$$

Hence, the slope of the current in the primary is:

$$\frac{di_1}{dt} = \frac{R_g}{n^2}(V_g+v_B) = \frac{2}{L_1}(V_g+v_B) \tag{4.19}$$

The voltage applied to the secondary with the residual flux is the output voltage of that phase.

$$n\frac{d\Phi_3}{dt} = -v_B \tag{4.20}$$

One gets an expression for the slope of i_3 by differentiating Eq. (4.17b) and substituting the slopes of the fluxes from Eqs. (4.18) and (4.20).

$$\frac{di_3}{dt} = -\frac{R_g}{n^2}(V_g+2v_B) = -\frac{1}{L_2}(Vg + 2v_B) \tag{4.21}$$

The slopes of the current are not what one may intuitively expect; they cannot be inferred by looking at the terminals of the inductors only since, for instance, the primary slope is not proportional to V_g but to V_g+v_B and the inductance associated with it is not L_1 but only half that value. The slopes of the two currents are very steep compared to those in

normal operation of the converter, thus one may expect the transient to die out fairly fast. However, this is not always the case as shown in the rest of this section.

Having calculated the slopes of the currents and knowing the initial values of the currents $i_3(nT_s^+)$ and $i_1(nT_s^+)$ one can calculate the length of time of that transient T_t, which is the time in which i_3 decays to zero, by integrating Eq. (4.21).

$$T_t = \frac{i_3(nT_s^+)L_2}{(V_g+2v_B)} \tag{4.22}$$

where $L_2 = \frac{n^2}{R_g}$.

It is important to find out if the period T_t ends before the current reaches I_{ref}. If T_t is greater than d_1T_s then the current will build up in the secondary and could reach values destructive to the output switches. This situation occurs only if:

$$\frac{i_3(nT_s^+)}{(V_g+2v_B)} > \frac{\Delta i_2}{(V_g+v_B)} \tag{4.23}$$

$$i_3(nT_s^+) = \Delta i_2 - \Delta i_3$$

$$\Delta i_2 = I_{ref} - i_2(nT_s^-) = I_{ref} - i_1(nT_s^+)$$

$$\Delta i_3 = I_{ref} - i_3(nT_s^-)$$

The above condition is satisfied as long as the final value of the secondary currents is less than or equal to I_{ref}, since $i_3(nT_s^+)$ will always be smaller than Δi_2. However, if the load is reactive, a motor for instance, then during a portion of the inversion cycle some power is reflected to the

converter, and so it is possible for that condition to be violated.

It is useful to think of the inductor in the inverter as being a reservoir that stores energy and that can be a source or a sink depending on the external conditions. Furthermore, in the case of the multiple output magnetics there are two reservoirs which are mostly separate but are connected during the period T_t. It is clear, from the above results, that the magnetic loop with the higher flux transfers some of its energy to the other loop, hence there is a smaller demand on the supply during that time. This energy is stored in the inductors and used during the portions of the cycle where there is a higher demand from the load.

The design of the switches and the inductors requires that one knows how large the currents become when the loads are reactive. However, before proceeding one needs to clarify what the different modes of operation are, and which are the ones of interest. The first mode of operation is when Δi_2 and Δi_3 are both positive, hence T_t is smaller than $d_1 T_s$. In this case, the current $i_3(nT_s^+)$ decays to zero and the slope of the input current becomes that given by Eqs. (4.10a) or (4.10b). The length of the period $d_1 T_s$ is calculated from the integration of the slopes of i_1 over the period $d_1 T_s$.

$$\int_{i_1(nT_s^+)}^{I_{ref}} di_1 = \int_0^{T_t} \frac{R_g}{n^2}(V_g + v_B)dt + \int_{T_t}^{d_1 T_s} \frac{R_g}{n^2} V_g dt \tag{4.24}$$

Hence, the length of $d_1 T_s$ is given by:

$$d_1 T_s = i_{eq} \frac{L_1}{V_g} \tag{4.25}$$

and

$$i_{eq} = \frac{i_2(nT_s^-) - i_3(nT_s^-)}{2} \tag{4.26}$$

is the average value of the final currents in the secondaries. Hence, the length of the period is the same as if the initial value of the primary current is the average of the secondary currents; this takes into account the case of the two currents being equal. This mode of operation covers the region where Eq. (4.23) is satisfied even if one of the secondary currents is greater than I_{ref}.

The second type of transition occurs when both secondary currents are higher than I_{ref}. The initial primary current is then also greater than I_{ref}, the control circuit will shut off the input switch immediately, and so the period $d_1 T_s$ can be assumed to be zero. In this case, the extra energy is not transferred from one output to the other, but remains separate. Thus the secondary currents rise above I_{ref} as the power is being reflected from the load. If one wants to transfer that extra energy back to the input then there has to be an extra switch in the circuit. However, with passive loads this energy is simply stored in the inductor to be used when the load requires it.

The final condition is when only one secondary current is higher than I_{ref} and Eq. (4.23) is not satisfied. The primary current starts at the smaller of the two values and rises with the slope given by Eq. (4.19) until it hits I_{ref} and the input switch is turned off. The residual secondary current decays during that time and some energy is transferred to the

other output.

The two last cases are the ones of interest for calculating the peak current in the secondary. To find the peak current value one needs to calculate the cumulative effect the whole time in which this condition occurs. The worst case is for a purely reactive load, and with the slopes of the two currents being assumed equal to simplify the calculation. The slopes by which the currents rise and decay are not equal and the rising current in the primary is slower than the decaying secondary current (for this to be true the output voltage effect has to be additive, which is guaranteed by the switches), hence the assumption of equal slopes is a conservative one. In this case, the region under consideration is the whole half cycle of the inversion frequency where Δi_3 is negative.

$$\Delta i_3 = \frac{d_m v_B T_s}{L}\cos\omega_m t = \frac{d_m^2 R T_s}{L} I_{ref}\sin 2\omega_m t$$

where

$$v_B = I_{ref} R d_m \sin\omega_m t$$

and R is the magnitude of the output impedance at the inversion frequency. Thus, the region of integration is from $2\omega_m t = 180°$ to $2\omega_m t = 360°$, and this covers both regions of operation defined above. In the first portion, from 180° to 300° the two secondaries are sharing part of the extra energy, and in the second each is separate.

$$i_{3peak} = I_{ref} + \int_{180°}^{300°} i_3(nT_s^+) - \frac{V_g + 2v_B}{V_g + v_B}\Delta i_2 d(2\omega_m t)$$

$$+ \int_{300°}^{360°} \Delta i_3 d(2\omega_m t) \tag{4.27}$$

The above equation becomes very simple when the assumption of equal slopes is taken into account.

$$i_{3peak} = I_{ref} + \int_{180°}^{360°} \Delta i_3 d(2\omega_m t)$$

$$= I_{ref} + \frac{d_m^2 R T_s}{L} I_{ref} = (1+4\varepsilon) I_{ref} \tag{4.28}$$

Thus the peak current in the secondary is proportional to $(1+4\varepsilon)$ which can be made almost equal to 1 by proper choice of the inductance or the switching frequency to minimize ε. From the results of Chapter 3 for the single-phase inverter one expects for the three-phase inverter that the distortion be proportional to ε, hence minimizing ε improves the general performance of the inverter.

Use of the assumption of equal slopes makes the above result fairly conservative. In practice the peak current is much smaller as there are losses in the inverter and the load is never purely reactive. Hence, the upper bound set by Eq. (4.28) is an absolute bound that will neither be exceeded nor even approached in practice. Thus, it has been shown that the two-phase inverter can handle reactive loads and a design equation has been derived for calculation of the peak currents the output switches are to handle.

4.6 Multiple-Input Magnetics

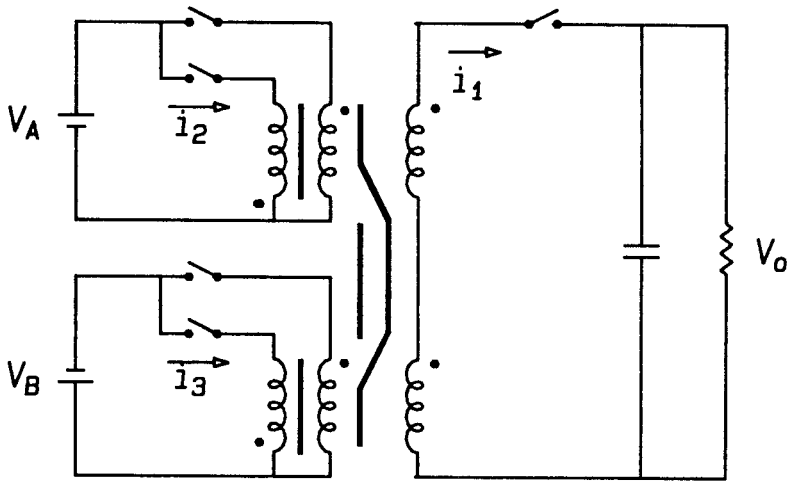

Fig. 4.10 The flyback converter with the space-multiplexed magnetics used as a multiple input circuit with dc inputs.

The magnetic structure has been studied in depth in the previous sections when used with a single input and several outputs. However, the three-phase ac-to-dc rectifiers have several inputs (the three-phase supply), and usually, though not necessarily, a single output (the dc output). Hence, one needs to study the operation of the magnetics when it has multiple inputs. For simplicity, the circuit is operated from two dc sources that have different values of voltage (Fig. 10). The steady state behaviour of the magnetics is the same as the cases studied in Section 4.4, and so the case of interest here is the switching instant from the inputs to the output.

Once more assume that the flux Φ_2 is larger than Φ_1, and so the reluctance model of the magnetics is as shown in Fig. 11(a). The situation is basically the same as in Section 4.5, except that instead of V_g the voltage on the series windings is $-V_o$ (Fig. 11(b))(the minus sign is due to the polarity reversal with respect to the dots on the windings). The resulting slopes are given by:

$$\frac{di_1}{dt} = \frac{R_g}{n^2}(-V_o+v_B) = \frac{-2}{L_1}(V_o-v_B) \tag{4.29}$$

$$\frac{di_3}{dt} = -\frac{R_g}{n^2}(-V_o+2v_B) = \frac{1}{L_2}(V_o-2v_B) \tag{4.30}$$

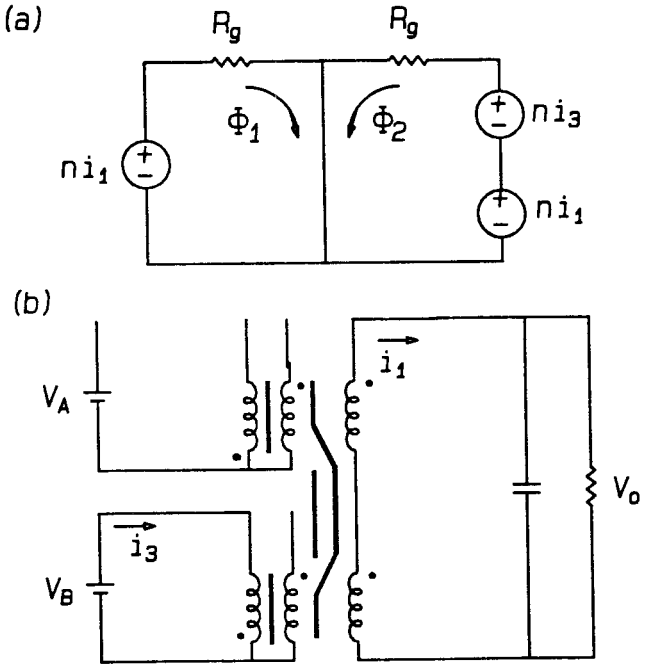

Fig. 4.11 (a) The reluctance model for the multiple input magnetics when the fluxes in the two loops are unequal. (b) The corresponding electric circuit with no special path for the residual current.

If V_o is larger than v_B then the fluxes do not converge to an equal value at the steady state. There is very little energy transfer from one loop to

the other. This is not a desirable situation as it is the loop with the lesser flux that is supporting the output, and as the input voltages are sinusoidal this means that when one of the input voltages is close to zero the output voltage will not be maintained.

It is possible to use a zener diode and a normal diode back to back to create a reverse current path (Fig. 12(a)). Thus, the loop with the smaller flux is the one with the two mmf sources, which are of opposite polarity (Fig. 12(b)), and the currents are as shown in Fig.12(c). Thus the output current starts out equal to the higher of the final input currents and decays with a slope:

$$\frac{di_1}{dt} = -\frac{R_g}{n^2}(V_o + V_Z) = \frac{-2}{L_1}(V_o + v_Z) \tag{4.31}$$

and the residual current i_3, which flows in the negative direction, rises up to zero with a slope of:

$$\frac{di_3}{dt} = \frac{R_g}{n^2}(V_o + 2v_Z) = \frac{1}{L_2}(V_o + 2v_Z) \tag{4.32}$$

The voltage of the zener diode has to be greater than the peak input voltage so that the winding is not clamped by that voltage. The equivalent starting current is calculated in the same manner as before and is found to be equal to the average value of the two final currents in the input windings.

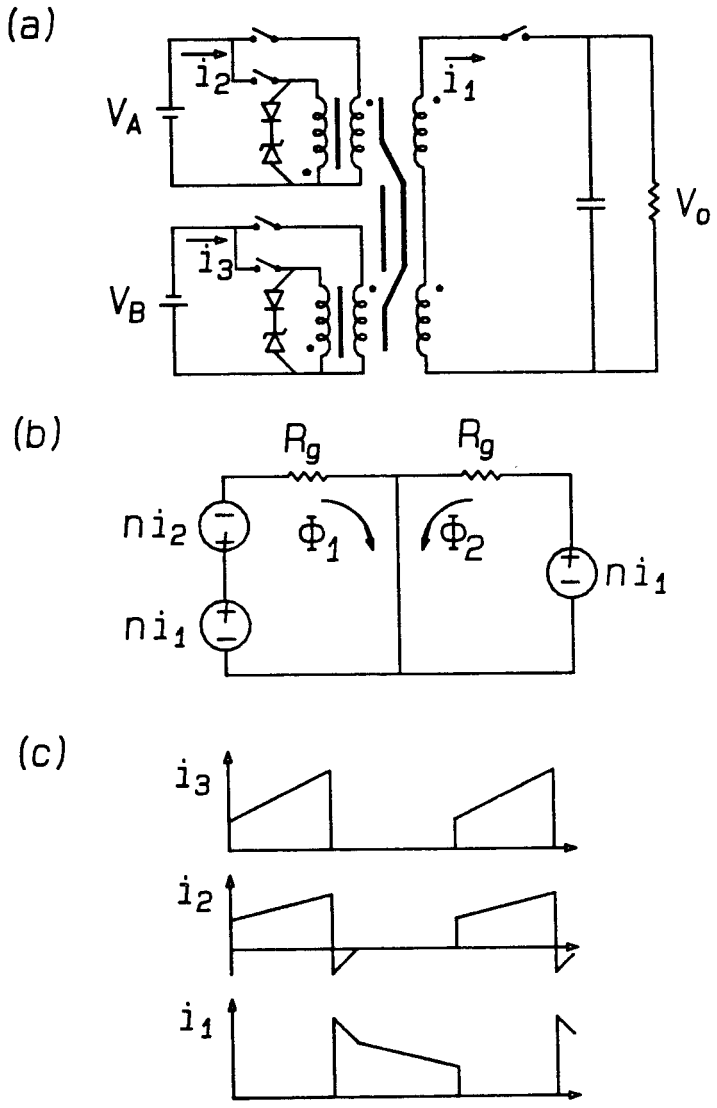

Fig. 4.12 (a) The multiple input flyback with the zener diode reverse path for the residual current in the input winding. (b) The reluctance model for this condition. (c) The current waveforms with the reverse path provided.

4.7 Time Multiplexed Magnetics

The multiple output magnetic structure studied so far in this chapter can be said to take the energy from the input and separate it into two halves, each half being stored in an inductor that is spatially separated from the other. This leads to another form of multiple output magnetics which can be called *time multiplexed magnetics*. As the space multiplexed magnetics supplies two or more different loads simultaneously from different inductors, the time multiplexed magnetics supplies two or more different loads from the same inductor at different times.

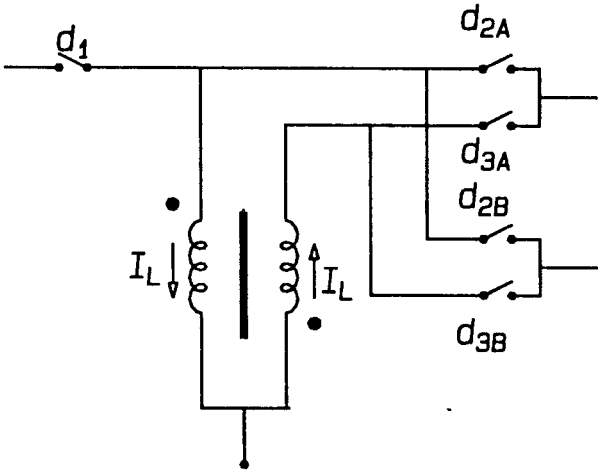

Fig. 4.13 The time-multiplexed coupled inductor magnetics. There is one switch on the dc side and four switches on the ac side. Thus each pair of switches is used to supply one of the outputs. This is obviously extended to any number of outputs within time and energy constraints.

One may look at the inverters of Section 1.3 in the light of time and space multiplexing. Thus, the push-pull inverters of Section 1.3.1 are the space multiplexed versions of the inverters and the sinusoidal inverters

of Section 1.3.2 are the time multiplexed versions. The similarity extends further as the time multiplexed inverters are smaller and lighter but require more complex control waveform generation schemes, and the same can be said of the time multiplexed magnetics.

The time-multiplexed magnetics consist of the coupled inductors that are used in the single-phase inverters of Chapter 1, but with two pairs of switches instead of one (Fig. 13). Each of these pairs of switches is connected to a load, and so the inductor is alternately connected to one output or the other. There are two different ways of making the connections: one way is to connect the inductor to both outputs within one switching cycle, the other is to alternate between the outputs cycle by cycle. The latter method is the one used here as it insures that the current starts at I_{ref} for both outputs and so the two outputs do not affect each other.

The sequence of operation, for the inverter shown in Fig. 14, is as follows: the input switch is on, and the inductor current rises to I_{ref}, then the input switch is turned off; simultaneously one of the output switches is turned on. The two complementary output switches d_{2A} and d_{2B} are turned on and off in such a way that the required output voltage is maintained. The switching period is constant, and at T_s the input switch is turned on again until the inductor current reaches I_{ref}. The same sequence of operation is repeated but for the other switches and with different duty ratios if needed.

Several of the basic properties of the space multiplexed magnetics are evident here although for different reasons. The steady state input voltage to output voltage gain of the inverter is divided by two because the

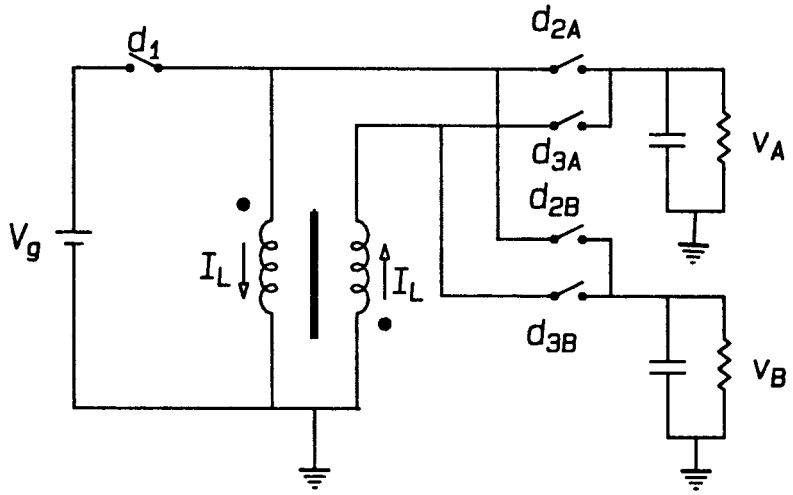

Fig. 4.14 The flyback independent two-phase inverter with time-multiplexed magnetics.

outputs are connected to the inductor once every two cycles. In the space multiplexed magnetics this occurs because the input voltage is connected to an inductor that is twice as large as the output inductor. This can also be explained as being a consequence of having the energy divided between two outputs. Similarly, when one of the outputs reflects power back to the inverter, the current rises in the inductor, and is used to supply the other output as before. Also, if both outputs are reflecting power the input period becomes very small and tends to zero.

One disadvantage of this method is that for the same switching frequency the output is connected to the inductor for only half the time. Hence, to obtain the same value of output voltage ripple, the output capacitor has to be twice as big as in the the inverter with the other magnetics. This results in a halving of the cutoff frequency of the inverter.

The switching frequency has to be doubled on the other hand if the same ripple specifications are required with the same capacitor values.

Hence, there are two distinct ways of getting multiple independent outputs using the magnetics. Each of these methods has its advantages and disadvantages when compared to each other. However, they both separate two or more outputs so that these outputs are independent. In the next chapters both methods are used to obtain the three-phase inverters, rectifiers and cycloconverters. The details of the control and drive waveform generation for each type of circuit are discussed with the two types of magnetics, with comparison of both.

4.8 Conclusion

A multiple output magnetic structure that separates the outputs from each other has been introduced. The values of the different inductors were calculated as were the transformation ratios for the currents and the voltages. As the primary consists of two similar windings in series, the transformation ratio for the voltages and currents are not as in a normal coupled inductor. The behavior of the magnetics at the switching instants was also studied. The fluxes in the two loops were shown to reach equality when the correct switches were on for a long enough time. It was also shown that the magnetics can handle a reactive load by proper design of the inductors to handle the extra energy reflected by the load.

The magnetic structure was also shown to operate in a multiple input circuit. It has the same steady state behavior as in the multiple-output case. The behavior at the switching instants is different, and

the energy transfer to the output to be optimized.

An alternative method of obtaining multiple-outputs from the same magnetic piece is introduced by use of time multiplexing of the magnetics as opposed to space multiplexing. The time multiplexed magnetics have several properties similar to the ones of the space multiplexed magnetics. It has the advantage of using less magnetics but requires either a doubling of the switching frequency or use of larger capacitors to hold the output longer. In Chapter 7, for example, the time multiplexed magnetics is the one that is mainly used for the cycloconverters.

CHAPTER 5

Three-Phase Inverters

5.1 Introduction

Three-phase systems are the workhorse of the industry. A three-phase inverter is useful in systems such as uninterruptible power supplies [3], where the three-phase line power is supplemented by batteries with the inverters being used to get the required ac output voltage. The same inverters with a bidirectional power handling capability are also used to recharge the batteries once the line voltage is restored. One can also foresee the use of ac induction motors, that are very simple and robust in construction, as variable speed actuators in areas where the supply is dc, such as on spacecraft or aircraft. Other possibilities exist for applications of these inverters; for instance, homeowners with solar cell arrays can sell back some power to the utilities during sunny periods, as a way of reducing the cost of electricity.

The multiple output magnetics introduced in the last chapter are used to obtain independent two-phase inverters from the single-phase inverters of Chapter 1. The independence of the outputs is a result of the use of CRP in the inverters in conjunction with their 3SN mode of operation. The multiple output magnetics separate the outputs and help reduce the interaction between them.

The three-phase load is connected between the terminals of the two-phase inverter. The two independent outputs are then modulated in such a way that a three-phase balanced load has a three-phase balanced output voltage. The use of the interrelation between the balanced three-phase outputs results in the smaller number of switches that characterize these inverters. The ability to generate the two independent phases is a result of the 3SN nature of the inverters and the use of CRP on the input switch.

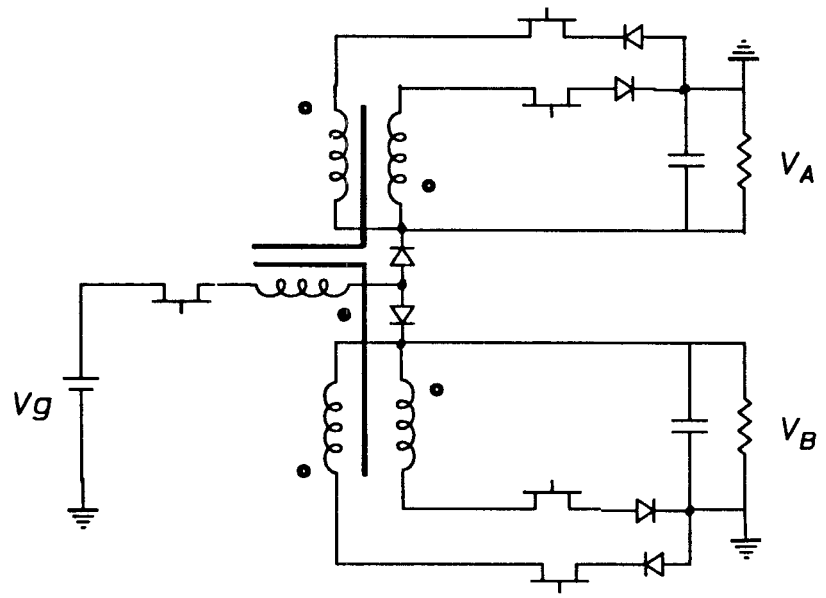

Fig. 5.1 The buck inverter with two independent ac outputs. Note the use of two back-to-back diodes to separate the outputs. This is the space-multiplexed version.

In this chapter, the three-phase inverters are derived from the corresponding single-phase ones. They are shown to exhibit the same characteristics as far as high linearity, single-pole dynamics and fast pulsed-load response are concerned. The large-signal non-linear analysis is done for the three-phase inverters as before. However, as these are

constant power systems, the application of the transformation to a rotating frame of reference is possible. It yields expressions for the small-signal dynamics of the inverters. The transformations, known as the abc-ofb transformation, are described in Appendix A. The chapter concludes with the experimental verification, made upon a three-phase flyback inverter, of the large-signal behavior.

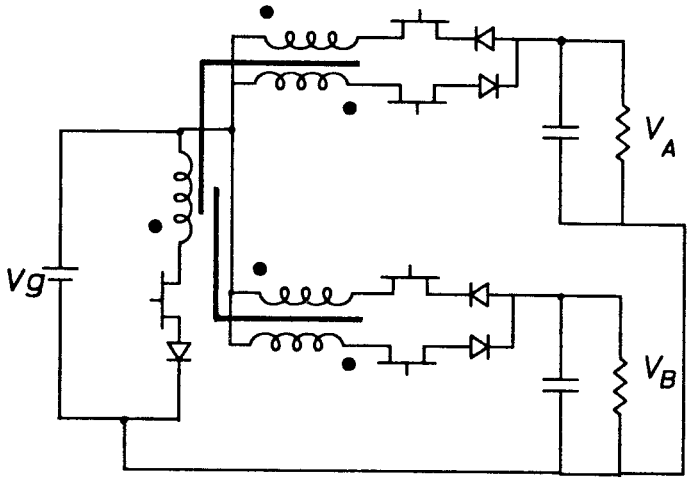

Fig. 5.2 The boost inverter with two independent ac outputs using the space-multiplexed magnetics.

5.2 Three-Phase Inverters

A 3SN dc-to-dc converter with CRP can function as a multiple-output converter with independent outputs [8] by using the magnetic structure with non-interactive secondaries that was presented in Chapter 4. It is possible to apply the same principle to the inverters to obtain two independent ac outputs [19]. In Chapter 4, the two-phase flyback inverter was briefly introduced. In this section, the other two-phase inverters are

presented and the three-phase inverters are derived from them.

The magnetic structure used with the flyback inverter can also be used with the other inverters to give the respective independent two-phase inverters (Fig. 1, 2, 3). The currents in the secondaries at the beginning of the second period are equal to I_{ref} when all windings have an equal number of turns. In the case of the buck inverter, the return path for the currents during the first period d_1 is the same so the two diodes shown in Fig. 1 are used to separate the two outputs. If these diodes are not there the output sections are in the same loop during a part of the switching cycle. The Ćuk converter has an output section similar to a buck, and so requires the added diode.

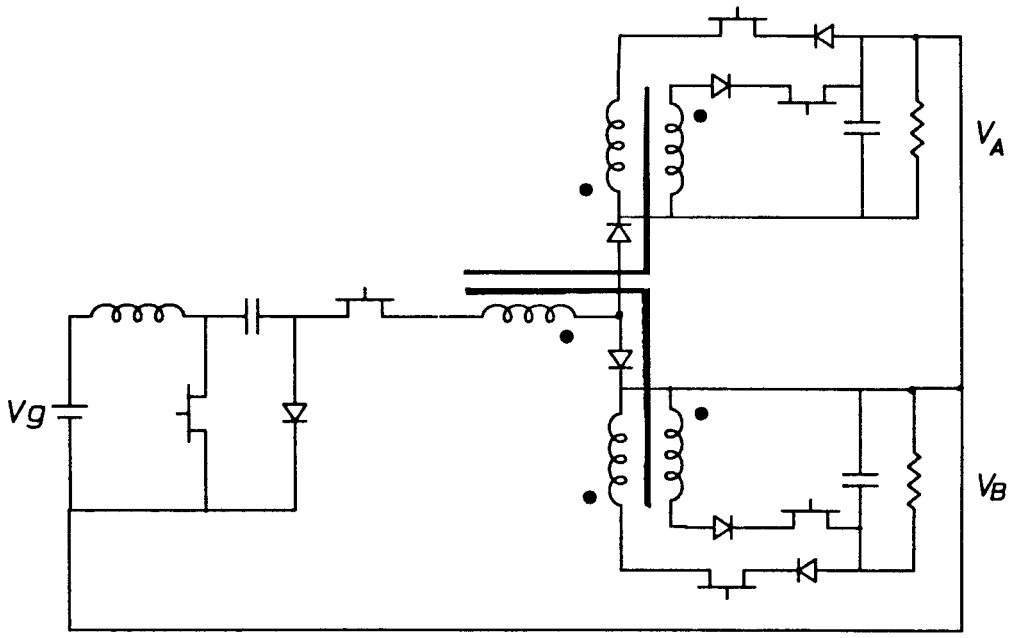

Fig. 5.3 The Ćuk inverter with two independent ac outputs, using the space-multiplexed magnetics.

It is also possible to obtain a set of three-phase inverters by use of the time multiplexed magnetics (Fig. 4). There is a net reduction in the amount of copper needed in this case as opposed to the amount needed in the case of the space multiplexed magnetics. However, there is not necessarily a reduction in the amount of magnetic material, as the same amount of energy is stored in the magnetics in both cases. The load is connected to the inductor once every two switching cycles. So the load requires a transfer of twice the energy as before, during that time, for the same output power. The equivalent switching frequency is half that of the previous case which entails a certain degradation in performance. There is also a slight increase in the complexity of the control circuit to generate the drive waveforms. Hence, there is once more an engineering trade-off that can only be resolved in terms of the specific application of the inverter.

As the discussion that follows is similar for both types of inverter, it is done only for the space multiplexed versions. It is clear from the discussion in Chapter 4 that there is very little interaction between the outputs because of the magnetics. Similarly, by virtue of the 3SN mode of operation, the output switch effective duty ratios are independent, where the effective duty ratios are $d_{2A}-d_{3A}$ and $d_{2B}-d_{3B}$ for the flyback and boost inverters, and $d_1+d_{2A}-d_{3A}$ and $d_1+d_{2B}-d_{3B}$ for the buck and Ćuk inverters. Because of the current programming, the output voltages are independent of the input voltage. Hence, the output voltages are basically independent from one another. The control to output relations for each phase are then the same as for the single-phase inverter. The control to output relations for the flyback two-phase inverter are:

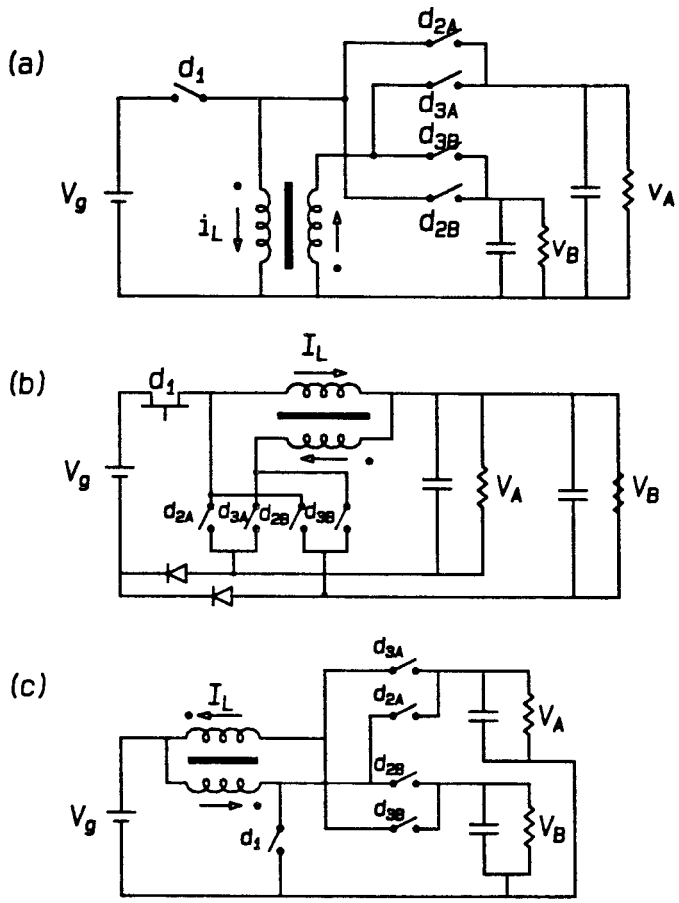

Fig. 5.4 The time-multiplexed inverters with two independent ac outputs: (a) the flyback, (b) the buck and (c) the boost inverters. The Cuk inverter has an output section similar to the buck and so is not shown here.

$$v_A = I_{ref} R_A (d_{3A} - d_{2A}) \tag{5.1}$$

$$v_B = I_{ref} R_B (d_{3B} - d_{2B}) \tag{5.2}$$

The outputs may have different frequencies, phases and amplitudes according to the modulation of the effective duty ratios, with very little interaction.

A balanced three-phase voltage system does not consist of three-independent voltages as there is a linear relation between them:

$$v_1 + v_2 + v_3 = 0 \tag{5.3}$$

where v_1, v_2, and v_3 form a three-phase balanced system. This is used to simplify the control circuit of the sinusoidal PWM inverters [1]. Only two input waveforms are generated and the third is calculated by use of an OP-AMP adder. In the same manner, a set of balanced three-phase voltages can be generated across a balanced three-phase load, in either a star or a delta connection, from two independent voltage sources of correct amplitude, phase and frequency. The above two-output inverters are extended to three phases simply by connection of the three-phase load between the outputs as shown in Fig. 5, and by generation of the correct voltages at the outputs of the inverter.

The two output voltages of the two-phase inverter (Fig. 5), represented by their phasors in the frequency domain $\bar{v}_A$ and $\bar{v}_B$, have to satisfy the following vector relations for the three load voltages to be balanced.

$$\bar{v}_A = \bar{v}_1 - \bar{v}_3 \tag{5.4}$$

$$\bar{v}_B = -\bar{v}_2 + \bar{v}_3 \tag{5.5}$$

From the vector diagram (Fig. 6), the voltages are:

$$\bar{v}_A = \sqrt{3}|v_1|\angle -30^\circ \tag{5.6}$$

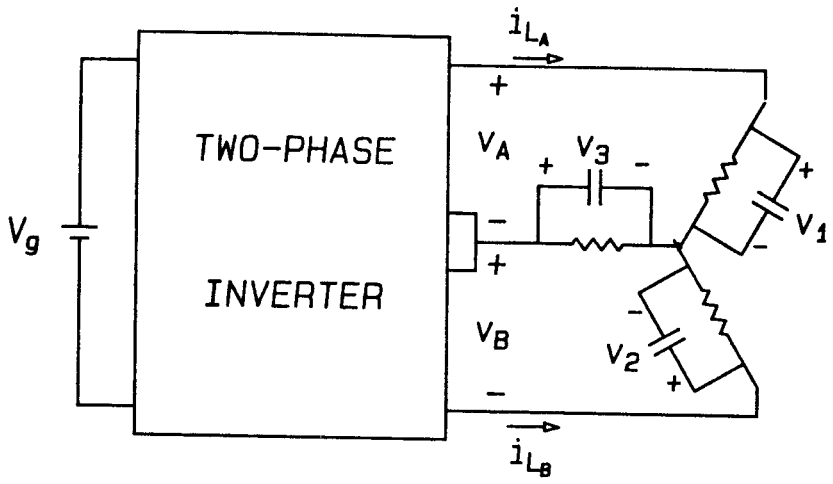

Fig. 5.5 The three-phase load is connected as shown to any of the two independent phase inverters to give a three-phase inverter.

$$\bar{v}_B = \sqrt{3}|v_1|\angle 90^\circ \tag{5.7}$$

The inverter output behaves as a current source. The output voltages v_1 and v_2 are the direct result of the inductor currents i_{L_A} and i_{L_B} flowing through the corresponding loads. Hence the output duty ratios are modulated sinusoidally with the same magnitude and out-of-phase by 120°, to result in a balanced three-phase output voltage. Thus for the flyback and boost inverters:

$$d_A = d_{3A} - d_{2A} = d_m \cos\omega_m t \tag{5.8a}$$

$$d_B = d_{3B} - d_{2B} = d_m \cos(\omega_m t - 120^\circ) \tag{5.8b}$$

and for the buck and Ćuk inverters:

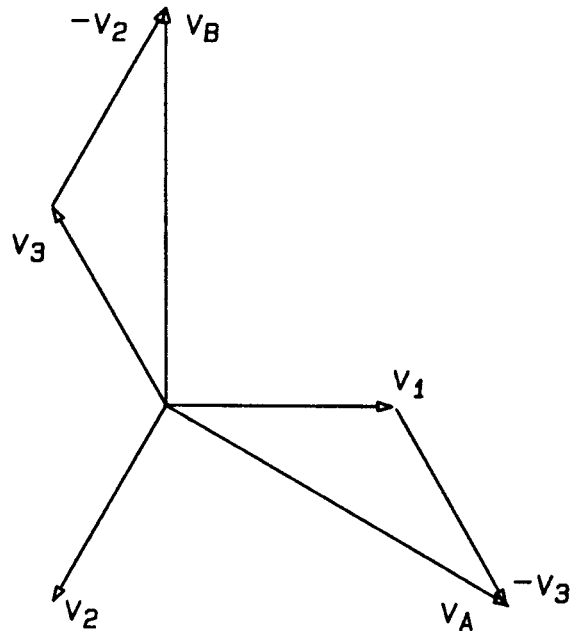

Fig. 5.6 The phasor diagram of the three-phase voltages v_1, v_2, and v_3 used to calculate the two required voltages, v_A and v_B, for balanced operation.

$$d_A = d_1 - d_{3A} + d_{2A} = d_m \cos\omega_m t \tag{5.9a}$$

$$d_B = d_1 - d_{3B} + d_{2B} = d_m \cos(\omega_m t - 120°) \tag{5.9b}$$

In the ideal case, that is, infinite switching frequency or infinite inductance, the voltages are purely sinusoidal. The power flow of a balanced three-phase system is constant [16] and the input voltage is dc. Under these ideal conditions, the current in the inductor is dc, under steady-state conditions. It is sufficient to maintain the input switch duty ratio at a fixed value to keep the current fixed. However, the inductor current is not a constrained state as it varies with the load variation. Hence, this cannot be used as a cheap way to avoid implementing current programming, as all the advantages of CRP are lost. Also, in practical circuits the outputs are neither balanced nor of a single frequency, as is

shown in the next section. Hence, the current feedback loop is still needed.

In case of unbalance in the load the inverter would still function, although the voltages appearing across the load vary according to whether the output voltage feedback loop is closed or not. When it is operated with an open voltage loop, the inverter behaves essentially as a current source, and will supply the load with balanced currents, and so the output voltages will be unbalanced. However, if the voltage feedback loop is closed (the error signal controls the output switches), the inverter behaves as a voltage source and the output voltages are balanced. Thus the inverter may be viewed as a current source or a voltage source depending on whether there is output voltage feedback or not.

5.3 Large-Signal Analysis of Three-Phase Flyback Inverter

Large-signal analysis for the three-phase inverters is done in a similar manner as for the single-phase inverters. There are some differences in setting up the state-space equations. In the case of the space multiplexed versions, the three-phase inverters have three separate inductors that carry three quasi-independent currents.

These three inductor currents are independent of each other during the periods in which they are flowing. However, they are related at the transition times by the initial and final conditions (Fig. 7a):

$$i_{L_A}(nd_1T_s) = i_{L_B}(nd_1T_s) = i_L(nd_1T_s) = I_{ref} \tag{5.10}$$

and:

$$i_L(nT_s) = \frac{i_{L_A}(nT_s) + i_{L_B}(nT_s)}{2}$$

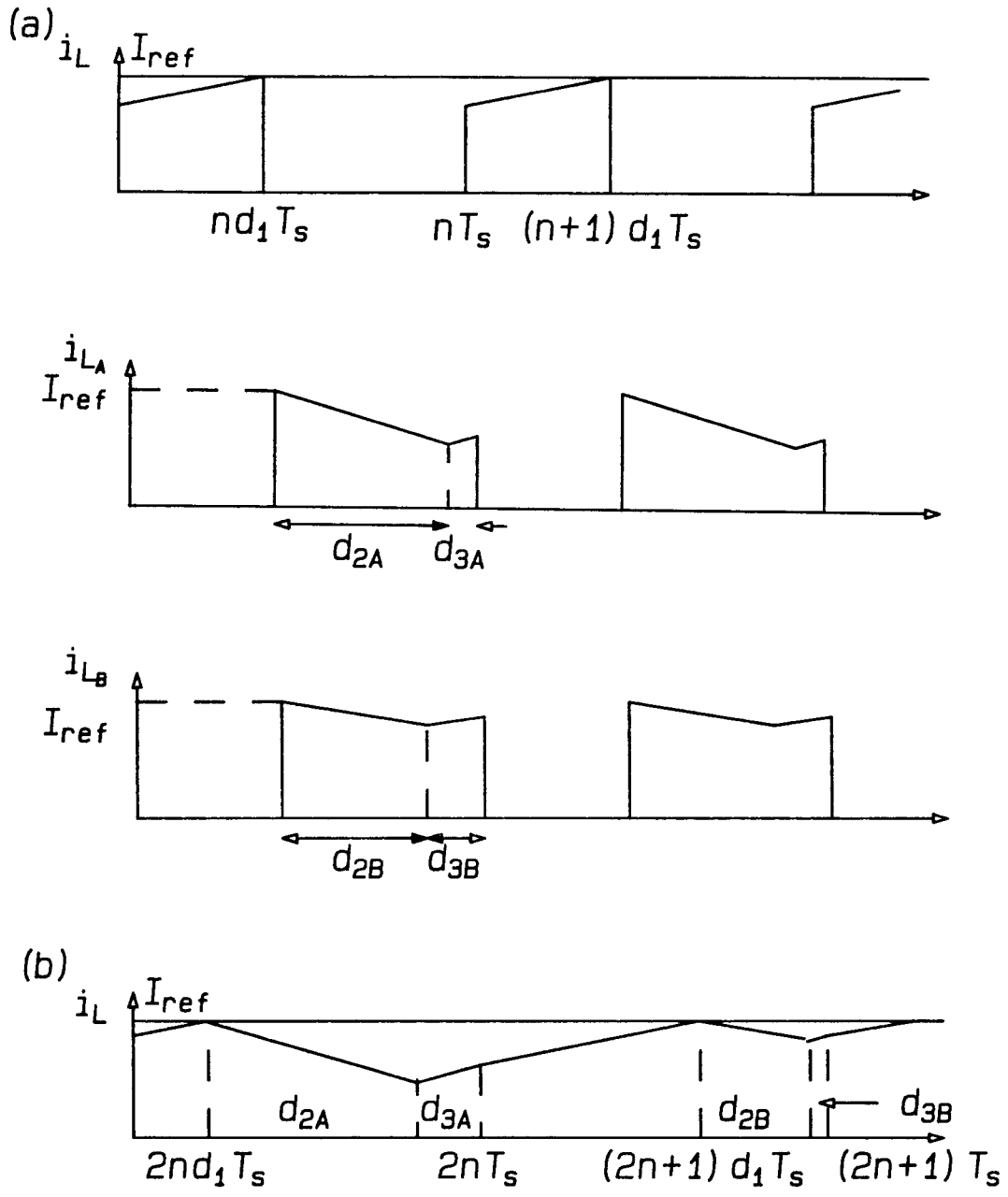

Fig. 5.7 (a) The three quasi-independent currents in a three-phase space multiplexed flyback inverter. (b) The single current of a time-multiplexed three-phase flyback inverter. It is shown over two cycles to illustrate the operation of the inverter.

(5.11)

when each half of the primary inductor and each of the secondary inductors have an equal number of turns.

The time multiplexed versions have only one inductor and hence only one current. However, that current behaves in different ways during the different periods of the switching cycle. It is therefore simpler for the mechanics of the analysis to treat it as three different currents taking into account the initial and final conditions of each (Fig. 7b).

$$i_L[nd_1T_s] = i_{L_A}[2nd_1T_s] = i_{L_B}[(2n+1)d_1T_s] = I_{ref} \tag{5.12}$$

$$i_L[2nT_s] = i_{L_A}[2nT_s] \tag{5.13a}$$

$$i_L[(2n+1)T_s] = i_{L_B}[(2n+1)T_s] \tag{5.13b}$$

The conditions of Eq. (5.10) and (5.12) effectively mean that the analysis for the output voltages for both types of inverter is the same.

The conditions given by Eq. (5.11), (5.13a) and (5.13b), are only important in setting the limits for operation of the inverter in the current programmed mode. It is clear that the conditions for the two types of inverters are not the same. For the space multiplexed versions the conditions are the same as for the single-phase inverter, except that the average of the two currents, voltages and load resistances are used instead of a single one. The conditions for the time multiplexed versions are the same as for the single-phase inverter but the output currents, voltages and loads have to satisfy the conditions for each output separately.

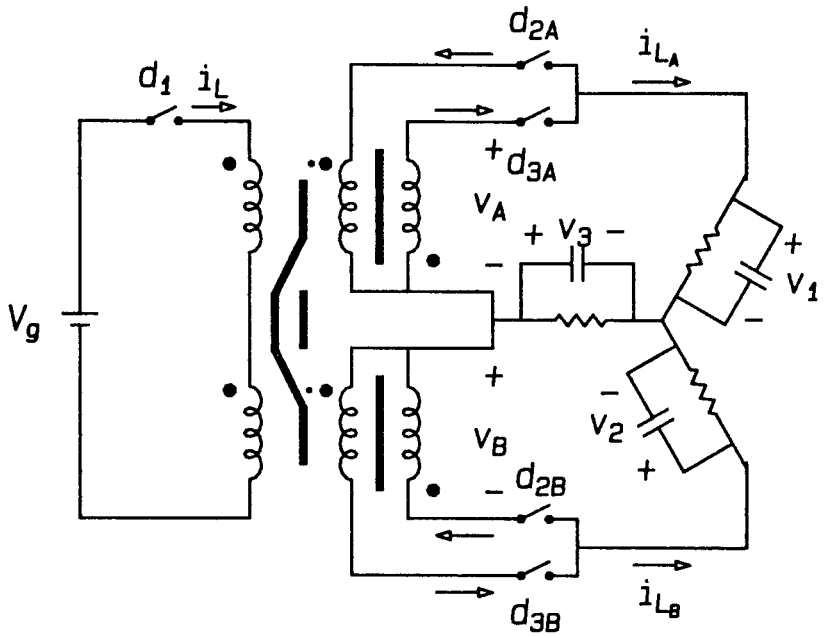

Fig. 5.8 The three-phase flyback space-multiplexed inverter. All the current directions and voltage polarities are shown that are used in the analysis.

The state vector is then extended to include those currents. Thus, the three currents are taken into account, each in its own period, and with use of the above conditions as initial values for the differential equations. The state-space equations are set up by averaging out the different switched-networks. The resulting averaged state-space equations for the three-phase flyback inverter of Fig. 8 are:

$$P\dot{x} = Ax + bV_g \tag{5.14}$$

where

$$P = \begin{bmatrix} L & 0 & 0 & 0 & 0 & 0 \\ 0 & L_A & 0 & 0 & 0 & 0 \\ 0 & 0 & L_B & 0 & 0 & 0 \\ 0 & 0 & 0 & C & 0 & 0 \\ 0 & 0 & 0 & 0 & C & 0 \\ 0 & 0 & 0 & 0 & 0 & C \end{bmatrix}$$

$$A = \begin{bmatrix} 0_3 & -A_d^T \\ A_d & A_r \end{bmatrix}$$

where 0_3 is a 3×3 zero matrix,

$$A_d = \begin{bmatrix} 0 & d_A & 0 \\ 0 & 0 & d_B \\ 0 & -d_A & -d_B \end{bmatrix}$$

and

$$A_r = \begin{bmatrix} -1/R & 0 & 0 \\ 0 & -1/R & 0 \\ 0 & 0 & -1/R \end{bmatrix}$$

and b is a vector with the first element equal to d_1 and all others equal to zero.

The solution for the currents can be written out by inspection of the current waveforms (Fig. 7) [20], as the initial values are given. The secondary currents both start at I_{ref}.

$$i_{L_A} = I_{ref} - \frac{d_A T_s}{2L}(v_1 - v_3) \tag{5.15}$$

$$i_{L_B} = I_{ref} - \frac{d_B T_s}{2L}(v_2 - v_3) \tag{5.16}$$

The solutions for the currents are substituted into the state equation. The differential equations for the output voltages are:

$$C\dot{v}_1 = \frac{-v_1}{R} + d_A\left[I_{ref} - \frac{d_A(v_1-v_3)T_s}{2L}\right] \tag{5.17}$$

$$C\dot{v}_2 = \frac{-v_2}{R} + d_B\left[I_{ref} - \frac{d_B(v_2-v_3)T_s}{2L}\right] \tag{5.18}$$

$$C\dot{v}_3 = \frac{-v_3}{R} - d_A\left[I_{ref} - \frac{d_A(v_1-v_3)T_s}{2L}\right] \tag{5.19}$$

$$- d_B\left[I_{ref} - \frac{d_B(v_2-v_3)T_s}{2L}\right]$$

To obtain a balanced three-phase system the duty ratio modulation has to be:

$$d_A = d_m \cos\omega_m t \tag{5.20}$$

$$d_B = d_m \cos(\omega_m t - 120^\circ) \tag{5.21}$$

The above duty ratios are substituted into the voltage equations. The three voltages v_1, v_2, and v_3 are expanded as power series in ε. It is clear that the existence of a common path for both inductor current introduces interactions between the two outputs. However, as before all non-idealities are of order ε and therefore are very small.

$$v_1 = v_{10} + \varepsilon v_{11} + \varepsilon^2 v_{12} \cdots \tag{5.22a}$$

$$v_2 = v_{20} + \varepsilon v_{21} + \varepsilon^2 v_{22} \cdots \tag{5.22b}$$

$$v_3 = v_{30} + \varepsilon v_{31} + \varepsilon^2 v_{32} \cdots \tag{5.22c}$$

The above equations are substituted into Eqs. (5.17),(5.18) and (5.19). The coefficients of the zeroth order of ε give the differential equations for the ideal inverter output voltages.

$$\frac{1}{\omega_p}\dot{v}_{10} + (1+\varepsilon)v_{10} = I_{ref} R d_m \cos\omega_m t \tag{5.23}$$

$$\frac{1}{\omega_p}\dot{v}_{20} + (1+\varepsilon)v_{20} = I_{ref} R d_m \cos(\omega_m t - 120°) \tag{5.24}$$

$$\frac{1}{\omega_p}\dot{v}_{30} + (1+\varepsilon)v_{30} = I_{ref} R d_m \cos(\omega_m t + 120°) \tag{5.25}$$

These equations are solved to give:

$$v_{10} = \frac{I_{ref} R d_m}{\sqrt{(1+\varepsilon)^2 + (\omega_m/\omega_p)^2}} \cos(\omega_m t - \tan^{-1}\frac{\omega_m}{(1+\varepsilon)\omega_p})$$

$$v_{20} = \frac{I_{ref} R d_m}{\sqrt{(1+\varepsilon)^2 + (\omega_m/\omega_p)^2}} \cos(\omega_m t - 120° - \tan^{-1}\frac{\omega_m}{(1+\varepsilon)\omega_p})$$

$$v_{30} = \frac{I_{ref} R d_m}{\sqrt{(1+\varepsilon)^2 + (\omega_m/\omega_p)^2}} \cos(\omega_m t + 120° - \tan^{-1}\frac{\omega_m}{(1+\varepsilon)\omega_p})$$

The equations for the higher powers of ε are solved in the same way. The algebra is quite involved and uninteresting as it does not provide any insight to the operation of the three-phase inverters. The structure of the output voltage of the single-phase inverter is preserved in its main points. As before, the fundamental component is much larger than the

harmonics. The only harmonics present in the flyback are the odd harmonics, and there are even harmonics in the boost and buck inverters.

The results are given for the flyback inverter:

$$v_1 = \frac{I_{ref} R d_m}{\sqrt{(1+\varepsilon)^2+(\omega_m/\omega_p)^2}} \left[\cos(\omega_m t-\varphi)\right.$$

$$+ \frac{\varepsilon}{\sqrt{(1+\varepsilon)^2+(\omega_m/\omega_p)^2}}\left[\cos(\omega_m t+120°-2\varphi)+\frac{\sqrt{3}}{2}\cos(\omega_m t+30°)\right] \quad (5.26)$$

$$\left. + \frac{\frac{\sqrt{3}}{2}\varepsilon}{\sqrt{(1+\varepsilon)^2+(3\omega_m/\omega_p)^2}}\cos(3\omega_m t+150°-\varphi-\varphi')\right]$$

$$v_2 = \frac{I_{ref} R d_m}{\sqrt{(1+\varepsilon)^2+(\omega_m/\omega_p)^2}} \left[\cos(\omega_m t-120°-\varphi)\right.$$

$$+ \frac{\varepsilon}{\sqrt{(1+\varepsilon)^2+(\omega_m/\omega_p)^2}}\left[\cos(\omega_m t+120°-2\varphi)+\frac{\sqrt{3}}{2}\cos(\omega_m t+30°)\right] \quad (5.27)$$

$$\left. + \frac{\frac{\sqrt{3}}{2}\varepsilon}{\sqrt{(1+\varepsilon)^2+(3\omega_m/\omega_p)^2}}\cos(3\omega_m t-150°-\varphi-\varphi')\right]$$

$$v_3 = \frac{I_{ref} R d_m}{\sqrt{(1+\varepsilon)^2+(\omega_m/\omega_p)^2}} \left[\cos(\omega_m t+120°-\varphi)\right. \quad (5.28)$$

$$+ \frac{2\varepsilon}{\sqrt{(1+\varepsilon)^2+(\omega_m/\omega_p)^2}}\left[\cos(\omega_m t-60°)\right]$$

$$\left. + \frac{\frac{3}{2}\varepsilon}{\sqrt{(1+\varepsilon)^2+(3\omega_m/\omega_p)^2}}\cos(3\omega_m t-\varphi-\varphi')\right]$$

where

$$\varphi = \tan^{-1}\frac{\omega_m}{(1+\varepsilon)wp} \qquad \varphi' = \tan^{-1}\frac{3\omega_m}{(1+\varepsilon)wp}$$

There is an unbalanced term in the fundamental component of the output voltage that is proportional to ε. The third harmonic components are also unbalanced. The unbalances in the results are mainly due to the fact that the voltage v_3 appears in the non-linear terms of the two currents i_A and i_B (Fig. 8). As for the single-phase inverter a vanishingly small ε reduces the inverter to the ideal case. Hence it appears that the three-phase inverter produces clean output waveforms while preserving all the properties of the single-phase versions including the smaller number of switches, the single pole dynamics and the fast pulsed load response.

5.4 Small-Signal Analysis of Three-Phase Inverters

The small-signal transfer functions of a three-phase inverter can be calculated using perturbation techniques. However, as the inverters are non-linear time varying systems, a transformation from the fixed frame of reference to a rotating frame of reference has to be applied [1,21]. In the new frame of reference the components of the state variables at the fundamental or inversion frequency appear as dc quantities. As shown in Chapter 3, this transformation exists only for constant power systems, so it cannot be applied to single-phase systems. Similarly, the transformation does not exist for a three-phase unbalanced system.

The results of the analysis in Section 5.3 show that the output of the coupled inductor three-phase inverters contains unbalanced terms of the second order. The unbalance disappears when some assumptions are made about the average inductor currents. Then the state equations are

set up with the new state variables. The abc-ofb transformations are then applied to the state equations. Perturbation of the new dc states yields the small-signal response of the system to variations in amplitude and inversion frequency.

In order to apply the transformation, the three inductor currents are replaced by a single current. This current closely approximates the behavior of the original three currents during the switching period, and is equal to their values at the switching instants. This operation affects the value of the ripple in the currents only. The equivalent assumption in the case of time-multiplexed inverters is to take the average value of the current during *two* switching cycles instead of one. The rest of the analysis for both types of inverters is the same.

Although the second-order terms of the current are quite small, the assumptions made do not neglect them altogether but only approximate their time dependence. The purpose of the transformation is to calculate the small-signal transfer functions of the inverter. Hence, the effect of the assumption of a single average current is only a third order effect. The required current is called i_L where

$$i_L = \frac{i_{L_A}+i_{L_B}}{2} \tag{5.29}$$

This is true for the space multiplexed inverter with $L_A = L_B = 1/2L$. For other ratios of inductances the constant on the right-hand side is other than half. It is also true for time multiplexed inverters with equal periods for both outputs.

The flyback three-phase inverter is taken as an example. Upon substitution of the current values from Eqs. (5.15) and (5.16) into (5.29), and control of the duty ratios as in Eqs. (5.20) and (5.21), the inductor current for the flyback inverter becomes:

$$i_L = I_{ref} - \frac{3d_m T_s}{4L} v \cos\varphi \tag{5.30}$$

where v is the amplitude of the output voltages, and φ is their phase angle relative to the duty ratio modulation. Note that in this section the voltage amplitude v, the amplitude of modulation d_m and the inversion frequency ω_m are time varying quantities. Equation (5.30) is obtained by use of the results of the previous section. However, the same result is obtainable independently by the analysis method used in the current section, thus showing that the abc-ofb transformation method gives a complete and accurate description of the system.

The state equations of the flyback three-phase inverter, obtained incorporating the assumption of a single current, are:

$$P\dot{\boldsymbol{x}} = A\boldsymbol{x} + \boldsymbol{b}V_g \tag{5.31}$$

where

$$P = \begin{bmatrix} L & 0 & 0 & 0 \\ 0 & C & 0 & 0 \\ 0 & 0 & C & 0 \\ 0 & 0 & 0 & C \end{bmatrix}$$

$$A=\begin{bmatrix} 0 & -d_A & -d_B & d_A+d_B \\ d_A & -1/R & 0 & 0 \\ d_B & 0 & -1/R & 0 \\ -d_A-d_B & 0 & 0 & -1/R \end{bmatrix} \qquad b=\begin{bmatrix} d_1 \\ 0 \\ 0 \\ 0 \end{bmatrix}$$

The following unitary transformation is applied to the system:

$$T = \begin{bmatrix} 1 & O_n^T \\ O_n & T_n \end{bmatrix} \tag{5.32}$$

where n is the number of phases, O_n is a zero vector of order n. In the case under consideration n is equal to three and T_3 is as given in Appendix A. The transformation applied to the flyback three-phase inverter under consideration gives a new state equation:

$$\tilde{P}\dot{\tilde{x}} = \tilde{A}\tilde{x} + \tilde{b}V_g \tag{5.33}$$

where

$$\tilde{x} = T^{-1}x = \begin{bmatrix} i_L \\ v_0 \\ v_f \\ v_b \end{bmatrix}$$

$$\tilde{P} = P \quad \tilde{A} = T^{-1}AT - T^{-1}P\dot{T} \quad \tilde{b} = T^{-1}b$$

and v_0, v_f and v_b are the zero sequence, forward, and backward phasors of the voltage in the rotating frame of reference.

The vector b remains the same as all its elements are equal to zero except for the first one. The matrix $\tilde{A}$ is the result of the summation of three matrices.

$$\tilde{A} = A_r + A_d d_m + A_\omega \omega_m \tag{5.34}$$

The first matrix contains the information about the load.

$$A_r = \begin{bmatrix} 0 & 0 & 0 & 0 \\ 0 & -1/R & 0 & 0 \\ 0 & 0 & -1/R & 0 \\ 0 & 0 & 0 & -1/R \end{bmatrix} \tag{5.35}$$

The second matrix contains the information about the effect of the amplitude of the duty ratio modulation on the states.

$$A_d = \begin{bmatrix} 0 & 0 & -\sqrt{3}/2 & -\sqrt{3}/2 \\ 0 & 0 & 0 & 0 \\ \sqrt{3}/2 & 0 & 0 & 0 \\ \sqrt{3}/2 & 0 & 0 & 0 \end{bmatrix} \tag{5.36}$$

The final matrix contains all the information relative to the inversion frequency.

$$A_\omega = -T^{-1}P\dot{T} = -j \begin{bmatrix} 0 & 0 & 0 & 0 \\ 0 & 0 & 0 & 0 \\ 0 & 0 & -C & 0 \\ 0 & 0 & 0 & C \end{bmatrix} \tag{5.37}$$

Before proceeding to the perturbation of the system described by Eq. (5.33) one can eliminate the zero sequence voltage from further consideration, as it is identically equal to zero. This results from the solution of the differential equation for v_0:

$$C\dot{v}_0 = -\frac{v_0}{R} \tag{5.38}$$

Hence, the system is reduced to one current i_L and two voltages v_f and v_b. The matrices given above remain the same except for the elimination of

the second row and the second column from them.

The transformed and reduced system is analysed by a perturbation method as described in Appendix B. The steady-state values are calculated by solution of the perturbed equation when the perturbations are equal to zero. The steady-state values of the voltages are simple to calculate in terms of the steady-state inductor current.

$$V_f = \frac{\sqrt{3}\, I_L R D_m}{2\left[1 - j\,\Omega_m / \omega_p\right]} \tag{5.39}$$

$$V_b = \frac{\sqrt{3}\, I_L R D_m}{2\left[1 + j\,\Omega_m / \omega_p\right]} \tag{5.40}$$

The steady-state voltages are complex because they are time varying at the inversion frequency, and the complex quantities represent the effect of the output RC-filter dynamics on their phase and amplitude. The above results indicate that the steady-state output voltages form a balanced three-phase system as they are DC in the rotating frame of reference. Thus, the steady-state inductor current is as given by Eq. (5.30), with steady-state values instead of time varying ones:

$$I_L = I_{ref} - \frac{3\varepsilon V \cos\varphi}{D_m} \tag{5.41}$$

The voltage $\frac{\sqrt{3}}{2} V \cos\varphi$ is the real part of the steady-state forward and backward voltages V_f and V_b, which is equal to $\frac{1}{2}(V_f + V_b)$.

$$V_r = \frac{\sqrt{3}}{2} V \cos\varphi = \frac{\sqrt{3}\, I_L R D_m}{2\left(1 + (\Omega_m / \omega_p)^2\right)} \tag{5.42}$$

The imaginary part of the steady-state voltages V_i is given by

$$V_i = -\tfrac{1}{2}j\,(V_f - V_b) = \frac{\sqrt{3}I_L R D_m \Omega_m / \omega_p}{2(1+(\Omega_m/\omega_p)^2)} \tag{5.43}$$

The expression for I_L given by Eq. (5.41) is substituted in the above equation to give $V\cos\varphi$:

$$V\cos\varphi = \frac{I_{ref} R D_m}{(1+3\varepsilon)+(\Omega_m/\omega_p)^2} \tag{5.44}$$

Hence, the steady-state forward and backward sequence voltages are given by:

$$V_f = \frac{\sqrt{3}\,I_{ref} R D_m \left[\dfrac{1+(\Omega_m/\omega_p)^2}{(1+3\varepsilon+(\Omega_m/\omega_p)^2)}\right]}{2\left[1 - j\Omega_m/\omega_p\right]} \tag{5.45}$$

$$V_b = \frac{\sqrt{3}\,I_{ref} R D_m \left[\dfrac{1+(\Omega_m/\omega_p)^2}{(1+3\varepsilon+(\Omega_m/\omega_p)^2)}\right]}{2\left[1 + j\Omega_m/\omega_p\right]} \tag{5.46}$$

The equations for the small-signal dynamics are linearized by elimination of all second-order perturbation terms. As shown in Appendix B, the Laplace transform is applied to the linearized equations. The transfer functions of the state variables relative to small-signal variations in the inversion frequency and the amplitude of modulation are easily found. These transfer functions are given below, with hatted terms indicating small-signal time varying quantities, all others being dc in the rotating frame of reference:

$$\frac{\hat{v}_f}{\hat{d}_m} = \frac{\frac{\sqrt{3}}{2}[I_{ref}R - \frac{6\varepsilon V\cos\varphi}{D_m}][(1+3\varepsilon)+j\frac{\Omega_m}{\omega_p}+\frac{s}{\omega_p}]}{K(s)} \tag{5.47}$$

$$\frac{\hat{v}_b}{\hat{d}_m} = \frac{\frac{\sqrt{3}}{2}[I_{ref}R - \frac{6\varepsilon V\cos\varphi}{D_m}]\ [(1+3\varepsilon)-j\frac{\Omega_m}{\omega_p}+\frac{s}{\omega_p}]}{K(s)} \tag{5.48}$$

$$\frac{\hat{v}_f}{\hat{\omega}_m} = \frac{j\frac{V_f}{\omega_p}\ [(1+3\varepsilon)-j\frac{\Omega_m}{\omega_p}+\frac{s}{\omega_p}]}{K(s)} \tag{5.49}$$

$$\frac{\hat{v}_b}{\hat{\omega}_m} = \frac{-j\frac{V_b}{\omega_p}\ [(1+3\varepsilon)-j\frac{\Omega_m}{\omega_p}+\frac{s}{\omega_p}]}{K(s)} \tag{5.50}$$

where

$$K(s) = 1 + \frac{s}{Q\omega_0} + (\frac{s}{\omega_0})^2 \tag{5.51}$$

$$\omega_0 = \omega_p\sqrt{(1+3/2\varepsilon)^2 + (\Omega_m/\omega_p)^2}$$

$$\frac{1}{Q} = \frac{(2+3\varepsilon)}{\sqrt{(1+3/2\varepsilon)^2 + (\Omega_m/\omega_p)^2}}$$

The minimum value of Q is 0.5, at a dc inversion frequency. That is not surprising as it means that the circuit reduces to a double pole at ω_0, with one pole and the zero cancelling out. The system simply reduces to what it would be as a dc-to-dc converter.

The above equations appear at first glance to have a second order complex pole and an extra zero. However, closer examination reveals that in each of the transfer functions one pole and the zero are so close that they effectively cancel each other out. It is therefore expected that

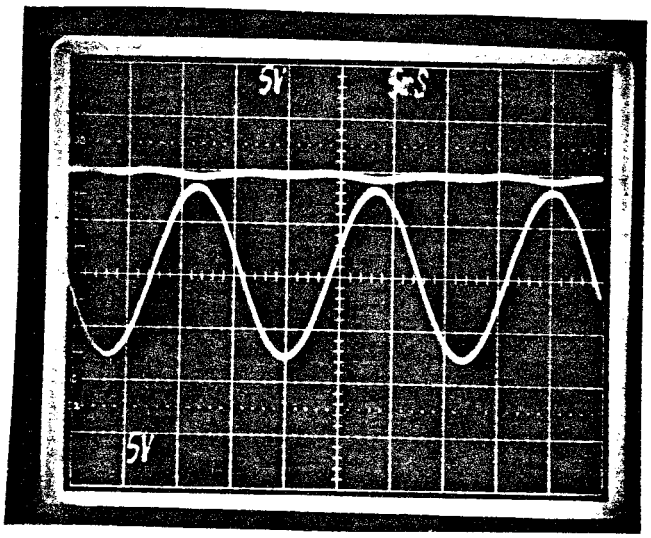

Fig. 5.9 The two independent output voltages of the two-phase flyback inverter with CRP. It is clear that although one is ac and the other dc there is minimal interaction. The output sections are both open loop.

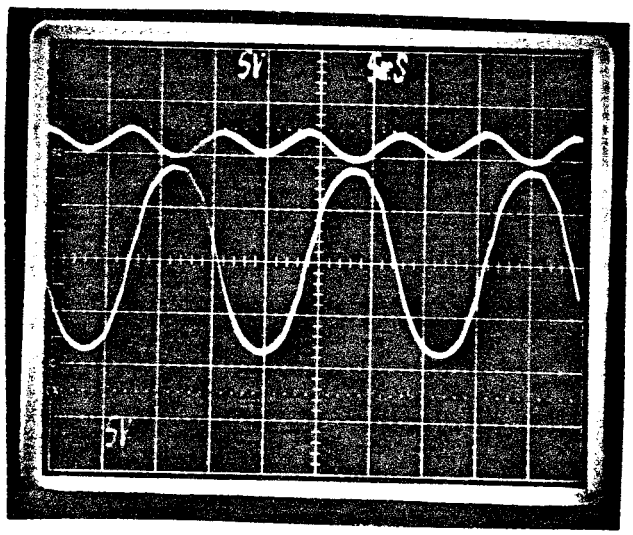

Fig. 5.10 The two outputs of the two-phase flyback inverter without CRP. The two voltages are obviously interacting. The output sections are controlled in exactly the same way as for Fig. 9.

the pole and zero will not affect the circuit significantly in practice. As a matter of fact, the difference between the pole and the zero cutoff frequencies is equal to $3/2\varepsilon$. Hence, once more as ε tends to zero the inverter reduces to the ideal case.

5.5 Experimental Verification

The three-phase flyback inverter using the space multiplexed inductors was built for experimental verification. Several aspects of the operation of this inverter are demonstrated qualitatively. The first aspect shown is the independence of the two outputs of the inverter when operated as an independent dual output converter. Figure 9 shows the two outputs of the converter when one is an ac voltage and the other a dc voltage, neither of which is regulated. It is clear that there is very little interaction.

The photograph of Fig. 10 shows the same two outputs when the current programming loop is taken out of the circuit. The two outputs are affecting each other much more than in the first case. Hence, the independence of the two outputs is a result of the use of current programming as well as the use of the multiple output magnetics. Finally, Fig. 11 shows the effect of the inequality of the currents in the secondary windings at the switch on instant of the input switch. The waveforms exhibit the phenomenon described in Chapter 4.

The generation of the gate or base drive waveforms for the three-phase inverter is done in the same manner as the single-phase flyback inverter. However, the input signals (the balanced sinusoids) need to be generated by special circuits in this case, whereas, for the single-

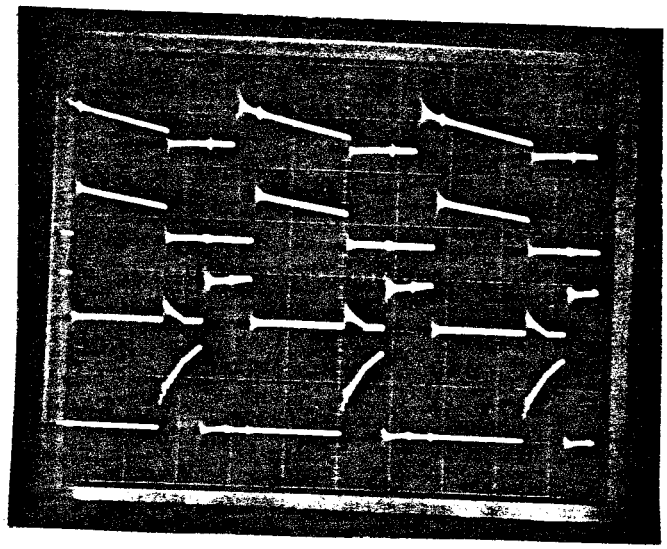

Fig. 5.11 The currents in a three-phase space-multiplexed flyback inverter. The top two traces show i_{3A} and i_{3B}, and the bottom two show i_{2B} and i_1. The final values of i_{3A} and i_{3B} are different. There is a residual current i_{2A} and i_1 exhibits the double slope explained in Ch. 4.

phase inverter, a sine wave generator could be used. This is due to the requirements that the input signals have variable frequency and amplitude yet are always out of phase by 120°.

As far as the demonstration of the operation of the three-phase inverter is concerned the simplest way to generate the signals is to read two EPROMs that have two sine waves stored in them, out of phase by 120° (Fig. 12). This method allows for simple change of frequency and amplitude by use of two potentiometers.

However, to measure the frequency response with the Automatic Measurement System used in the Power Electronics Lab the inputs to the system must track the output of the NF waveform synthesizer. This is because the analyzer is a narrow-band tracking voltmeter that only

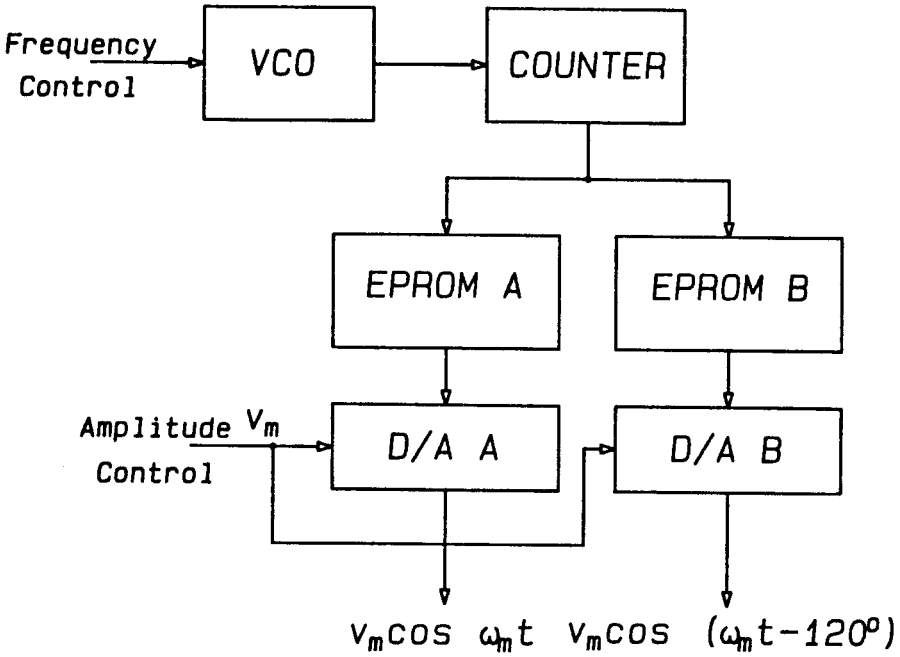

Fig. 5.12 The block diagram representation of the input signal generation circuit. The output of the VCO acts as a clock for the counter that read the addresses of the EPROM. The amplitude of the signal is set by the reference voltage input to the D/A converter.

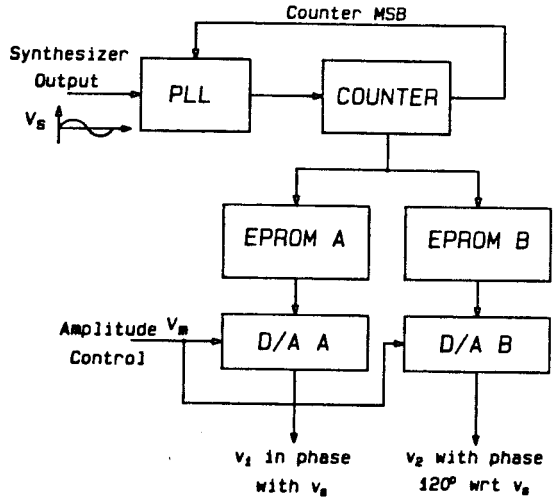

Fig. 5.13 The block diagram of the input signal generation circuit for a signal locked to the analyzer center frequency. It is the same as the above one except for the use of a phase-locked loop to generate the clock signal.

measures frequencies close to the synthesizer output. The same circuit used before is then modified to track the output voltage frequency of the synthesizer by use of a phase locked loop (Fig. 13).

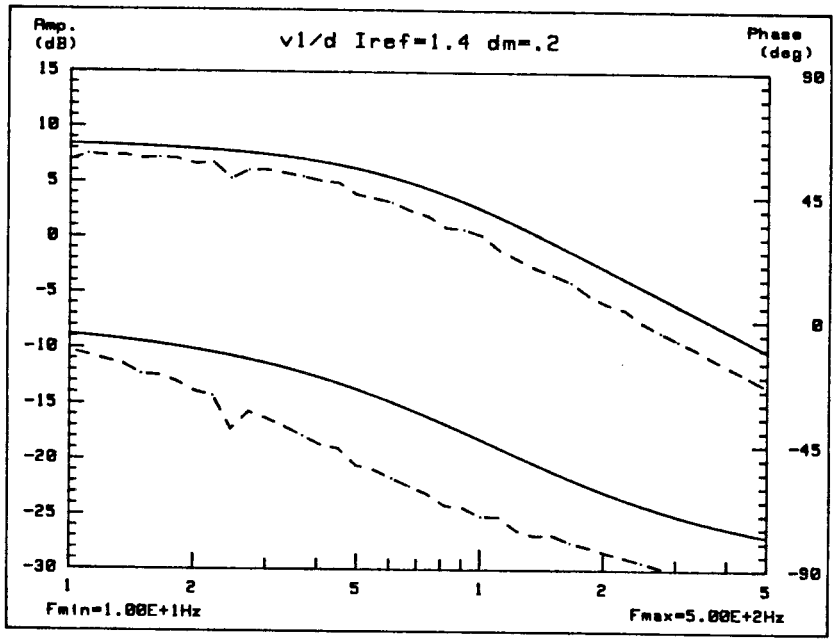

Fig. 5.15 Comparison of measurement (dashed line) and theoretical prediction (solid line) for the control-to-output transfer function of the three-phase flyback inverter. The reference current is equal to 1.4A, and the duty ratio modulation amplitude is 0.2.

The large-signal response of the three-phase flyback inverter (Fig. 14) is measured using the NF analyzer driven from the HP9826 desk-top computer. The measurements are compared to theoretical calculations of the output voltage obtained from Eq. (5.26) for v_1. The measured phase is greater than the predicted phase because of the phase lag introduced by the phase-locked loop. The PLL does not affect the amplitude, thus the predictions and measurements are close.

The fundamental and third harmonic components are measured for v_3, and compared to the theoretical prediction calculated from Eq. (5.28). As for the single-phase inverters, the agreement for the fundamental component is very good (Fig. 15). The agreement for the third harmonics is not as good, for the same reasons cited in Chapter 3. It confirms, however, the order of the magnitude of the harmonic components, and hence the linearity of the inverter.

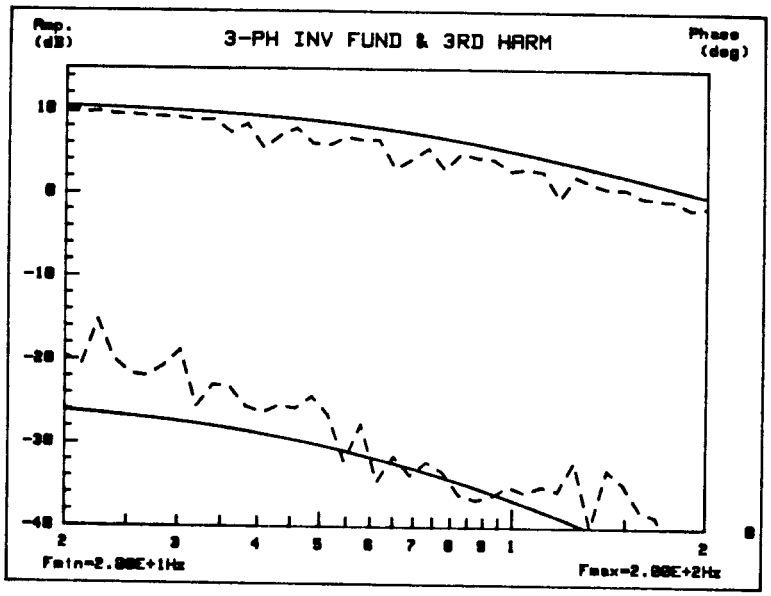

Fig. 5.15 Comparison of measured fundamental and third harmonic components (dashed lines) with the predictions for v_3. The agreement is very good for the fundamental (top), quite good for the harmonics (bottom).

5.6 Conclusions

The three-phase versions of the coupled inductor inverters are obtained. The two types of multiple output magnetics introduced in Chapter 4 are used with the four basic single-phase inverters to generate the three-phase inverters. Similarly to the single-phase case the large

signal analysis using a power series expansion of the voltages is made. The result of that analysis confirms that the three-phase inverters preserve the main advantages of the corresponding single-phase inverters which are: a smaller number of switches, high linearity, improved dynamics and fast pulsed load response.

With some manipulation of the states the abc-ofb transformation is applied to the system. Thus, small-signal perturbation is used to calculate the small-signal response of the system. The importance of this analysis is to offer a basis of comparison with other systems where this method has been applied. Similarly, the transformation method is extensively used in the calculation of the small-signal transfer functions of electrical machines. In systems where the three-phase inverter drives a three-phase motor, for instance, those transfer functions are useful in the design of the feedback loop.

CHAPTER 6

Three-Phase Ac-to-dc Rectifiers

6.1 Introduction

Rectifiers have been in use since the beginnings of ac power generation. For instance, all modern electronic appliances from computers to hifis have a rectifier circuit that forms the interface between the ac power lines and the internal dc power. Until recently rectifier circuits consisted mainly of uncontrolled switches (diodes) that were turned on or off according to the polarity of the voltage applied to them. One of the main drawbacks of this type of rectifier is the input current waveform that pulsates at the line frequency or at half the line frequency [22,23], depending on whether the rectifier is a full wave or a half wave one. Furthermore, a 60 Hz (or 50 Hz) transformer is required at the input to bring down the line voltage to a value closer to the output voltage. The rectified waveform is then filtered by a large capacitor followed by a linear regulator to give the required output voltage.

The line frequency transformer is a very bulky and heavy component in the circuit. It has been eliminated by the use of off-line switchers [24]. These consist of the rectifier and filter portions as before without the transformer. These are followed by a dc-to-dc converter that steps down the voltage to the required value and regulates it simultaneously. The converter switches at a high frequency (usually greater than 20 kHz). The size and weight of the magnetics is then much smaller

than with the linear regulator. There is also a reduction in the losses as opposed to the linear regulator. Hence, the overall power supply is much smaller than before.

However, that system still suffers from the pulsating input current at the line frequency, as well as an inductive power factor. These two aspects of rectifiers affect other users as the inductive type of load sends back power to the line. The pulsating current also is a drawback as it might affect other users close-by. The generally inductive type of load encountered by the utilities forces them to build costly power factor correction circuitry that generally reduce the efficiency of the overall power system. The pulsating currents at the input of the rectifier also affect the generators as they cause load pulsation at the line frequency, thus making it impossible to filter out.

A rectifier system that has sinusoidal input currents with no phase lag or even a phase lead is a highly desirable system. The three-phase inverters of Chapter 5 are very easily transformed into such rectifiers. The load and input voltages are simply interchanged, the output ac switches becoming the input switches and vice versa. These rectifiers are introduced in this chapter. It is shown that there is a way to operate the rectifiers with current programming and at the same time to maintain the sinusoidal input current property with control over the phase angle. The transfer function for the rectifier is derived, and experimental verification is done with a flyback type of rectifier.

6.2 Description of Three-phase Ac-to-dc Coupled-Inductor Rectifiers

The rectifier power circuit is basically the same as the three-phase inverter circuit (Fig. 1). As before, there are two types of coupled inductor rectifiers: the time-multiplexed and the space-multiplexed ones. However, the multiple output magnetics now are multiple input magnetics. In order to avoid confusion in the notation the switches and their duty ratios have the same names as in the inverters. Hence, the ac switches are d_{2A}, d_{2B}, d_{3A}, and d_{3B}, and the dc switch (the output switch) is d_1. The numbers do not indicate the order of switching.

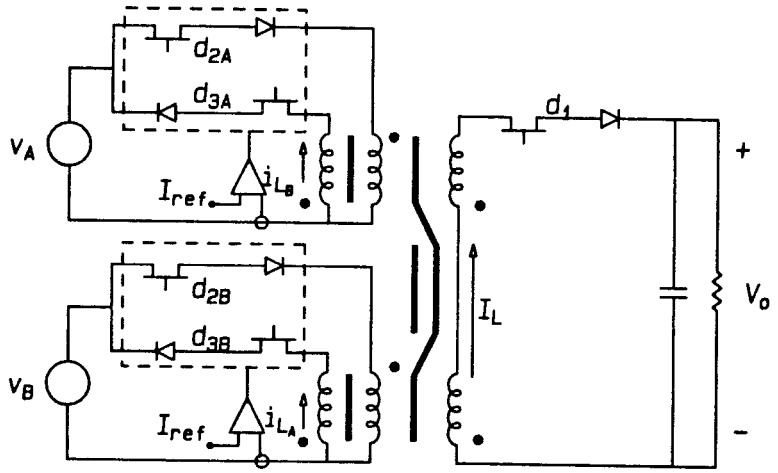

Fig. 6.1 A flyback space-multiplexed rectifier with the current loops. The reset diodes are not shown, but they are as in Ch. 4.

The time-multiplexed magnetics behave in a similar manner in both the inverter and the rectifier. However, the space-multiplexed magnetics are not reciprocal. This results from the analysis of the magnetics done in Section 4.8. One practical aspect of the non-

reciprocality of the magnetics is the need to create a reverse path for the residual currents in the input inductor. As shown in Section 4.8 this is achieved by the addition of a back-to-back diode and zener diode (Fig. 1).

The choice of the zener voltage is determined by several practical considerations. The zener voltage, on the one hand, has to be larger than the peak input voltage so that it does not conduct during the input period. The reverse current flows through the zener diode when the fluxes in the two input sections are unequal. The current slope is proportional to the zener voltage and positive. As the current direction is negative it decays to zero. Hence, the larger the zener voltage the shorter the transient period. On the other hand the switches must be able to handle the voltage stresses and this sets an upper bound on the zener voltage.

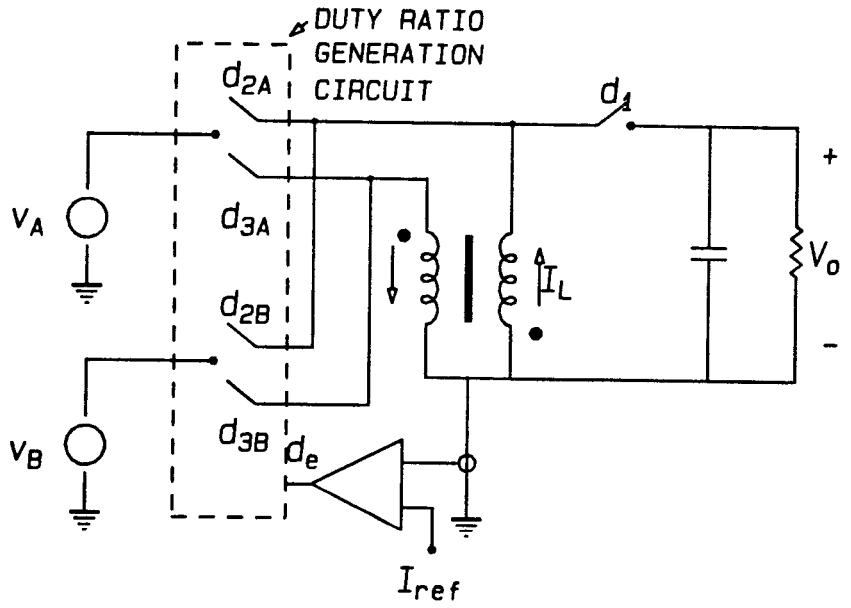

Fig. 6.2 The time-multiplexed flyback rectifier. There is only one current sense circuit required. There is also no need for the diode reset circuit.

Furthermore, the implementation of CRP in the inverter requires the sensing of both inductor currents. Current programming must be applied to the input switches to yield results similar to the ones obtained for the inverters. Thus, the current transformers have to be on the ac switch side. Hence, there have to be two current sense circuits, one for each pair of coupled inductors. In the rectifiers with time multiplexed magnetics only one current sense circuit is required (Fig. 2).

The current under consideration in the space multiplexed case is the current in the single (the output) inductor. The results of Chapter 4 for the multiple input magnetics show that the initial current in the output inductor is approximately equal to the mean value of the final input currents. Hence, the controlled value of current in the rectifier is the mean of the two input currents. The current sense circuits also have a bridge rectifier at the output as the input currents are bidirectional yet are compared to a fixed dc level (Fig. 3).

The rectification action is done by the switches at the input side. The polarity of the voltage applied to the inductor is almost instantaneously changed according to which of the two switches is on. As the flux is constant in the inductor this means that the current changes direction. Hence, regardless of the polarity of the input voltage the switching can always be done in such a way that energy is stored in the inductor during the input switching period. That input switching period is defined, in this case, as being $d_2 + d_3$.

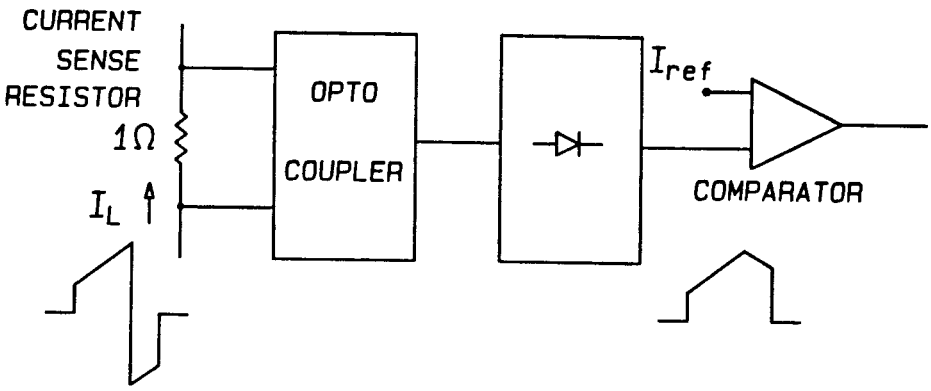

Fig. 6.3 The current sense circuit. The circuit is optically coupled for isolation. The rectified output is compared to a dc level.

6.3 Operation of Three-Phase to Dc Rectifier

Recall that in the inverter circuit the single input switch is controlled only by the CRP loop. The output switches were then capable of generating any attainable output voltage while maintaining the length of switching period constant. In the rectifier, however, the paired switches are controlled by the CRP loop, determine the shape of the current and still maintain the length of the switching period constant. Hence, there are many more ways of controlling those switches than in the case of the inverter. It is, therefore, the aim of this section to describe the different modes of operation that are possible with these rectifier topologies. The discussion centers mainly on the flyback topology (Fig. 4) although the same can be said for the others with slight modifications.

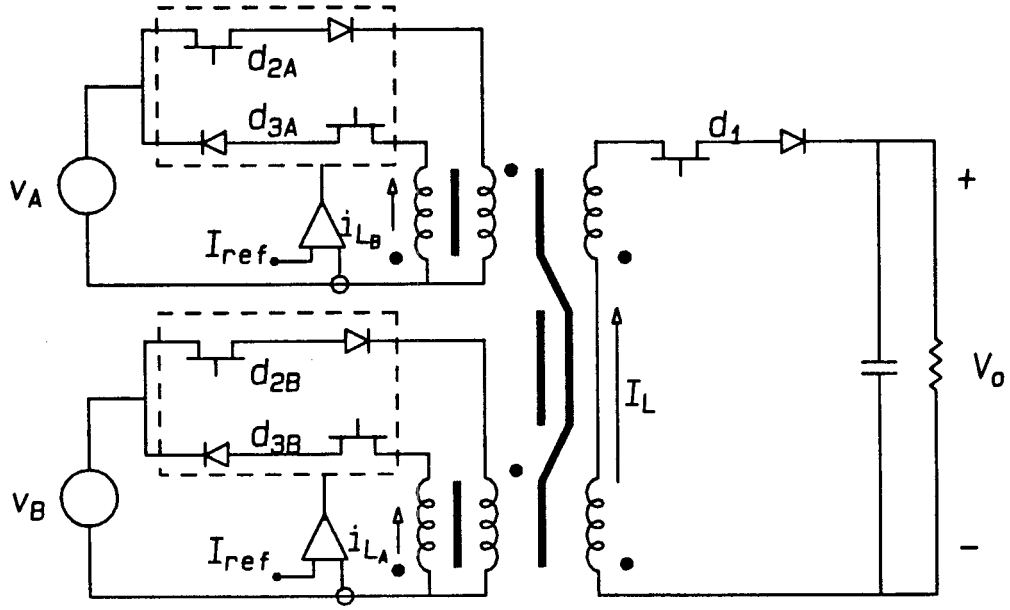

Fig. 6.4 The flyback space-multiplexed rectifier.

As mentioned before, there are three main specifications that should be achieved by the rectifiers. The first two concern the input current waveforms: they should ideally be sinusoidal and have a zero phase with respect to the input voltages. The third specification concerns the internal operation of the rectifier: the inductor current must be programmed, that is it must reach a fixed value at the end of the input switching period.

6.3.1 Sinusoidal Input Currents

It is possible that the specifications are so restrictive that they cannot be simultaneously satisfied. However, if one assumes, at first, that the system under consideration is ideal, that is the switching frequency or the inductor value is infinite, then a sinusoidal input current in phase with the input voltages gives a fixed current in the inductor.

A constant power flow argument proves the above statement. Let the load and output voltage be fixed. Then the output power is constant. As the rectifier is assumed to be ideal there are no losses and so the input power is equal to the output power. There is an infinite number of input currents waveform that satisfy this criterion from a three-phase input voltage. For example, a three-phase ac-to-dc rectifier with diodes has constant power flow with pulsating input currents. More significantly a set of balanced sinusoidal input currents also guarantee constant power flow.

$$\begin{aligned} p &= v_1 i_1 + v_2 i_2 + v_3 i_3 \\ &= VI(\cos^2 \omega_m t + \cos^2 (\omega_m t - 120°) + \cos^2(\omega_m t + 120°)) \\ &= 3/2\, VI \end{aligned} \tag{6.1}$$

where v_1, v_2, and v_3 form a positive sequence balanced three-phase system and i_1, i_2, and i_3 are the corresponding phase currents.

The currents in the above equation are in phase with their respective phase voltages. However, the voltages applied to the inductors are not the phase voltages, but are given by:

$$v_A = v_1 - v_3 = \sqrt{3} V \cos(\omega_m t - 30°) \tag{6.2}$$

$$v_B = v_2 - v_3 = \sqrt{3} V \cos(\omega_m t - 90°) \tag{6.3}$$

The inductor currents iA and iB are respectively equal to the phase currents i_1 and i_2. Thus, under ideal conditions, it is sufficient to modulate the input switches sinusoidally in phase with the phase voltages to achieve the desired characteristics.

$$I_{final}-I_1 = \frac{T_s}{2L}[v_A d_m \cos \omega_m t + v_B d_m \cos (\omega_m t - 120°)]$$

$$= \frac{3}{2}\frac{d_m V T_s}{L} \qquad (6.4)$$

In the above relation if I_1 is the same at the beginning of every input cycle then I_{final} will be a constant value. This condition is satisfied when the load is constant and the input voltage amplitude does not change.

Hence, under idealized conditions, the application of a sinusoidal modulation to the duty ratios is equivalent to CRP. It is, however, an open loop system and is not practically useful as far as implementing the CRP is concerned. It is possible to refine it slightly by introducing some feed-forward from the input voltage in such a way that the modulation amplitude times the input voltage amplitude remains invariant. In this manner input voltage fluctuations do not affect the operation of the rectifer, but load variations still affect it.

6.3.2 Current Programming in Rectifiers

Some form of feedback is then needed to maintain the current in the inductor regardless of changes in the operating conditions. Furthermore, that feedback loop must operate on a pulse by pulse basis as in the inverters. The advantage of this is that it responds to disturbances within a switching cycle. The inductor then looks like a current source to the output. It should be pointed out that a fixed inductor current does not imply sinusoidal input waveforms.

An important property of the switches used in practical circuits should be described before proceeding. If the two transistors connected to the same coupled-inductor pair are turned on simultaneously the one that conducts is the one with the current of positive slope. This is due to the natural turn-on of the diode with the positive voltage applied to it, while the other is back-biased. As far as the inductor is concerned it requires only one path to maintain continuity of flux.

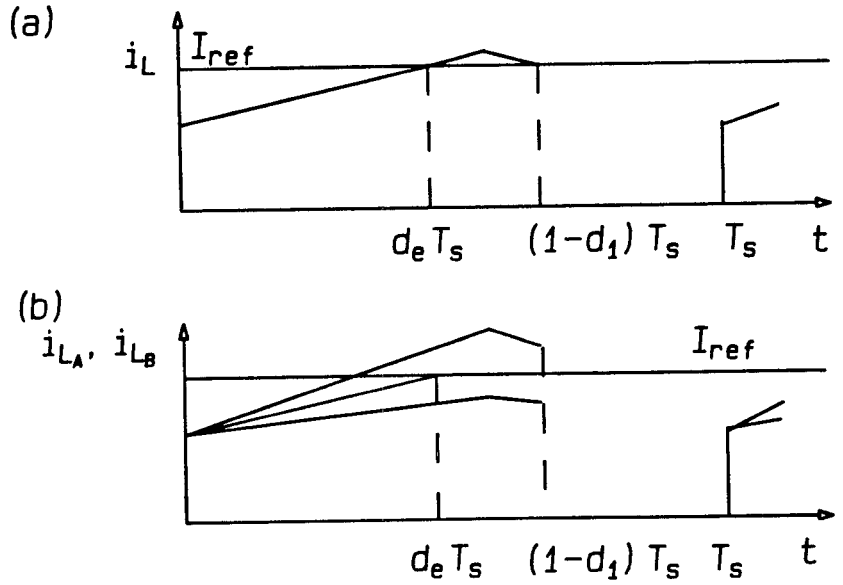

Fig. 6.5 (a) The rectified inductor current in a time-multiplexed rectifier. The larger of the two input voltages is chosen and the switches connected to that input are the only ones turned on. (b) The currents in the space-multiplexed rectifier. The control circuit senses the instant the current reaches I_{ref}, and pads the rest of the period so that the final current is equal to I_{ref}.

The importance of this property resides in the fact that if the current is allowed to ramp down initially, there is a causality problem. The length of the ramping down period is determined *after* the current reaches I_{ref}. Clearly if the current begins to ramp down it does not reach

I_{ref} and ending that period presupposes the knowledge of the length of the ramp-up period. Hence, one does not need to worry about the correct switching sequence as the circuit takes care of it naturally.

If, at first, one relaxes the current waveform constraint a relatively simple CRP loop can be implemented. In the case of the time-multiplexed rectifier there is a simple control algorithm. Choose the higher of the two input voltages, connect the inductors to that voltage, let the current ramp up until it reaches I_{ref}, then fill up the rest of the period (that is let $d_2+d_3=1-d_1$ (Fig. 5a)). This case is the simpler one because there is only one current to monitor and to control.

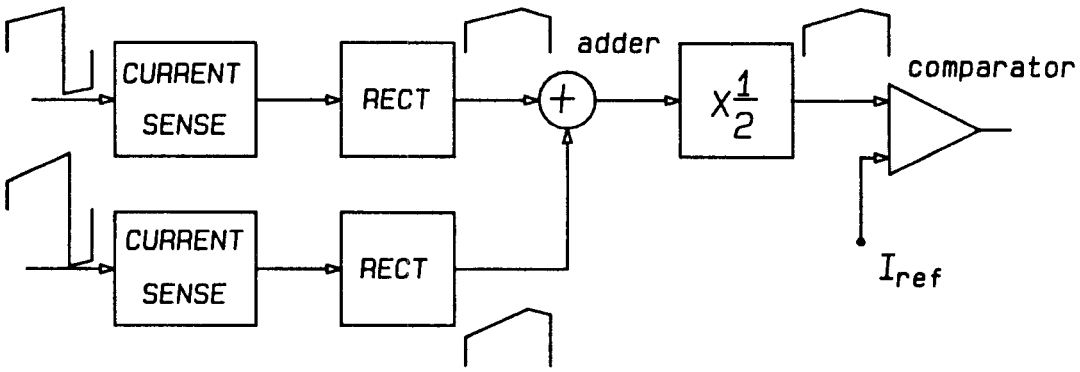

Fig. 6.6 Block diagram of the current sense circuit and the generation of the switching signal for the space-multiplexed rectifiers.

As mentioned before the current value of interest in a space-multiplexed rectifier is the mean of the two input currents (Fig. 5(b)). The mean of the rectified outputs of the two current sense circuits is

calculated using an OP-AMP adder. The output of the OP-AMP is input to the comparator (Fig 6). The comparator in the current programming loop fires at the point in the cycle where the average of the input currents is equal to I_{ref}. The length of that period is called $d_e T_s$ to indicate it is the effective length required for implementation of current programming. From the current waveforms in Fig. 5b one gets:

$$I_{ref} - I_1 = d_e T_s \frac{(|v_A| + |v_B|)}{2L}$$

when $L_A = L_B = \frac{1}{2}L$. The modulus of the input voltages is taken as it indicates the rectification action that results from the switching method. That value d_e is then used to calculate the lengths of the periods d_{2A}, d_{2B}, d_{3A} and d_{3B} that satisfy the following equations:

$$1 - d_1 = d_{2A} + d_{3A} = d_{2B} + d_{3B} \tag{6.5}$$

$$d_e = |d_{2A} - d_{3A}| = |d_{2B} - d_{3B}| \tag{6.6}$$

The above relations imply that the currents in the two phases flow for the same amount of time. If one assumes that the current ripple is very small then the average input currents are equal to:

$$i_{L_A} = i_{L_B} = I_{ref} d_e$$

$$= I_{ref} \frac{2L}{T_s(|v_A| + |v_B|)} \tag{6.7}$$

The shape of the rectified voltage function is shown in Fig. 7. It does not have a simple description as it is discontinuous. However, it is clear that the current shape is not sinusoidal.

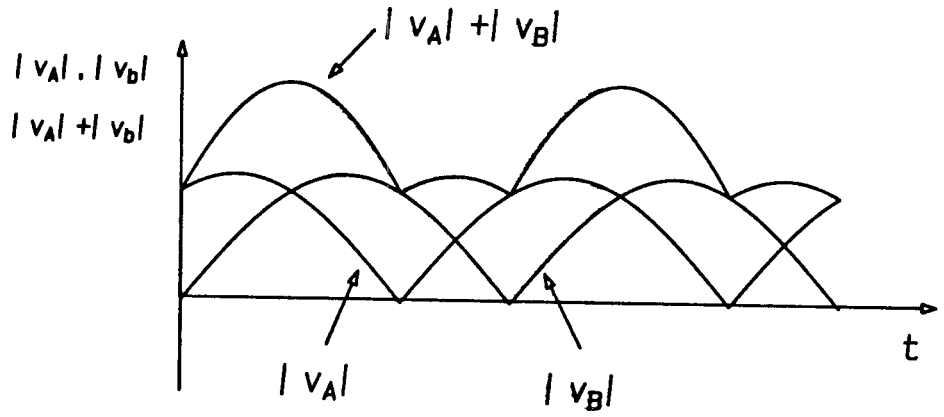

Fig. 6.7 The rectified input voltages and their sum. It is not possible to describe that function mathematically in a closed form.

6.3.3 Current Programming and Sinusoidal Currents

The first method shows that under ideal conditions a sinusoidal switch modulation yields a fixed current in the inductor. The second shows how CRP can be implemented simply if the current shaping requirements are completely relaxed. It is then possible to implement the feedback by sacrificing some of the purity of the sinusoidal input current waveforms. The switches are essentially modulated sinusoidally, as before. However, the amplitude of modulation is varied on a cycle by cycle basis according to the requirements of the CRP loop. In other words, the basic sinusoidal signal is amplitude modulated by the current programming loop.

Once more, one comes face-to-face with a causality problem. The problem is more acute in the case of the space-multiplexed rectifier as everything happens simultaneously. The problem is that one must calculate

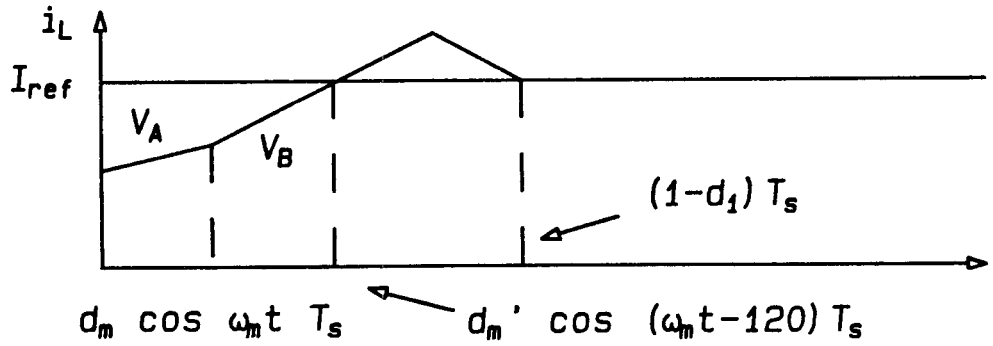

Fig. 6.8 Rectified inductor current in a time-multiplexed rectifier operated with current programming and sinusoidal input currents. The length of the first period is set by use of d_m calculated from the previous cycle. The second period length is set by the CRP loop. The third period is just for padding. The new d_m is calculated for use in the next cycle.

the lengths of the periods in such a way that at the *end* of the input period the currents satisfy $\frac{1}{2}(i_{L_A}+i_{L_B})=I_{ref}$. To compound the problem, under certain conditions, the current in one inductor must start the ramp-down period *before* the mean has reached I_{ref}.

The solution of this problem in the time-multiplexed rectifier is easier to find (Fig. 8). It also gives a hint on how to solve it in the other case. Let the effective duty ratios at the cycle under consideration be such that $d_A = d_m\cos\omega_m t < d_B = d_m\cos(\omega_m t-120°)$. Assume that one knows the amplitude of modulation d_m from the previous cycle. That value is then used to calculate the length of the ramp-up period for the shorter of the two. Phase A is turned on first. At $d_A T_s$ phase A is turned off and

phase B is turned on. It is then left on until the current reaches I_{ref}. The effective length of this period is then used to calculate the new d_m for use in the next cycle. That is done by assuming that the length of the second period is equal to $d'_m \cos(\omega_m t - 120°) T_s$. The period is then padded out in the usual manner. The next cycle uses the new value of d_m to calculate the shorter duty ratio.

The above method uses the property of balanced three-phase systems shown in Section 6.3.1. Thus under steady state conditions the currents are sinusoidal and the inductor current is at I_{ref}. Under transient conditions the currents are quasi-sinusoidal, yet the CRP is still in effect. When the new steady state is reached the currents are again sinusoidal. This solution resembles the CRP in the inverter, insofar as it is one switch that determines the value of the current from a certain point on.

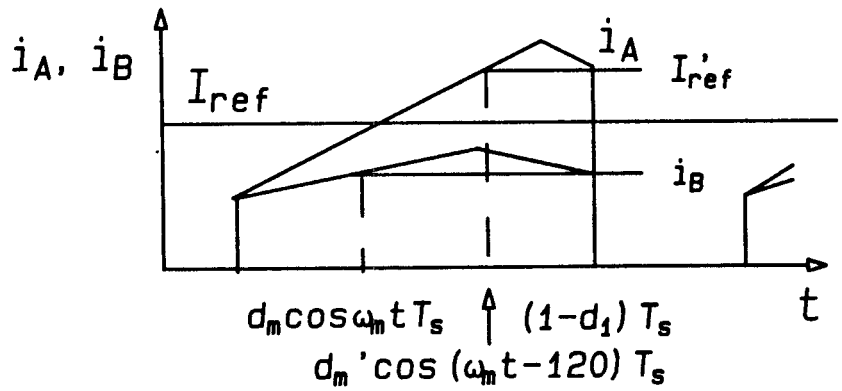

Fig. 6.9 The rectified inductor currents in a space-multiplexed rectifier with CRP and sinusoidal input currents. The control algorithm is similar to that of the time-multiplexed rectifier.

As stated before the solution for the space-multiplexed version is more complex. The reason for this is that the two phases are affecting the final value of the inductor current. There is no easy way of decoupling the effects of the two phases as happens in the time-multiplexed version. In the time-multiplexed case the final current for one phase is the starting current for the next one, and the length of the remaining period is known. So the generation of the switching waveforms is straightforward. Both currents are flowing during the whole period in the space multiplexed magnetics. However it is possible to find out the final value of the current in either phase before the end of the input period. The reason for this is that the current in the inductor at the effective duty ratio instant is equal to the final current at the end of the input period (Fig. 9).

The ramp-up periods are started first for both phases at the same time. Phase A is once more switched to give $d_A = d_m \cos\omega_m t$ with the amplitude obtained from the previous cycle. The value of the inductor current i_{L_A} at $d_A T_s$ is retained so as to calculate the reference value that is actually used for the other switch.

Hence the new reference value that is input to the comparator is given by:

$$I'_{ref} = 2I_{ref} - i_{L_A}[nd_A T_s] \tag{6.8}$$

The current in phase B is then switched in such a way that $i_{L_B}(d_B T_s) = I'_{ref}$. The period is padded out as usual. Thus the final value in phase A is $i_{L_A}(nd_A T_s)$ and the one in phase B is I'_{ref} and so the initial value in the output inductor is:

$$i_L[n(1-d_1)T_s] = \frac{I_{ref} + i_{L_A}[nd_A T_s]}{2}$$

$$= I_{ref} \tag{6.9}$$

The time-multiplexed and space-multiplexed versions of the inverters are comparable in qualities and drawbacks. There is no absolute preference for one type over the other. However, in the case of the rectifiers it appears that the time-multiplexed versions have several advantages. There is no need, for example, to use the extra diodes for resetting the input inductors. They also need only one current sense circuit and the amount of calculations is much smaller. In the next chapter on cycloconverters it will be seen that the time-multiplexed versions are the only practically useful ones.

6.4 Analysis of Coupled-Inductor Rectifier

The analysis of the rectifiers is quite simple as opposed to that of the inverters. The difficulty for the inverters resides in that the output states are time-varying. In the case of the rectifier the states are all dc. The inputs are balanced three-phase sinusoids. However, as long as the current programming loop functions properly, as described in the previous section, the output is decoupled from the input.

It is therefore required to give the ranges of input voltages and loads that allow the rectifier to operate with CRP. The same arguments used in Chapter 2 are used here. The relations for the maximum load are the same as in Chapter 2. The ones for the input voltages are slightly different. The same relation has to be satisfied for the time and the

space-multiplexed versions, however subject to different restrictions. The main relation for the input voltages is:

$$v_A d_A + v_B d_B \geq V_o \, d_1 \tag{6.10}$$

with the following condition for the time-multiplexed rectifier:

$$d_A + d_B \leq 1 - d_1 \tag{6.11}$$

and for the space-multiplexed rectifier:

$$d_A \leq 1 - d_1 \quad \text{and} \quad d_B \leq 1 - d_1 \tag{6.12}$$

These conditions are assumed to hold for the rest of the analysis.

The inductor always carries the same value of current. The output relations can then be written out by inspection:

$$V_o = I_{ref} R d_1$$

for the ideal case (infinite inductor or switching frequency). In the practical case there is a current droop that must be accounted for:

$$V_o = [I_{ref} - \frac{V_o D_1 T_s}{2L}] \, RD_1$$

$$= \frac{I_{ref} RD_1}{(1+2\varepsilon)} \tag{6.13}$$

where $\varepsilon = D_1^2 RT_s / 4L$.

It is also simple to construct the state equations for calculation of the small-signal dynamics:

$$\begin{bmatrix} L & 0 \\ 0 & C \end{bmatrix} \dot{\boldsymbol{x}} = \begin{bmatrix} -1/R & -d_1 \\ d_1 & -1/R \end{bmatrix} \boldsymbol{x} + \begin{bmatrix} d_A & d_B \\ 0 & 0 \end{bmatrix} \begin{bmatrix} v_A \\ v_B \end{bmatrix} \tag{6.14}$$

where

$$\boldsymbol{x} = \begin{bmatrix} i_L \\ v_o \end{bmatrix}$$

The operation of the CRP loop allows the current to be determined exactly from the following equation:

$$i_L = I_{ref} - \frac{d_1 T_s}{2L} v_o \tag{6.15}$$

This equation for the current is substituted in Eq. (6.14). The differential equation for the voltage results:

$$\frac{1}{\omega_p} \dot{v}_o = I_{ref} R d_1 - \frac{d_1^2 R T_s}{2L} v_o - v_o \tag{6.16}$$

The above equation is non-linear, but as the steady-state values of the state variables are dc it is solved by small-signal perturbation. As before the variables are assumed to consist of a large steady-state value plus a small-signal ac perturbation.

$$v = V + \hat{v} \qquad d_1 = D_1 + \hat{d}_1 \tag{6.17}$$

The small-signal perturbed equations are obtained by substitution of Eq. (6.17) into Eq. (6.16). Note that the steady-state results obtained by inspection in Eq. (6.13) may also be calculated from the perturbed equation by letting the perturbations equal zero and solving the equation for $\dot{X}=0$. As before the term $\frac{D_1^2 R T_s}{2L}$ is substituted for by 2ε. The

equations are linearized by neglecting all higher order perturbations.

$$\frac{1}{\omega_p}\dot{\hat{v}}_o - (1+2\varepsilon)\hat{v}_o = (I_{ref}R - \frac{4\varepsilon}{D_1}V_o)\hat{d}_1 \tag{6.18}$$

The Laplace Transform of the above equation is applied to give the small-signal transfer function of the flyback coupled-inductor rectifier.

$$\frac{\hat{v}}{\hat{d}_1}(s) = \frac{I_{ref}R - \frac{4\varepsilon}{D_1}V_o}{[(1+2\varepsilon)+s/\omega_p]} \tag{6.19}$$

As expected the system is of the first order. The rectifier operated with current programming has the same properties as the inverter. Those properties are linear gain characteristics, single-pole dynamics and very fast pulsed load response.

Another property of the rectifier circuit presented here is that it may have very large step-down ratios without going to extreme duty ratio values. A 2SN dc-to-dc flyback converter, for example, has a steady-state gain that is given by:

$$V_o = -\frac{D}{(1-D)}V_g \tag{6.20}$$

where V_g is the input dc voltage. To obtain a large step down in voltage, say 1:10, D has to be approximately equal to 0.1. In general, the operation of the dc-to-dc converters close to the limits of the duty ratios is not a very good idea as these are the regions of least efficiency. As the switching is extremely fast at such small duty ratios, the switching losses are proportionately larger. This problem is usually solved in the case of 2SN converters by use of an isolation transformer with a large step-down ratio.

The voltage is then regulated by the duty ratio control.

The coupled-inductor rectifier, on the other hand, may have a large step down ratio without going to extreme duty ratios. The reason is that the input effective duty ratio is the result of the subtraction of two real duty ratios. It may be very small without either of the two duty ratios being small. The choice of duty ratio values can be optimized for maximum efficiency by proper choice of I_{ref} and of D_1 given the specified load conditions. The problem has not been analyzed quantitatively yet, but it is possible that the drawback of large circulating currents in the coupled-inductor rectifiers with CRP can be overcome by the reduction of the switching losses. It is still an open question, yet it is quite tractable; it opens up possible avenues of future research.

The coupled-inductor rectifier then performs the role of rectifier, step-down transformer and regulator. As most rectifier applications require large step down ratios from the ac line voltages that are in the hundreds of volts down to the dc suply voltages that are typically of the order of five or fifteen volts. Hence, the coupled-inductor rectifier has added advantages of simplicity, compactness and reduced parts count over other systems.

It should be noted that, although the control circuits are slightly more complex than in other systems, it is not necessarily a drawback. Recent advances in integrated circuit manufacturing and design allow the increasing use of semi-custom and custom designed ICs. The control circuit for all its complexity may be integrated on one chip as it uses standard gates and components. Thus the complexity of the control circuit is reduced to one custom designed chip and allied to the advantages of the

power circuit results in a total system that is very useful and compact.

6.5 Experimental Verification

The experimental version of the flyback space-multiplexed rectifier is built to verify some of the results givne above. The rectifier is tested under the two types of operation described in Section 6.3.1 and 6.3.2. In the first case a simple sinusoidal modulation is applied to the input switches. The order of switching is not important in this case. A switching scheme such as the one used for the three-phase inverters is used here.

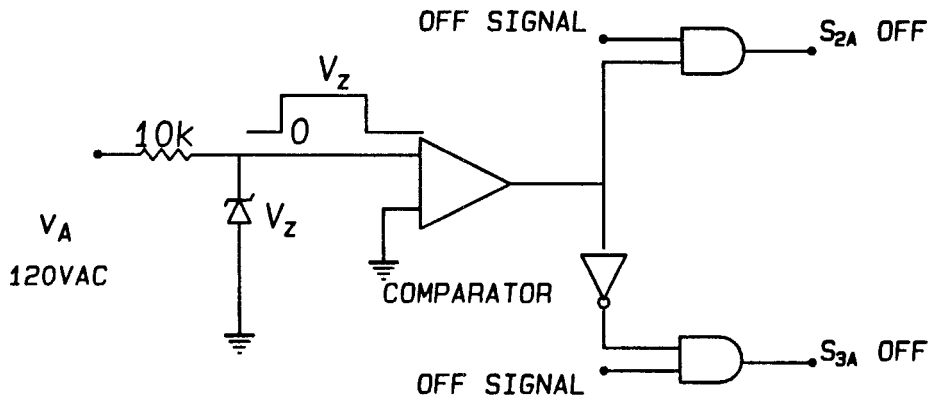

Fig. 6.10 The circuit used to determine the switch that is to be turned off. This is done by sensing the polarity of the input voltage.

The control circuit is different for the current programmed rectifier. All the switches are turned on at the same time. Because of the diodes only the ones with positive current slope at that moment conduct. The control circuit must sense which of the switches are conducting as it needs to generate the off signal for that switch. The input voltage is then

sensed and according to its polarity one of the two switches will be turned off. At the end of the input period $(1-d_1)$ the other two switches are turned off and the output switch is turned on. Hence, the on signal for the input switches is the same as the off signal of the output switch, one set of input switches is turned off by a signal from the current sense circuit, finally the remaining switches are turned off by the same signal that turns the output switch on.

The off pulse is switched from one input switch to the other by a signal generated from a comparator set up as a zero crossing detector (Fig. 10). Each phase voltage is sensed through a large resistor and a zener diode to bring the voltage down to digital signal levels. As mentioned before the complexity of the signal generation scheme is not a real drawback. All the circuits used are standard comparators, OP-AMPs and logic gates.

It should be noted that the off instant for the first output switch is not the instant that the mean current reaches I_{ref}. That instant is equal to d_e and the actual switch off instant is d_2 or d_3. These values are chosen to satisfy the two constraints given by Eqs. (6.5) and (6.6). Thus, the current comparator output is used to give the hold signal to a sample and hold circuit. This sample-and-hold circuit stores the current value of the ramp voltage v_e (Fig. 11). The voltage v_2 (or v_3) is then calculated from the following relation:

$$v_2 = \frac{V_{max} - v_1 + v_e}{2} \tag{6.21}$$

The voltage v_2 is the voltage corresponding to the turn off instant of the

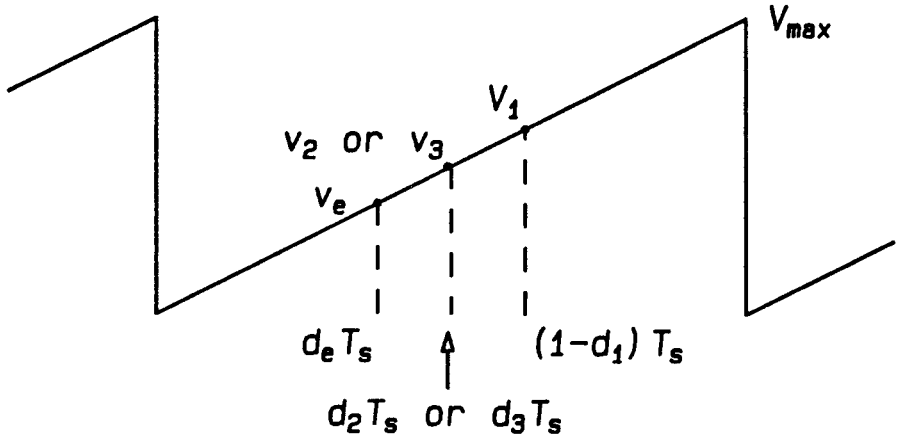

Fig. 6.11 The ramp voltage shows the relation between the different control voltages and the switching instants. The voltage v_e corresponds to the instant the current reaches I_{ref}. It is then used to calculate with v_1 the actual switching instant.

two switches with current of positive slope regardless of the polarity of the voltage.

The waveform photographs of Fig. 12 show the sinusoidal input current in the first case. The actual current is a sinusoidally modulated PWM. The current shown is filtered to show the sine wave. In practical circuits there is always an input filter to reduce conducted electromagnetic interference (EMI). Thus, in practice the currents shown are the actual currents at the input of the rectifier. The photograph of Fig. 13 shows the currents in the space-multiplexed inductor and the reset diodes when the fluxes are unequal in the two loops. This confirms the prediction of Chapter 4.

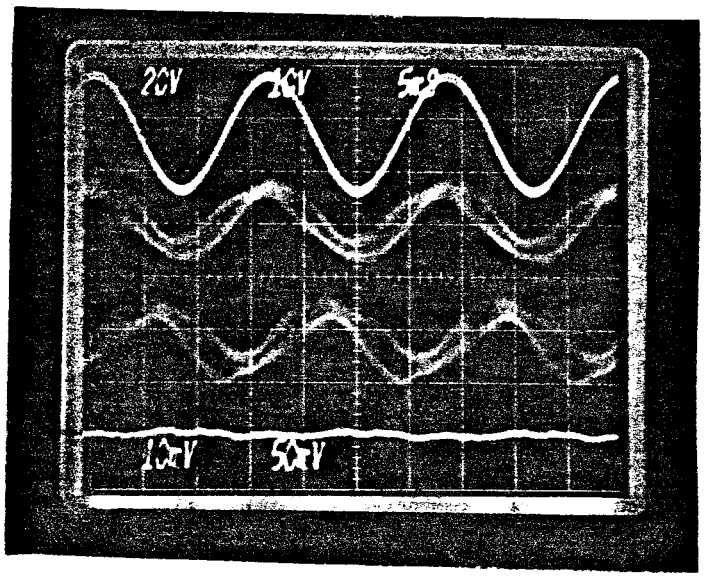

Fig. 6.12 The top trace is one of the input voltage phases. The next two traces are the input currents to the rectifier. They are sinusoidal and in phase with the voltages. The bottom trace is the output voltage. The rectifier is operated without any feedback.

The output voltage to duty ratio transfer function is measured by injecting the small-signal ac perturbation on top of the steady-state dc. The rectifier in this case is being operated with current programming without sinusoidal input currents. The experimental results are compared to the theoretical calculations in Fig. 14. There is good agreement between the two. The transfer function has a single pole type of response which is to be expected.

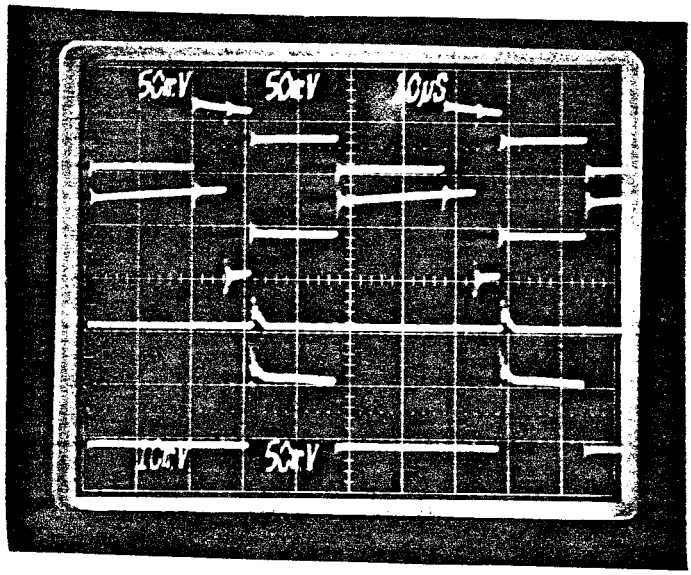

Fig. 6.13 The top two traces are the input current phases to the rectifier. The next trace is the reset diode current. The lower trace is the output current. This confirms the prediction of Chapter 4 for the currents. Note that the scale on the bottom two traces is twice that of the top ones.

6.6 Conclusions

The coupled-inductor rectifiers, that perform the reciprocal function of the three-phase inverters, are introduced in this chapter. They are found to exhibit the same properties as the inverters. However, the switching schemes required to attain the same level of performance are much more complex than the ones of the inverters. That is found to be not a problem of the topologies but an inherent problem due to the fact that all the performance specifications must be achieved by the input switches. The input switches, are required not only to maintain the programmed current in the inductor but must also simultaneously shape the input current waveform and keep the switching period constant.

All the objectives stated above are attainable by the coupled inductor rectifiers. The rectifiers with the time-multiplexed magnetics are found to be simpler to control. They also require only one current sense circuit and very few calculations, as opposed to two current sense circuits and a fair amount of calculations in the space-multiplexed rectifiers. Furthermore, the space multiplexed rectifier require an additional pair of diodes and zener diodes to reset the input windings when the final fluxes are unequal.

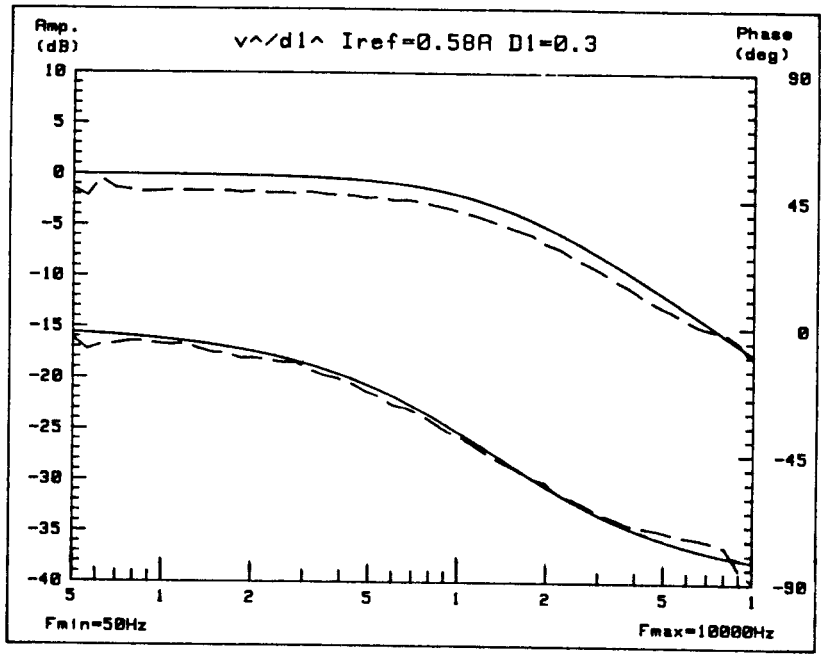

Fig. 6.14 The transfer function of the rectifier operated in the current programming mode. The solid lines show the predictions and the dashed lines show the measurement.

Thus, it seems that the time-multiplexed versions of the rectifier have a substantial edge over the space-multiplexed ones. This is in contrast to the inverters where there was really no clear cut preference for one over the other. It is seen, in the next chapter, that the time-multiplexed cycloconverters are so preferable to the space-multiplexed

ones that they are the only ones considered.

The steady-state and small-signal ac analysis of the rectifiers is made. Compared to the analysis for the inverters it is relatively simple to perform and in fact, is very similar to that for dc-to-dc converters. The theoretical calculations are verified by the experimental measurements. Two of the three modes of operation are also verified. The third one is but the concatenation of the two, and so does not require separate verification.

The coupled-inductor rectifiers are seen to be very compact and well-behaved circuits. They incorporate the best qualities aimed for by rectifier systems. They have the main basic characteristics of the coupled-inductor power processing devices, namely the smaller number of switches, the single pole dynamics, the high linearity and the fast pulsed load response. The power circuit is very simple in construction, especially in the time-multiplexed versions. The added complexity of the control circuit is not a severe drawback in the lights of the most recent advances in integrated circuits. In the next chapter the coupled inductor cycloconverters are introduced.

CHAPTER 7

Polyphase Ac-to-Ac Cycloconverters

7.1 Introduction

Use of the coupled-inductor method to generate the three-phase inverters and rectifiers leads to the introduction of the final power processing circuit: the polyphase ac-to-ac cycloconverter. A cycloconverter with variable output frequency and amplitude introduces a new dimension in the area of variable speed motor drives. Whereas ac motors have in general been limited to fixed speed applications this restriction disappears with the use of cycloconverters.

Slow switching cycloconverters with square output waveshapes have been in use for some time [25]. However, the maximum output frequency is restricted by the speed of the switches that were used. They typically run up to frequencies of 400-600 Hz. The square waveforms introduce losses in the machine in the form of harmonic currents and torque fluctuations. The design of the ac motor has to be very conservative to handle this type of input. Thus, the existence of simple, high performance cycloconverters with low harmonic outputs leads to a totally new outlook for variable speed applications.

As for the inverters and rectifiers presented in this thesis, the cycloconverters introduced here are not the first fast switching ones [1]. However, they share the same advantages as the corresponding rectifiers and inverters over the previous versions. These advantages are once more:

smaller number of components, single-pole dynamic response, high linearity of the output characteristics, and extremely fast pulsed load response.

The ac-to-ac cycloconversion function is simple to obtain by a cascade of a rectifier and an inverter. However, as with most simple ideas, this does not leads to a satisfactory result. Although the cascaded rectifier and inverter is an ac-to-ac cycloconverter, as a power processing circuit it is highly inefficient. As a first step it shows that ac-to-ac power processing is possible with the coupled-inductor principle. Several improvements are made on the simple minded coupled-inductor cycloconverter, which leads to a very compact circuit, with the minimal number of components. The coupled-inductor cycloconverters are well behaved as far as control is concerned, and have the same good waveforms as the corresponding inverters and rectifiers.

In contrast to the inverters and rectifiers, where the choice between the time and space multiplexed magnetics is not easy to make, the choice here is in favor of the time multiplexed magnetics. As a matter of fact, the idea of time multiplexed magnetics was discovered as a simplification of the cycloconverter circuits. The results of the analysis that has been done for the rectifier and the inverter are directly applicable to the cycloconverter. Hence, this chapter is mainly concerned with the description and operation of the cycloconverters. Similarly, the experimental confirmation in the previous chapters applies to the cycloconverters, so none is presented in this chapter.

7.2 Description of Ac-to-Ac Cycloconverters

It is of interest to follow the sequence of development of the cycloconverter from the inverter and rectifier, as it illustrates why the time-multiplexed versions are preferred. The first approach, as stated before, is simply to cascade the two circuits as shown in Figure 1, to obtain a flyback cycloconverter. It is immediately clear that the center section being a dc section can be merged into one (Fig. 2). Thus at this stage the coupled-inductor cycloconverter requires nine switches and ten windings.

The number of windings on the single core is very large. There are five windings on each outer leg. This sets a severe restriction on the maximum inductor value as the possible number of turns is limited by the available window area of the core. Thus, the performance of the circuit has to be sacrificed by choice of small inductor values (recall that the amount of distortion is inversely proportional to the inductor value). It is possible to use a larger core to have a larger window area but the core would be underused and too heavy for the actual energy requirements.

As an initial simplification, in the case of the flyback topology, one may get rid of a few windings by eliminating the two output phases. The output switches are then connected to the input coupled inductors as shown in Fig. 3. The reason this connection works is that the coupled inductors are either connected to the input or to the output. A similar approach may be used with the other topologies.

The dc winding is needed to equalize the fluxes in the two halves of the core. The fluxes in the two windings at the beginning of the output period are equal. In general, the sequence of operation of the switches

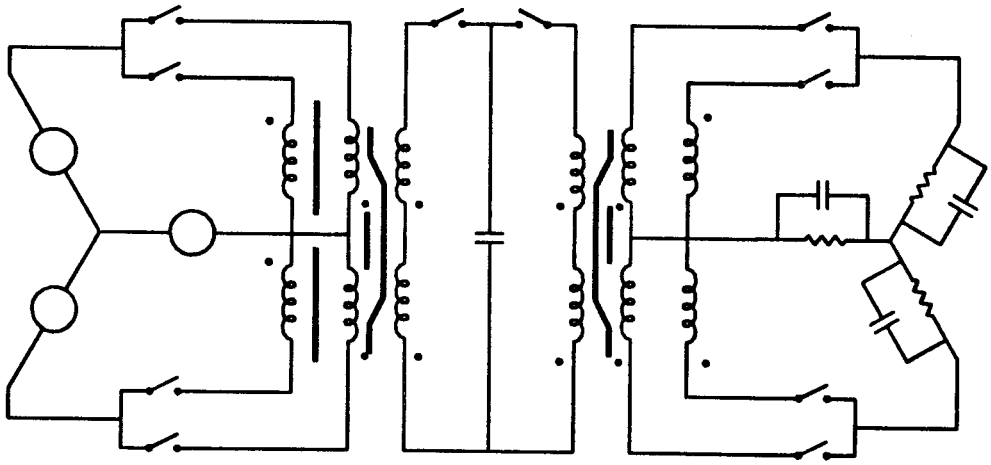

Fig. 7.1 A cycloconverter formed by the cascade of rectifier and an inverter.

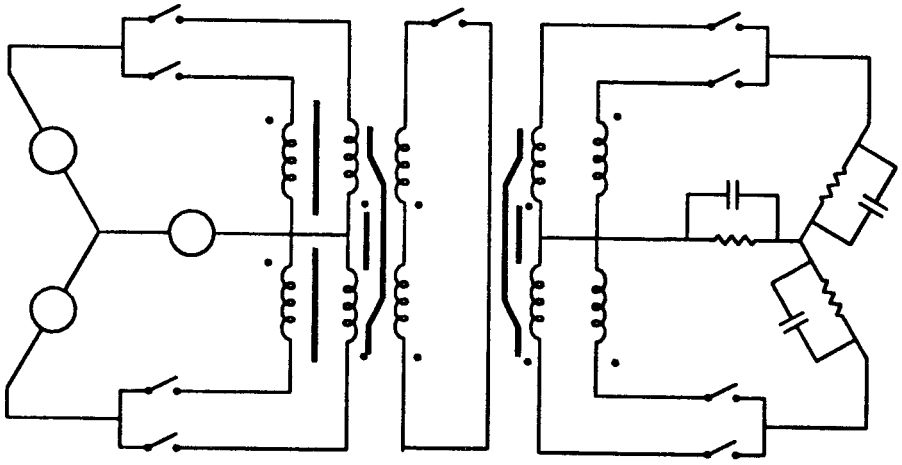

Fig. 7.2 First step reduction of the cascaded cycloconverter.

with CRP is as follows: the input switches turn on so that the inductor current reaches I_{ref}, the dc switch turns on to reset the fluxes, then finally the output switches turn on to supply the loads.

The dc section cannot be omitted because of power flow considerations. If the dc winding were not there, then each set of coupled-inductors form a single-phase ac-to-ac cycloconverter. The problem with this is that the power in a single-phase system is fluctuating and goes to zero twice in every cycle. It is then clear that the operation of the cycloconverter is not at all satisfactory.

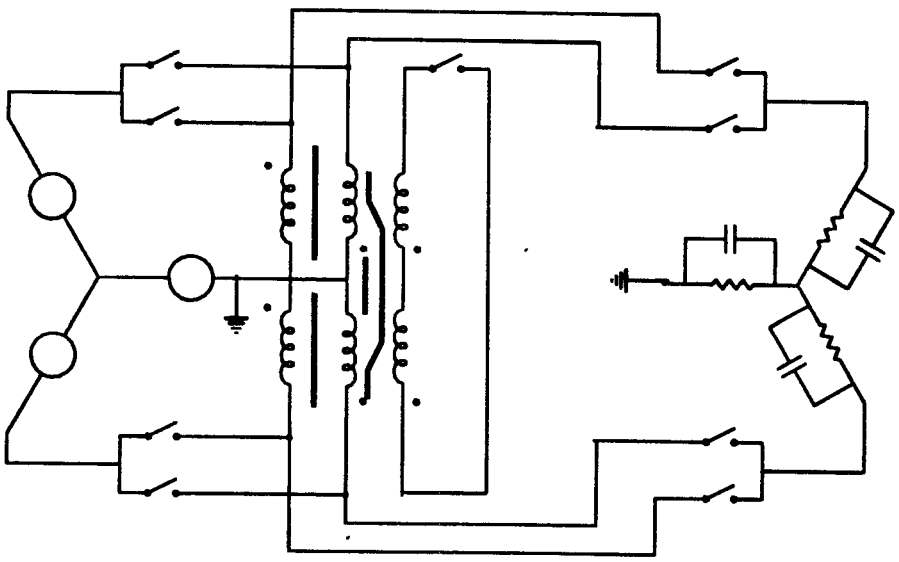

Fig. 7.3 A second step simplification of the flyback cycloconverter. The input and output switches are connected to the same inductors. The dc section serves only to equalize the fluxes in the two halves of the core.

The importance of the above circuit is that the same pairs of coupled-inductors are used once on the input and once on the output sides. This principle, pushed to its logical conclusion, results in the time-

multiplexed flyback cycloconverter (Fig. 4). The concept is applicable to the other basic topologies. The cycloconverters derived from the buck, and the boost converters are shown in Figs. 5, 6. It is clear that the complexity of the circuits is reduced to the minimum. The number of windings is down to two from a high of ten. The dc switch is also eliminated. The coupled-inductor cycloconverters require only eight switches while other types may require up to twelve switches. Note that the switch names are d_1 and d_2 for the input side, d_3 and d_4 for the output side, with a phase A and a phase B on each side. There is no relation between the phases of the same name on the input and output sides.

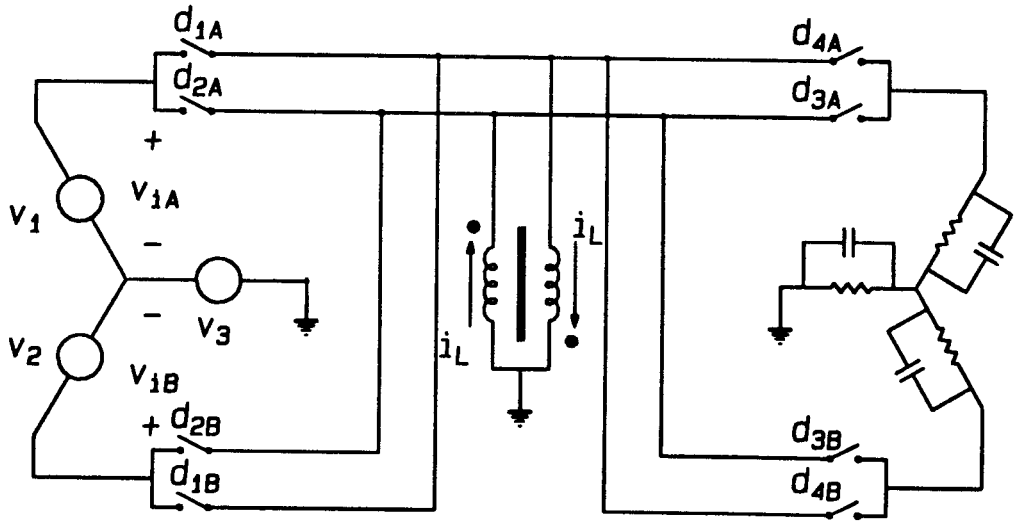

Fig. 7.4 The flyback time-multiplexed cycloconverter. The circuit is clearly more simple and compact than the space multiplexed version.

The cycloconverter input section is the same as the rectifier. Thus, the space-multiplexed versions have two extra diode-zener pairs as well as two current sense transformers. It is clear that the time-multiplexed cycloconverters are more compact, have fewer components and are simpler to operate than the space-multiplexed ones. Thus, the subsequent discussion concentrates on the time-multiplexed ones only.

7.3 Operation of Coupled-Inductor Cycloconverters

All the above circuits require only one current sense circuit, similar to the rectifiers of Ch. 6. The input switches are controlled in the same manner as the rectifier input switches. The output switches, on the other hand, are controlled as the output switches of the inverters of Ch. 5. However, whereas in the rectifier the input switches are required to maintain the length of the period constant, in this case the output switches take care of that condition. This simplifies the generation of the gate or base drive waveforms as they are closer to those of the inverters than the rectifiers.

The allowable lengths of the different switching intervals need to be calculated for proper operation. The conditions that need to be satisfied by the duty ratios can be written as:

$$d_{iA}(2nT_s) + d_{iB}(2nT_s) + d_{3A}(2nT_s) + d_{4A}(2nT_s) = 1 \qquad (7.1a)$$

$$d_{iA}((2n+1)T_s) + d_{iB}((2n+1)T_s) + d_{3B}((2n+1)T_s) + d_{4B}((2n+1)T_s) = 1 \qquad (7.1b)$$

where the i subscript denotes the effective input switch duty ratios. The

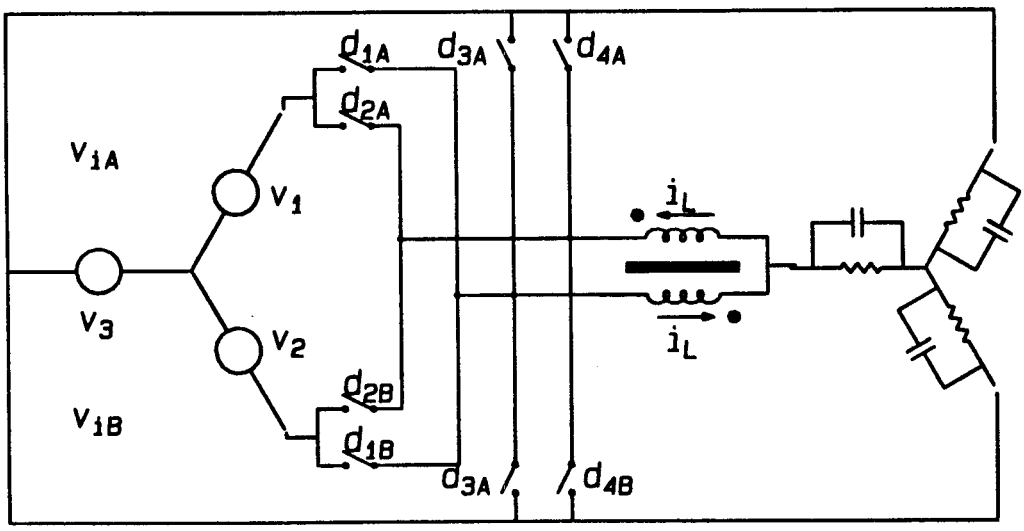

Fig. 7.5 The time-multiplexed buck coupled-inductor cycloconverter.

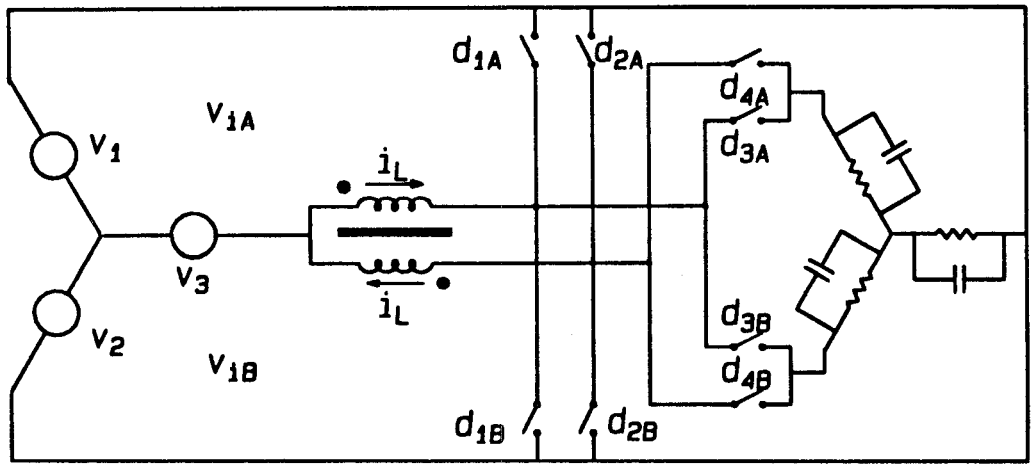

Fig. 7.6 The time-multiplexed boost coupled-inductor cycloconverter.

effective input duty ratios in the above equations are always positive as they are equal to d_2 or d_3 of the given phase according to the input voltage polarity. This is expressed mathematically as:

$$d_{iA} = \begin{cases} d_{1A} & v_A > 0 \\ d_{2A} & v_A < 0 \end{cases} \tag{7.2a}$$

$$d_{iB} = \begin{cases} d_{1B} & v_B > 0 \\ d_{2B} & v_B < 0 \end{cases} \tag{7.2b}$$

The operation of the cycloconverter with sinusoidal input currents and current programming is described very briefly here. The input switches with the shorter duty ratio are turned on at the beginning of the switching cycle for a predetermined length of time. The on-time of that switch is calculated by assuming that there has been no change in the required d_m from the previous cycle, and that the modulation is sinusoidal and in phase with the input voltage. Because of the natural diode commutation only the switch with positive inductor current slope conducts as specified by Eqs. (7.2a) and (7.2b). The switches on the other input phase are then turned on until the current reaches I_{ref}. The length of this period is assumed to be sinusoidal and in phase with the input voltage. The value of d_m is calculated and used for the next cycle.

The sinusoidal current switching scheme described above yields the following input duty ratios:

$$d_{iA} = d_{im} |\cos \omega_{im} t| \tag{7.3}$$

$$d_{iB} = d_{im}|\cos(\omega_{im}t - 120°)| \tag{7.4}$$

The maximum length of the input switching period for a given d_{im} is:

$$(d_{iA} + d_{iB})_{max} = \sqrt{3}d_{im} \tag{7.5}$$

This relation is then substituted in the general relations for the duty ratio lengths (Eq. (7.1a) and (7.1b)) to give the allowable duty ratio swings:

$$\sqrt{3}d_{im} + d_{3A}(2nT_s) + d_{4A}(2nT_s) = 1 \tag{7.6a}$$

$$\sqrt{3}d_{im} + d_{3B}((2n+1)T_s) + d_{4B}((2n+1)T_s) = 1 \tag{7.6b}$$

As for the rectifier circuits, the switching algorithm described yields pure sinusoidal currents at steady-state operation with some distortion as the operating condition changes. The current programming, however, is satisfied within the operating range of the cycloconverter. The range of operation is defined in the next section.

The switches of each phase of the input section are on for some time every switching cycle. The output section phases are connected to the inductor only every other switching cycle. The reason for this is for the outputs to receive equal amounts of energy. The inductor current at the start of each output period is equal to I_{ref}. The outputs do not affect each other as they are buffered by the input period. At the start of each output cycle the current value in the inductor is I_{ref}. Hence, the value of the output voltages depends only upon the corresponding effective duty ratio.

The output switch duty ratios are determined by the required output voltages. For a balanced three-phase sinusoidal output the effective output duty ratios for the flyback and boost cycloconverters are:

$$d_{oA}(2nT_s) = d_{3A}(2nT_s) - d_{4A}(2nT_s)$$

$$= d_{om}\cos(\omega_{om}t) \tag{7.7a}$$

$$d_{oB}((2n+1)T_s) = d_{3B}((2n+1)T_s) - d_{4B}((2n+1)T_s)$$

$$= d_{om}\cos(\omega_{om}t-120°) \tag{7.7b}$$

The effective duty ratios for the buck cycloconverter are:

$$d_{oA}(2nT_s) = d_{iA}(2nT_s) + d_{iB}(2nTs) + d_{3A}(2nT_s) - d_{4A}(2nT_s)$$

$$= d_{om}\cos(\omega_{om}t) \tag{7.8a}$$

$$d_{oB}((2n+1)T_s) = d_{iA}((2n+1)T_s) + d_{iB}((2n+1)T_s) + d_{3B}((2n+1)T_s)$$

$$- d_{4B}((2n+1)T_s) = d_{om}\cos(\omega_{om}t) \tag{7.8b}$$

The input duty ratios are not independent as they are constrained by the CRP loop as well as the sinusoidal input current requirement. These conditions are derived in the next section.

7.4 Analysis of Coupled-Inductor Cycloconverters

As far as the outputs of the cycloconverters are concerned, what happens during the input cycles is transparent as long as the CRP conditions hold. The conditions are that the inductor current reaches the reference value within the input cycle, $d_{iA} + d_{iB}$. The output section of the

cycloconverter is topologically the same as that of the corresponding inverter. It is operated in exactly the same manner and under the same conditions. Thus, the results obtained for the control-to-output large- and small-signal characteristics are immediately applicable here.

Hence, the region of operation of the CRP loop has to be defined for the cycloconverter. As for the rectifier there are several possible ways of operating the input section: sinusoidal currents, current programming or a combination of both. The one of interest is the CRP with sinusoidal input currents.

The maximum load that is supplied by the cycloconverter in the CRP mode is the same as the one given in Chapter 2. The minimum input voltage required to reach the reference current during a single input cycle calculated given the input voltages and currents are balanced three-phase sinusoids and so are the outputs.

$$\Delta I_{max} = v_{iA} d_{iA} + v_{iB} d_{iB} = V_o d_{om} \tag{7.9}$$

where ΔI_{max} is the maximum allowable inductor current ripple that ensures proper operation, v_{iA} and v_{iB} are the instantaneous input voltages, V_o is the magnitude of the output voltage and d_{om} is the output amplitude of modulation. The above equation is a general one for the time-multiplexed cycloconverters. For the special case of sinusoidal input currents, recall that the input voltages are:

$$v_{iA} = \sqrt{3}\, V_i \cos\,(\omega_{im} t - 30°) \tag{7.10}$$

$$v_{iB} = \sqrt{3}\, V_i \cos\,(\omega_{im} t - 90°) \tag{7.11}$$

where V_i is the amplitude of the phase voltages. Substitution of the above equations into Eq. (7.9) gives the following condition for the amplitude of the input voltages:

$$\sqrt{3} V_i d_{im}\, [\cos\,(\omega_{im} t)\, \cos(\omega_{im} t - 30°)$$

$$+ \cos\,(\omega_{im} t - 120°)\, \cos(\omega_{im} t - 90°)] = \frac{3}{2} V_i d_{im}$$

$$= V_o d_{om} \tag{7.12}$$

The above equation is rewritten as:

$$V_i \geq \frac{2 V_o d_{om}}{3 d_{im}} \tag{7.13}$$

The above condition is subject to the maximum duty ratio conditions given in the previous section.

It is clear that the stability of the CRP loop is the same as that of the single-phase inverter. This is especially true for the flyback and boost cycloconverters which reject disturbances within one cycle. For the buck cycloconverter the same conditions hold on the length of the input period as in Eq. (2.14). However, this translates to a different maximum output voltage for stability.

The conditions on the duty ratios for stability of the CRP loop obtained for the buck single-phase inverter need to be slightly modified. The condition setting the maximum input period is:

$$(d_{iA} + d_{iB})_{max} = 0.25 \tag{7.14}$$

The maximum length of the input period is directly related to the modulation amplitude of the input duty ratios.

$$(d_{iA} + d_{iB})_{max} = \sqrt{3} d_{im} \tag{7.15}$$

Thus the condition on the maximum allowable input duty ratio is:

$$d_{im} \leq \frac{0.25}{\sqrt{3}} \tag{7.16}$$

This translates to a maximum output voltage amplitude for the buck cycloconverter that is equal to:

$$V_o = \frac{3}{2} V_i \frac{d_{im}}{d_{om}} = \frac{\sqrt{3}}{4} V_i \tag{7.17}$$

Thus the output voltage can only be approximately equal to $0.43 V_i$.

As long as the cycloconverters are operating within the regions of stable CRP, their output sections are exactly the same as the three-phase inverter output sections. The results obtained in Chapter 5, and the methods used to obtain them, are immediately applicable here. The outputs of the cycloconverters have the same low distortion, the control-to-output transfer functions are of the first order, and the pulsed load response is very fast.

The fact that the cycloconverters have the same characteristics as the other circuits is not suprising as they are the generalized power processing circuit. It is easy to see that by keeping certain switches on at all times or off at all times different power processing functions are

obtained. For example, if one kept all the input switches except one off all the time one has a three-phase inverter. As a matter of fact, other power processing functions exist in the cycloconverter that have not been discussed in this thesis, such as a dual output rectifier with independent outputs, or a multiple input dc-to-dc converter.

7.5 Conclusions

The ac-to-ac cycloconverters are discussed in this chapter. The cycloconverters derived from the basic dc-to-dc converters are described. The time-multiplexed versions are found to be clearly superior to the space-multiplexed ones. The operation is described; it is found to be the same as rectifiers on the input side, and as the inverter on the output side. The analysis of the rectifier and inverter is then sufficient to describe the cycloconverters.

The regions of operation and stability of the CRP loop are derived. Within these regions the cycloconverters exhibit the advantages of the coupled inductor rectifiers on the input, mainly the low distortion sinusoidal input currents and the phase angle correction. On the output side, it has the advantages of the three-phase rectifiers: single-pole response, high linearity, and fast pulsed load response. All these advantages are added to the small number of switches that are required, which is one of the principal properties of the coupled-inductor circuits.

The coupled-inductor cycloconverters are in fact the generalized coupled-inductor power processing circuit. The eight switches in these circuits have enough degrees of freedom to be able to generate any desired power processing function. This is achieved by constraint of some

switches to be on at all times or off at all times. Hence, it is clear that all the power processing circuits including dc-to-dc converters are but a special case of cycloconversion. There are also potential applications in areas not studied in this thesis, such as multiple output dc-to-dc converters.

CONCLUSION

A pair of negatively coupled inductors substituted for the single inductor in the basic dc-to-dc converters yields a complete family of power processing circuits. All the functions of power procesing are represented in this family: dc-to-ac, ac-to-dc, and ac-to-ac conversion.

The coupled-inductor circuits all require a smaller number of switches than other existing types of power processing circuits. The reduction in the number of parts icreases the simplicity and reliability of the circuits while reducing the cost. This is not achieved at the expense of performance. On the contrary, the use of the coupled inductors introduce a third switched network that, added to the application of current programming, make these circuits close to optimal in performance.

The circuits exhibit high linearity with resulting low distortion in the waveforms. Thus, the inverters have very clean sinusoidal outputs, and the rectifiers approach the ideal operation of sinusoidal input currents with zero phase angle. The circuits are very simple to control as the dynamics are of the first order. This is very useful as far as integration of these converters in different systems is concerned. The response to changes in loads is extremely fast, thus making these circuits ideal for pulsed load applications.

The different coupled-inductor power processing circuits are described starting from the single-phase inverters to the polyphase

cycloconverters. The application of current reference programming to these circuits is discussed in detail. The advantages gained from the use of that control technique allied to the three switched-network mode of operation is emphasized. The stability of the coupled-inductor circuits' CRP loop is investigated. The flyback and boost are found to be stable at all operating points which makes them very attractive to use in practice.

Some interesting concepts in the application of magnetics to the problem of multiple independent output converters are presented. The time- and space-multiplexed magnetics are both studied in detail in all modes of operation. The observed behavior of the currents in the multiple output magnetics is explained by use of reluctance model analysis. The behavior of the currents in the multiple input magnetics is predicted and confirmed experimentally. These magnetics are applied to the three-phase versions of the inverters as they help reduce the number of switches.

Extensive experimental verification has been made of most of the theoretical results. The single-phase flyback and boost inverters were built. The stability of the CRP loop is confirmed as well as the fast pulsed load response. The measurements are made of the control-to-output transfer function. The harmonic content of the output waveform is also calculated. The single-pole response and high linearity of the circuits are proved. The same measurements are taken for a flyback three-phase inverter. The comparison of the measurements and theoretical results are equally good in that case.

The flyback coupled-inductor rectifier is built to verify the operation and analysis. It is seen that the coupled-inductor rectifier has the main characteristics of an ideal rectifier. These characteristics are:

sinusoidal input currents with control over the phase. The rectifiers still have the principal advantages common to the coupled-inductor circuits with CRP. The measurements of the control-to-output transfer function are taken and compared to the predictions with good agreement.

Thus, the coupled-inductor circuits are a family of simple and relatively inexpensive yet of high performance power processing circuits. It is to be hoped that, with the advent of such circuits, the cost of the electronics goes down, its performance increases, and it becomes more attractive to use in different applications.

The range of potential application is too large to list comprehensively, but a few can be pointed out. In the field of robotics, for example, it is becoming apparent that traditional motors and their drives are a severe limitation because of low torque-weight ratios. The existence of new motor drives with high quality sinusoidal outputs allow for the consideration of ac motors as an alternative to the motors currently in use.

The inputs to the motor being sinusoidal help reduce the losses and torque fluctuations in the motor. The design of the motor itself can be redone with substantial savings in weight. It is still an open problem whether ac motors can supersede the dc motors in variable speed applications. However, it is an important question to investigate in the light of the innovations in power electronics such as the coupled-inductor circuits.

There are other areas of application, such as the use of inverters as interfaces between solar arrays and the three-phase ac lines of the distribution system. The inverters could help making the installation of

solar arrays in homes more economic by allowing the homeowners to sell the power to the utilities. It also eliminates the cost of rewiring the houses and the use of special appliances that run off the dc voltage of the solar arrays.

As mentioned previously, the application of such circuits to the problem of power factor correction is of primary importance. Most loads in use are inductive in nature. Large capacitors are used by the utilities to correct the power factor as a small power factor means that a huge amount of power is being reflected to the source. The cycloconverters can be used as impedance converters making the inductive loads appear to be resistive.

The different circuits require a lot of further studies. The effect of different types of loads on the operation of these circuits needs to be investigated. The choices of current reference values and duty ratio modulations for maximization of the efficiency is another point of interest. There are also some offshoots of the work presented here. The 4SN Ćuk converter is an circuit with many properties that requires further study.

The operation of coupled inductor circuits with variable switching frequencies helps increase the efficiency. This type of operation eliminates the lossy current return period that is mainly there to maintain the fixed switching frequency. The most obvious drawback is how to filter the conducted electro-magnetic interference with a variable switching frequency. Another question of interest is whether there is an optimal frequency range for the magnetics and the switching losses.

Every answered question or solved problem uncovers a greater number of new questions and problems. It is also the case here. However, it is clear that the field of power electronics is maturing from its beginnings with dc-to-dc converters to the present with the generalized power processing circuits. It is to be hoped that other fields of engineering would take advantage of the new advances in power electronics. Power electronics has a potentially revolutionary impact on mature fields such as motor design as well as recent areas such as robotics and maybe even some as yet unknown applications.

APPENDIX A

Small-Signal Perturbation of State-Space Equations

Take a general state-space description of an inverter written in the form:

$$P\dot{\boldsymbol{x}} = (\boldsymbol{A}_r + \boldsymbol{A}_d d_m + \boldsymbol{A}_\omega \omega_m)\boldsymbol{x} + \boldsymbol{b} V_g \tag{A.1}$$

The variables in the above equation are time-varying and the equation is non-linear as d_m and ω_m are inputs to the system. One method of solving the above equation is to assume that the variables consist of a large steady-state value and a small perturbation.

$$\boldsymbol{x} = \tilde{\boldsymbol{X}} + \hat{\boldsymbol{x}}$$

$$d_m = D_m + \hat{d}_m \qquad \omega_m = \Omega_m + \hat{\omega}_m$$

where uppercase letters denote steady-state quantities and lowercase ones with carets denote small-signal ac quantities. Small-signal perturbations in V_g are neglected in the analysis as they are effectively decoupled from the output by the CRP loop. Similarly, perturbations in d_1 are not an input to the system as they result from perturbations in the other states. The system is now described by:

$$P\dot{\hat{\boldsymbol{x}}} = (\boldsymbol{A}_r + \boldsymbol{A}_d(D_m + \hat{d}_m) + \boldsymbol{A}_\omega(\Omega_m + \hat{\omega}_m))(\boldsymbol{X} + \hat{\boldsymbol{x}}) + \boldsymbol{b} V_g$$

$$= (A_r + A_d D_m + A_\omega \Omega_m)X + b V_g \tag{A.2}$$

$$+ (A_r + A_d D_m + A_\omega \Omega_m)\hat{x} + A_d \hat{d}_m + A_\omega \hat{\omega}_m$$

$$+ \textit{higher order perturbations}$$

The steady-state values are found by solution of the above equation when the perturbations are equal to zero. The steady-state equation is:

$$(A_r + A_d D_m + A_\omega \Omega_m)X = 0 \tag{A.3}$$

The small-signal equation is then linearized by neglecting the higher order perturbations.

$$P\dot{\hat{x}} = A\hat{x} + A_d X\hat{d}_m + A_\omega X\hat{\omega}_m \tag{A.4}$$

where $A = (A_r + A_d D_m + A_\omega \Omega_m)$. The transfer functions are then found by taking the Laplace Transform of the above equation.

$$\hat{x}(s) = (sP - A)^{-1}[A_d X\hat{d}_m + A_\omega X\hat{\omega}_m] \tag{A.5}$$

APPENDIX B

The abc-ofb Transformation

Let $\boldsymbol{v}$ be a vector of balanced three-phase voltages in stationary (abc) frame of reference.

$$\boldsymbol{v} = \begin{bmatrix} v_1 \\ v_2 \\ v_3 \end{bmatrix} = \begin{bmatrix} v\cos(\omega_m t - \varphi) \\ v\cos(\omega_m t + 120° - \varphi) \\ v\cos(\omega_m t - 120° - \varphi) \end{bmatrix} \tag{B.1}$$

where φ is a phase angle relative to some arbitrary reference. Then $\boldsymbol{v}$ can be transformed to a rotating (ofb) frame of reference by:

$$\boldsymbol{v} = T_3 \mathfrak{V} \qquad \mathfrak{V} = T_3^{-1} \boldsymbol{v}$$

where the transformation T_3 is given by:

$$T_3 = \frac{1}{\sqrt{3}} \begin{bmatrix} 1 & e^{-j\omega_m t} & e^{j\omega_m t} \\ 1 & e^{-j(\omega_m t - 120°)} & e^{j(\omega_m t - 120°)} \\ 1 & e^{-j(\omega_m t + 120°)} & e^{j(\omega_m t + 120°)} \end{bmatrix} \tag{B.2}$$

The transformation here is assumed to have no phase relative to the arbitrary reference. However, it may have some angle φ_T. In this case, the transformed voltage vector $\mathfrak{V}$ is given by:

$$\mathfrak{V} = \begin{bmatrix} v_0 \\ v_f \\ v_b \end{bmatrix} = \begin{bmatrix} 0 \\ \frac{\sqrt{3}}{2} v e^{j\varphi} \\ \frac{\sqrt{3}}{2} v e^{-j\varphi} \end{bmatrix} \tag{B.3}$$

where v_0, v_f and v_b are the zero sequence, forward and backward phasor

of the transformed voltage.

The above relation gives the transformed vector of the *steady state* voltages. Hence, one cannot assume that v_0 is identically equal to zero in the inverter output. It will be seen that, for the flyback inverter, v_0 is identically equal to zero.

REFERENCES

[1] Khai D.T. Ngo, "Topology and Analysis in PWM Inversion, Rectification, and Cycloconversion," PhD Thesis, California Institute of Technology, May 1984.

[2] Robert W. Erickson and R. D. Middlebrook, "Large-Signal Modelling and Analysis of Distortion in Switching Amplifiers," Power Electronics Group, California Institute of Technology, Jan. 1982.

[3] Farhad Barzegar and Slobodan Ćuk, "A New Switched-Mode Power Amplifier Produces Clean Three Phase Power," Proceedings Ninth International Power Conversion Conference (Powercon 9), pp. E3.1-E3.15, July 1982.

[4] B. D. Bedford and R. G. Hoft, *Principles of Inverter Circuits*, John Wiley and Sons, 1984.

[5] B. K. Bose, ed., *Adjustable Speed Ac Drive Systems*, IEEE Press, 1981.

[6] R. D. Middlebrook and Slobodan Ćuk, "Advances in Switched-Mode Power Conversion," Volumes I and II, second edition, TESLAco, Pasadena, 1983.

[7] D. T. Paris and F. K. Hurd, *Basic Electromagnetic Theory*, McGraw-Hill, 1969.

[8] R. Mahadevan, S. El-Hamamsy, W.M. Polivka and S. Ćuk, "A Converter With Three Switched-Networks Improves Regulation, Dynamics and Control," Proceedings Tenth International Power Conversion Conference (Powercon 10), pp. E1.1-E1.19, March 1983.

[9] Slobodan Ćuk, "Modelling, Analysis and Design of Switching Converters," PhD Thesis, California Institute of Technology, Nov. 1976.

[10] C. W. Deisch, "Simple Switching Control Method Changes Power Converter into a Current Source," IEEE Power Electronics Specialists Conference,1978 Record, pp. 300-306,
(IEEE Publication 78CH1337-5 AES).

[11] Shi-Ping Hsu, Art Brown, Loman Rensink and R.D. Middlebrook, "Modelling and Analysis of Switching Dc-to-dc Converters in Constant-Frequency Current-Programming Mode," IEEE Power Electronics Specialists Conference, 1979 Record, pp. 284-301.
(IEEE Publication 79CH 1461-3 AES)

[12] R.D. Middlebrook, "Topics in Multiple-loop Regulators and Current-mode Programming," IEEE Power Electronics Specialists Conference, 1985 Record,
(IEEE Publication 85CH 2117-0 AES)

[13] Arthur R. Brown and R. D. Middlebrook,"Sampled-Data Modelling of Switching Regulators," Proc. IEEE Power Electronics Specialist Conference, 1981 Record, Boulder, Colorado, June 1981,pp. 349-369.
(IEEE Publication 81CH1652-7)

[14] Dennis J. Packard, "Discrete Modelling and Analysis of Switching Regulators," PhD Thesis, California Institute of Technology, May 1976; also, Report No. M76-43, Hughes Aircraft Co., Aerospace Groups,Culver City, Calif.

[15] J. R. Ragazzini and G. F. Franklin, *Sampled Data Control Systems*, McGraw-Hill, 1958.

[16] D.C. White and H.H. Woodson, *Electromechanical Energy Conversion*, John Wiley and Sons, 1959.

[17] Slobodan Ćuk and R.D. Middlebrook, "A General Unified Approach to Modelling Switching Dc-to-dc Converters in Discontinous Conduction Mode," IEEE Power Electronics Specialists Conference, 1977 Record.
(IEEE Publication 77CH 1213-8 AES)

[18] Farhad Barzegar, Slobodan Ćuk, and R. D. Middlebrook, "Using Small Computers to Model and Measure Regulator Transfer Functions and Loop Gains," Proc. Eighth International Solid State Power Conversion Conference (Powercon 8), pp. H1.1-H1.28, April 1981.

[19] Sayed-Amr El-Hamamsy and R. D. Middlebrook, "A New Family of Single-Phase and Three-Phase Inverters," Proc. International PCI'85 Conference, October 1985, pp.84-98.

[20] Slobodan Ćuk and R.D. Middlebrook, "A General Unified Approach to Modelling Switching Dc-to-dc Converters in Discontinous Conduction Mode," IEEE Power Electronics Specialists Conference, 1977 Record. (IEEE Publication 77CH 1213-8 AES)

[21] Khai D.T. Ngo, Slobodan Ćuk, and R.D.Middlebrook, "A New Flyback Dc-to-Three-Phase Converter With Sinusoidal Outputs," IEEE Power Electronics Specialists Conference, 1983 Record, pp. 377-388. (IEEE Publication 83CH 1877-0 AES)

[22] N. J. Barabas, "Simplified Control Algorithm for Power Factor Correction," Proc. International PCI'85 Conference, October 1985, pp. 1-9.

[23] J. E. Murray and D. C. Griffith, "The Line Driven Switcher as a Black Box Load," Proc. International PCI'85 Conference, October 1985, pp. 10-18.

[24] M. J. Kocher and R. L. Steigewald, "An Ac to Dc Converter with High Quality Input Waveforms," IEEE Power Electronics Specialists Conference, 1982 Record, pp. 63-75.
(IEEE Publication 82CH 1762-4 AES)

[25] B. R. Pelly, *Thyristor Phase-Controlled Converters and Cycloconverters*, John Wiley and Sons, 1971.